A Sensitivity Investigation upon the Dynamic Structural Response of a Nuclear Plant on Aseismic Isolating Devices

I. MICHELI ANSALDO ENERGIA Nuclear Division I-16161 Genova, ITALY
A. COLAIUDA ENEA Accelerator Driven System Project I-40129 Bologna, ITALY

1. ABSTRACT

The ADS (Accelerator Driven System) is a hybrid reactor, basically consisting of an ion-beam accelerator and of a subcritical reactor, currently developed in Europe as an innovative and inherently safe concept for nuclear high-level waste management and power generation.

Object of this paper is a sensitivity analysis of the behaviour of a typical isolating device in an application for the Nuclear Island of an ADS Plant, with a preliminary assessment of isolation main effects on the building response under a reference design basis earthquake excitation.

After a general description of isolators and main underlying principles, an estimation is given of different building responses under a seismic load for classical foundations and for two different types of isolators, making use of a three dimensional finite element model of the building and of simplified extrapolations.

The comparison is focused on the acceleration floor response spectra at the reactor support level, a basic concern in the main vessel seismic design.

Specific criteria for the design verification of the isolating system are also investigated.

2. SEISMIC ISOLATORS

2.1 Basic Principles of Seismic Isolation

Seismic isolation is one of the most significant engineering developments in recent years: several examples of application to bridges, non-nuclear plants and structures already exist in highly seismic areas, like Japan, California and European countries (like Italy and Greece).

Unlike the conventional design approach, which is based upon an increased resistance (strengthening) of the structures, the seismic isolation concept is aimed at a decrease of dynamic loads induced by the earthquake at the base of the structures themselves.

This concept has proven especially reliable for the prevention of damage to non-structural members and inner equipment (like typically existing in nuclear plants).

Seismic isolation is practically obtained by means of an insertion of special devices (the “isolators”) between the base of the structure and its foundations. Isolators must have a high flexibility, so as to move the fundamental periods of the main structure well beyond the range associated to the soil motion amplification (see Figure 1): this can be easily achieved for medium or hard soil, whereas a particular care is required for applications upon soft soils. As a result, the soil excitation is filtered and accelerations at the base of the structure are drastically reduced.

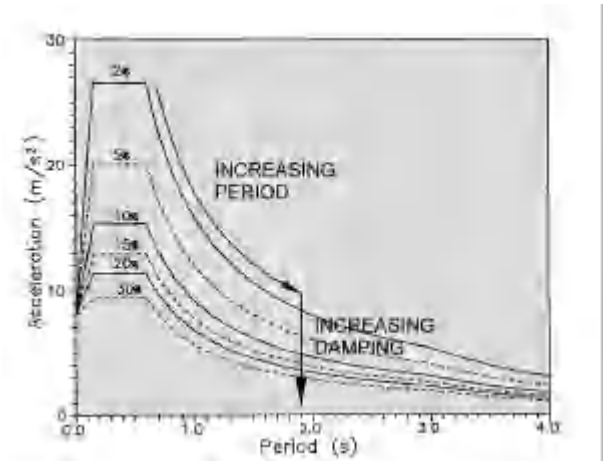

Figure 1 - Acceleration response spectrum as a function of damping (from Eurocodes EC8 for ground acceleration 0.8g and medium soil)

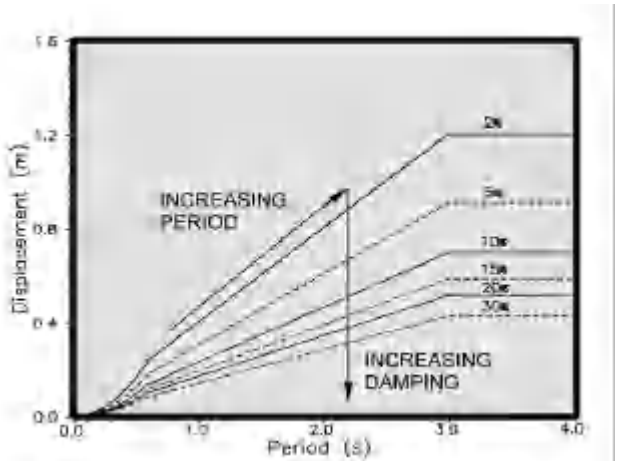

Figure 2 - Displacement response spectrum as a function of damping (from Eurocodes EC8 for ground acceleration 0.8g and medium soil)

In principle, a structure may be isolated in both horizontal and vertical directions: at present, however, seismic isolation is usually limited to horizontal directions. The main reason is that seismic loads are generally quite lower in the vertical direction (due to lower soil excitation levels and to a reduced amplification across the structure); also, 3-D isolation design is rather complicated by potential rocking modes of vibration.

The strong reduction in structural accelerations has its obvious reverse in large rigid-body displacements, which are to be limited by means of dissipating elements, leading to significant increases of structural damping (see Figure 2).

Isolators should also have a high self-centring capability, i.e. the capability of carrying back the isolated structure to its initial position after each peak of seismic excitation, a safety feature with respect to potential earthquake aftershocks.

Finally, the horizontal stiffness of isolation devices, which is quite low at large excitations, should be, on the contrary, high enough at low excitations, as typically induced by small earthquakes or winds, in order to avoid significant vibrations in case of these relatively frequent events.

All basic principles of seismic isolation have been successfully integrated in the HDRB (High Damping Rubber Bearing), a recently developed 2-D isolator, which has been selected for application to the ADS Nuclear Island.

2.2 Main Features of the HDRB

The HDRB is a steel-laminated bearing consisting of alternate layers of rubber and steel plates bonded by vulcanisation: it is able to support high vertical loads with negligible deflection, still providing an efficient isolation with respect to the horizontal seismic excitation [1] (see Figure 3).

This device is very efficient as regards both filtering and dissipation functions, the main effects of which are:

- the fundamental frequency of the isolated structure is moved in the low range (between 0.33 and 1 HZ), where the seismic motion energy is very low;
- the structure displacements in case of large earthquakes are reduced below allowable limits, by means of a large amount of energy dissipation.

Figure 3 - Typical High Damping Rubber Bearing

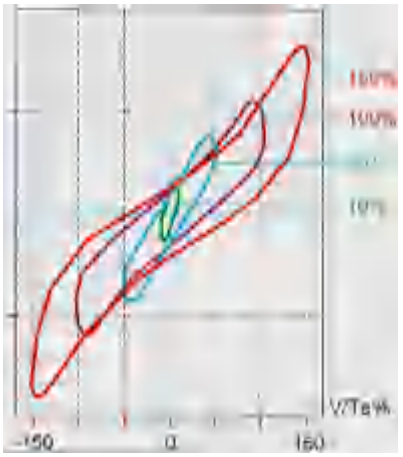

Figure 4 - Typical load/deflection plot of a HDRB

With respect to standard isolators, the HDRB peculiar characteristics are:

- a high damping capability due to a large area of the hysteresis loop (see Figure 4): the equivalent viscous damping is not less than 10% of critical damping;
- a highly proven good self-centring capability;
- a high horizontal stiffness at low excitations, so as to minimise the effects of frequently occurring events (like wind loads): the wind control region of shear strain is 2÷5%, as the earthquake region is 50÷125%;
- the horizontal stiffness, quite low in the large deformation range, increases again for shear strains exceeding 200%, which is useful to avoid excessive displacements even for extremely strong earthquakes;
- a very high vertical stiffness, in order to withstand deadweight and vertical seismic loads, as well as to prevent rocking movements during seismic excitation;
- the fixation to the structure is not based on friction but on positive connections, namely by recess or dowels (see Figure 5) or by bolt joints (see Figure 6);
- the mean lifetime is over 60 years.

The stiffness of HDRB isolators depends on the rubber compound modulus, bearing plan dimensions, height and number of layers. The allowable maximum vertical and horizontal displacements depend on the anchor system as well.

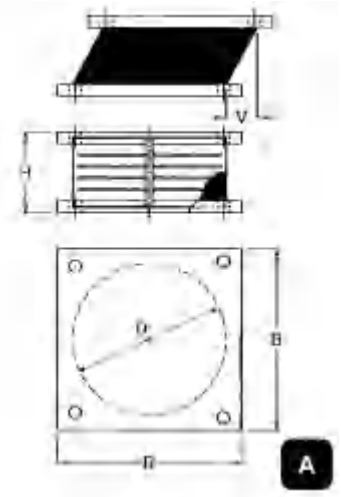

Figure 5 - HDRB with fixation by recess (type A)

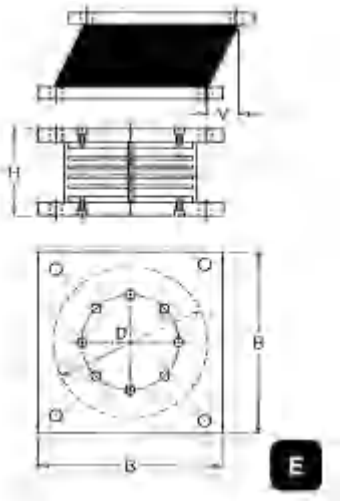

Figure 6 - HDRB with fixation by bolts (type E)

Stiffness and damping characteristics are shown in following Figures 7 and 8 and in Tables 1a and 1b for HDRB isolators with soft rubber compound (HDS) or hard rubber compound (HDH) [2].

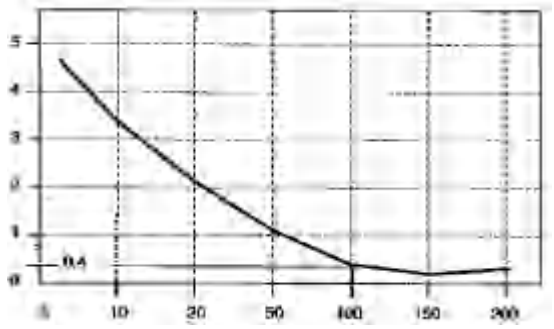

Figure 7a HDS Isolators
G modulus (MPa) versus Shear Strain %

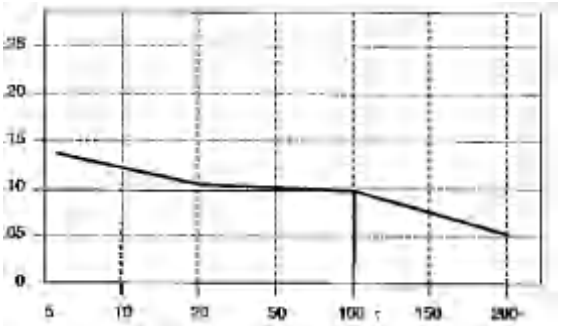

Figure 7b HDS Isolators
Damping Ratio versus Shear Strain %

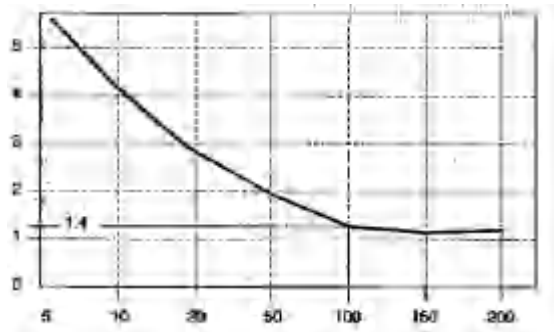

Figure 8a HDH Isolators
G modulus (MPa) versus Shear Strain %

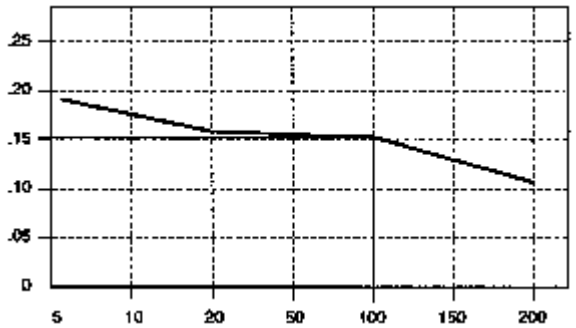

Figure 8b HDH Isolators
Damping Ratio versus Shear Strain %

It is shown that the damping ratio of these isolators is nearly constant for shear strains between 20 and 100%: its value is about 0.10 for soft/medium compounds and about 0.15 for hard compounds. The horizontal stiffness, nearly constant for shear strains between 100 and 200%, rises to several times more for shear strains of 5%: at 100% shear strains, soft and hard compound shear moduli G are, respectively, about 0.4 and 1.4 N/mm^2.

For self-centring 2-D isolators like the HDRB, an ultimate safety system ("fail-safe system") should be foreseen to withstand vertical loads in case of failure of the isolation system, unless it can be shown by qualification tests that isolators are able to support the structure under seismic loads as high as five times the SSE loads.

Table 1a. Dimensions and Properties of HDS.A Isolators

HDH.A	Vertical load max (kN)	Displacement max (mm)	Horiz. stiffness at 100% strain (kN/mm)	Dimensions Te = total rubber thk. (mm)			
	Fz	V	k_h	D	H	B	Te
HDH.A 300	1000	112	1.24	300	177	380	80
HDH.A 400	1850	146	1.69	400	210	480	104
HDH.A 500	2900	179	2.15	500	243	580	128
HDH.A 600	4200	218	2.54	600	274	680	156
HDH.A 700	5700	252	2.99	700	326	800	180
HDH.A 800	7500	280	3.45	800	374	900	204
HDH.A 900	9500	280	4.37	900	374	1000	204
HDH.A 1000	11000	280	5.24	1000	398	1140	210
HDH.A 1100	14000	280	6.34	1100	398	1240	210
HDH.A 1200	16000	280	7.54	1200	398	1340	210

Table 1b. Dimensions and Properties of HDH.A Isolators

HDH.A	Vertical load max (kN)	Displacement max (mm)	Horiz. stiffness at 100% strain (kN/mm)	Dimensions Te = total rubber thk. (mm)			
	Fz	V	k_h	D	H	B	Te
HDH.A 300	1000	112	1.24	300	177	380	80
HDH.A 400	1850	146	1.69	400	210	480	104
HDH.A 500	2900	179	2.15	500	243	580	128
HDH.A 600	4200	218	2.54	600	274	680	156
HDH.A 700	5700	252	2.99	700	326	800	180
HDH.A 800	7500	280	3.45	800	374	900	204
HDH.A 900	9500	280	4.37	900	374	1000	204
HDH.A 1000	11000	280	5.24	1000	398	1140	210
HDH.A 1100	14000	280	6.34	1100	398	1240	210
HDH.A 1200	16000	280	7.54	1200	398	1340	210

The HDRB isolators have already been employed in the aseismic design of several important civil and industrial buildings and structures. Among the most impressing applications [1]:

a) the Telecom Centre in Ancona (Italy), see Figures 9 and 10;
b) the Corinth Canal Bridge (Greece), see Figures 11 and 12;
c) the Riace's Bronzes in Reggio Calabria (Italy), see Figures 13 and 14;
d) the chemical plant in Visp (Switzerland), see Figures 15 and 16;
e) the bridge over Tagus River in Santarem (Portugal), see Figures 17 and 18.

Figure 9 – Ancona Telecom Centre building

Figure 10 - Details of the HDRB Isolator

Figure 11 - Corinth canal bridge under construction

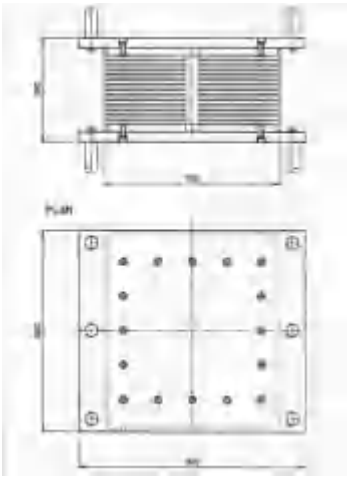

Figure 12 - HDRB sketch for Corinth canal bridge

Figure 13 - The maquette of a Riace's Bronze on its antiseismic support during tests

Figure 14 - Detail of the segmented HDRB

Figure 15 - Visp chemical plant: the base isolated tank

Figure 16 - Detail of the HDRB

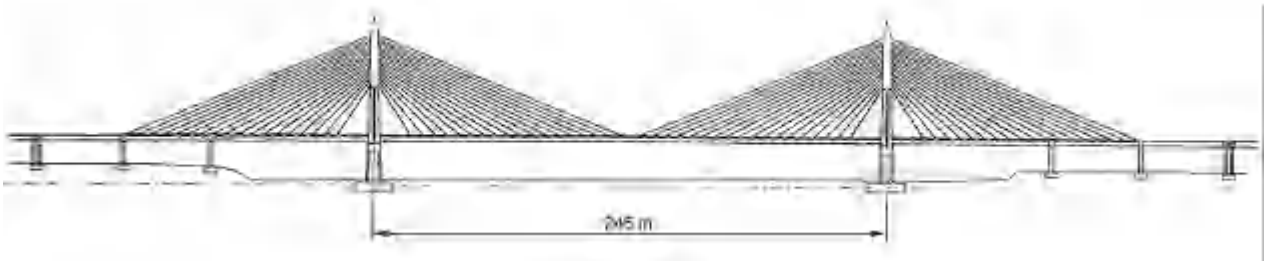

Figure 17 - The bridge over Tagus River in Santarem, central part

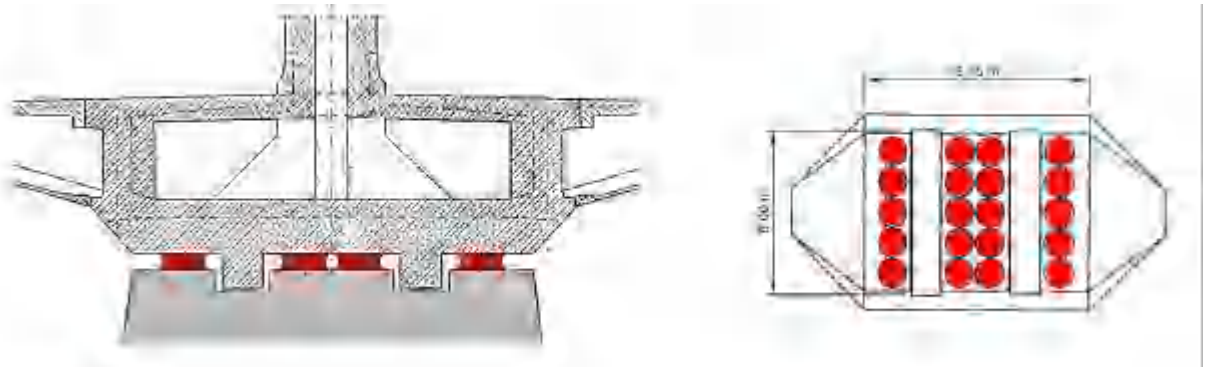

Figure 18 – Bridge over Tagus River: disposition of the HDRB on the piers of the main span

2.3 Isolation Design

The isolating system is to be designed to withstand dead, live and seismic loads.

The best-fit isolator layout should minimise the global torsion mode of the supported structure, so as to get nearly uniform horizontal displacements: this can be achieved along with a stiffness centre of the isolation system as close as possible to the projection of the centre of mass of the isolated structure onto the plane of isolators.

Isolators should be at least located under load concentrations zones such as main walls. Also, for an easy in-service inspection, they should be installed on concrete pedestals in a gap between a lower and an upper basemat, at an adequate mutual distance.

As to the dynamic behaviour, the isolator choice is based upon the following procedure:

a) calculation by hand of main horizontal isolation frequency: $f_i = (\sqrt{(K/M)})/2\pi$, with M total mass of the isolated building and K global horizontal stiffness of the isolation system (f_i should be in the range 0.33-1 Hz);
b) verification of the expected isolation frequency by means of a finite element model of the building and evaluation of the mean isolator horizontal displacement and associated shear strain and efficient stiffness;
c) subsequent iterative calculations of isolator displacements and stiffness until convergence is reached.

3. APPLICATION TO ADS NUCLEAR ISLAND BUILDING

3.1 FEM Model

The general arrangement of the ADS Nuclear Island buildings is shown in Figure 19.

Figure 20 shows the ADS Reactor Vessel and main Components.

The 3-D finite element model of the building structures was built up by means of ANSYS Computer Program [3] (see Figures 21 thru 23). Beam elements were used for the simplified stick models of auxiliary buildings, whereas the reactor building was simulated by shell elements and the reactor containment wall by solid brick elements; the main component, the reactor vessel supported by the containment, was represented by a simplified beam model reproducing the main horizontal mode of vibration.

The isolating devices were simulated by horizontal springs at 267 selected locations below the upper basemat (see Figure 24). The lower basemat was represented by a single massive node rigidly linked to isolator anchor points with respect to horizontal and torsion movements and to the upper basemat with respect to vertical and rocking movement (because of the negligible isolator vertical flexibility): the soil/structure interaction was simulated by six springs at the massive node, thus representing the global soil stiffness along each considered degree of freedom, as evaluated by means of the “soil impedance” method recommended by ASCE Standards [4].

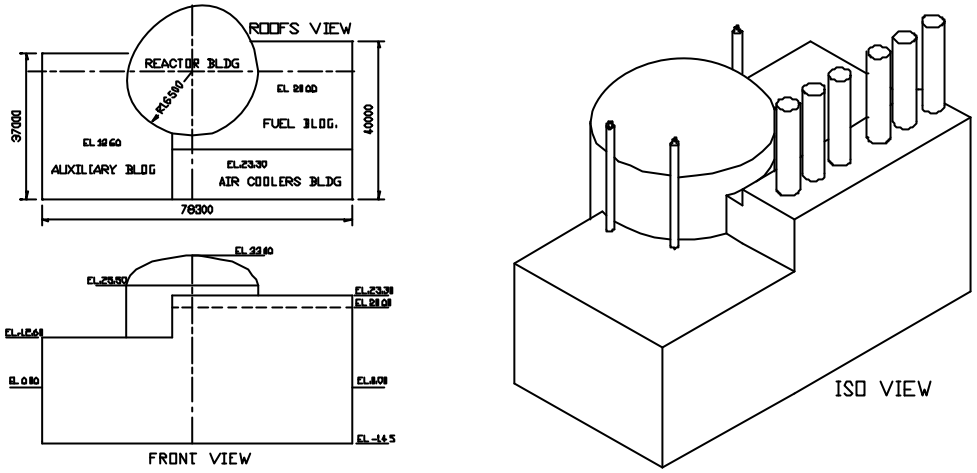

Figure 19 – ADS Nuclear Island Buildings – General Arrangement

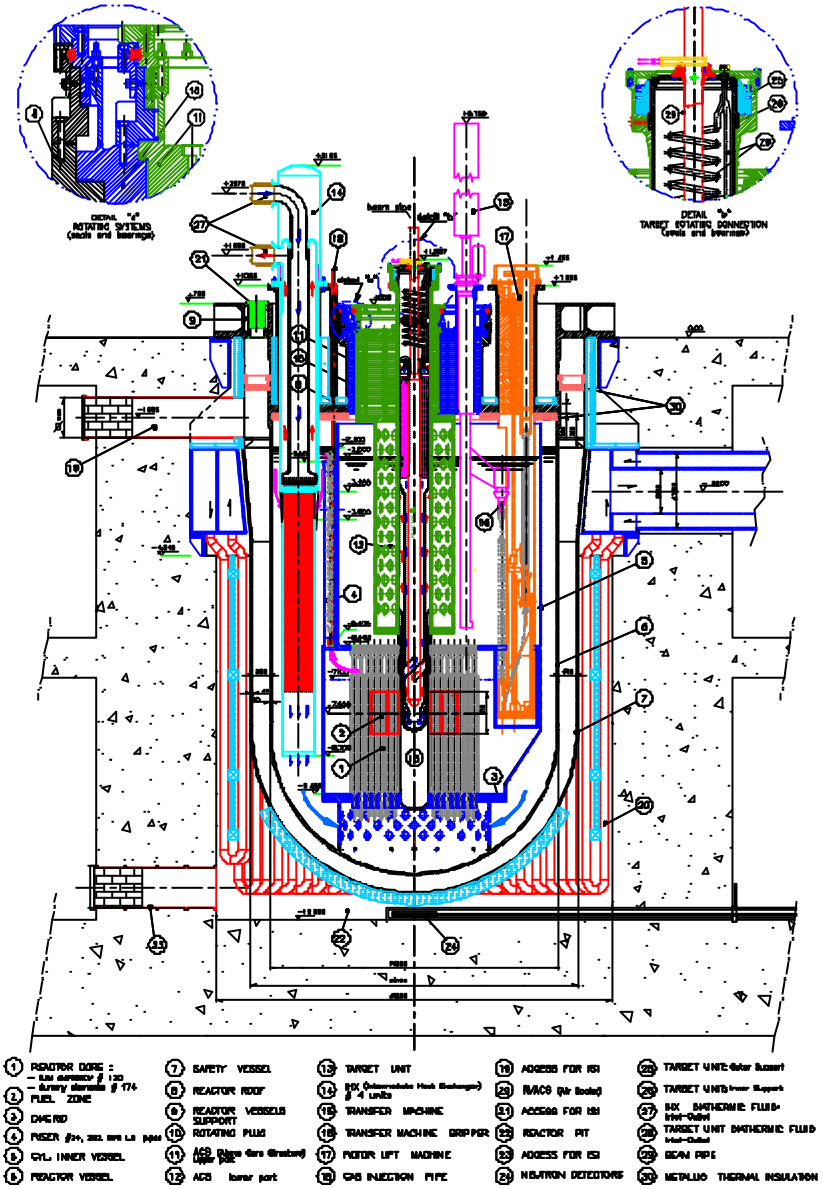

Figure 20 – ADS Nuclear Reactor Vessel and Main Components

The dynamic excitation corresponding to a SSE (Safe Shutdown Earthquake) was simulated by means of the EUR free-field design response spectra, with a ZPA acceleration of 0.25 g along each global direction.

The overall finite element model with isolators has a total of 14817 active degrees of freedom.

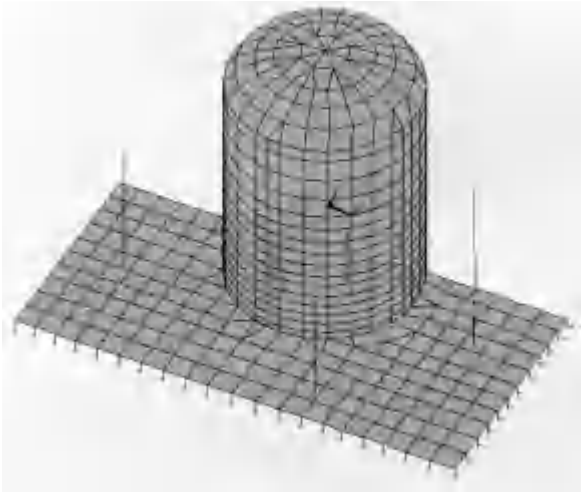

Figure 21 ADS Nuclear Island – ANSYS 3-D Finite Element Model

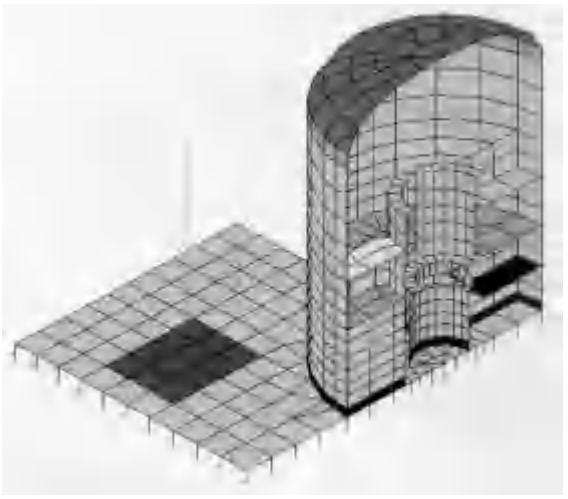

Figure 22 ADS Nuclear Island – ANSYS 3-D Finite Element Model – Section along YY

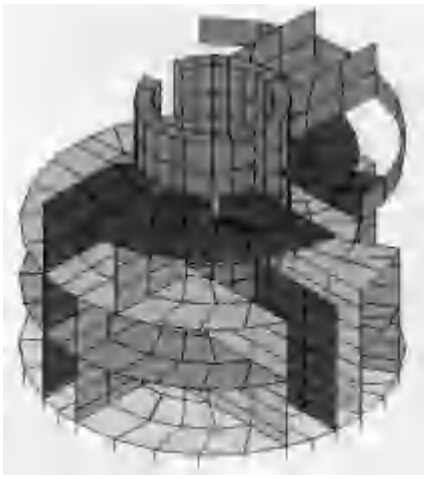

Figure 23 ADS Nuclear Island – ANSYS 3-D Finite Element Model - Structures inside Reactor Wall

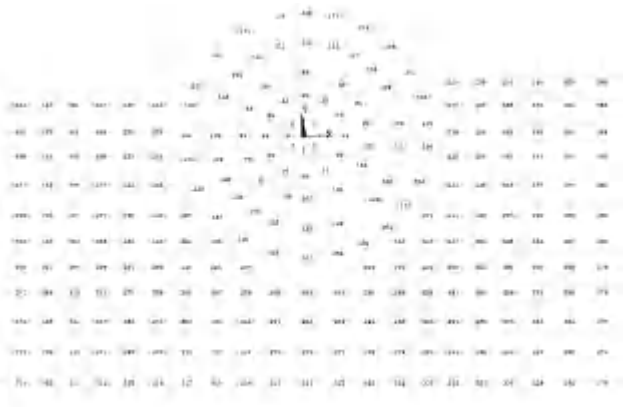

Figure 24 Considered Layout of Isolating Devices

3.2 Choice of Isolators

Two types of isolators were investigated in the dynamic analysis of the ADS buildings:

a) HDS.A900, with K_h = 1.25 kN/mm

b) HDH.A800, with K_h = 3.45 kN/mm,

K_h being the horizontal stiffness at 100% shear strain [2].

HDS (HDH) isolators are made from a soft (hard) compound rubber. The choice of HDS.A900 and HDH.A800 is related to the need of keeping the maximum vertical load on each isolator under the specific nominal limit, for each load combination taken into account: in this case, the combined maximum vertical load is given by the dead load plus the vertical component of the earthquake load (which is not reduced by the 2-D devices here investigated).

From the non-isolated building modal analysis, the maximum vertical acceleration associated to the global vertical mode is about 4.33 m/s^2 (in the most pessimistic case of soft soil, with 97.5% of the overall mass answering at the first vertical frequency of 2.64 Hz): in this case, with a downward seismic vertical excitation, the total vertical acceleration, to be conservatively applied to the whole building, is thus 9.81+4.33=14.14 m/s^2. As the overall building mass is 106150 t, the total vertical load to be supported by isolators is thus 106150·14.14 ≅ 1500 MN (in the worst case).

Assuming an isolator layout as shown in Figure 24 (an isolator at each of the upper basemat 267 nodes, underlying main walls of reactor and auxiliary buildings) with a uniform load distribution, the average load on isolators is thus:

$1500000/267 \cong 5620$ kN (conservative evaluation).

Isolators referred to as HDS.A900 and HDH.A800 have maximum allowed vertical loads of 7700 and 7500 kN, respectively (see Table 1a and 1b), thus ensuring a 30% margin or more. However, for the considered buildings, these isolators should be equipped with the fail-safe system above mentioned (see § 2.2).

3.3 Evaluation of the Isolation Frequency

For both selected types of isolator, the first-approach theoretical isolation frequency is evaluated by the horizontal stiffness at 100% shear strain:

a) for isolators HDS.A900, $f_i=(\sqrt{(K/M)})/2\pi \cong 0.28$ Hz, where $K=K_h \cdot N=1.25 \cdot 267 \cong 334$ kN/mm and $M \cong 106150$ t;

b) for isolators HDH.A800, $f_i \cong 0.47$ Hz, with $K=K_h \cdot N=3.45 \cdot 267 \cong 921$ kN/mm.

The actual dynamic response of the isolated building is checked by the ANSYS model, which includes the simulation of the isolator stiffness: spectral analysis results show that main calculated frequencies for selected isolators are in very good agreement with above theoretical values (see Table 2).

Table 2. Most Significant Response Parameters for Selected Isolators

Isolator Type	Total Rubber Thickness $\mathbf{T_e}$(mm)	Horizontal Stiffness $\mathbf{K_h}$(kN/mm)	Isolation Frequency $\mathbf{f_i}$(Hz)	Average Displacement $\mathbf{d_h}$(mm)	% Shear Strain $\mathbf{100 d_h/T_e}$	Efficient Stiffness $\mathbf{K_h'}$(kN/mm)
HDS.A900	204	1.25	0.28/0.30	120.7	59.2	3.45
HDH.A800	204	3.45	0.46/0.49	86.9	42.6	5.40

Table 2 also reports the average displacements at the isolator locations and corresponding shear strains from maximum and minimum SRSS horizontal displacements (combined along X and Y) at isolator top faces, as issued by ANSYS for a 3-D earthquake load combination (it is to be noted that horizontal displacements of an isolated building are uniform only in the ideal case of an isolator stiffness centre on the vertical projection of the global centre of mass, in which case the torsion mode is not excited). We observe that in a case like this, in which, due to isolation, nearly 100% of the building mass participates to a single mode (in both X and Y directions), a first approach value of the horizontal displacement due to earthquake may be obtained from the first mode displacements (by combining X and Y contributions). This is not completely true for the considered building, as a little error is brought about by an interaction between the first mode along Y and the torsion mode (see Sect. 3.5).

As the shear strain is lower than the assumed 100%, an iterative process should follow to achieve convergence between the assumed stiffness and the resulting shear strain (linked by the non-linear relationships of Figures 7 and 8).

This is done by a simplified by-hand approach through following steps:

a) an efficient stiffness K_h' is drawn from diagrams giving the stiffness variation of the considered isolators with the shear strain percent (Figures 7 and 8);

b) a corrected value of isolation frequency (f_i') is evaluated from K_h', by assuming a constant mass participation to horizontal modes (same "M" in equation for f_i): this is true in cases like this, with isolation frequencies far from soil/structure interaction frequencies (as shown in Sect. 3.5);

c) a corresponding new value of horizontal displacement (δ_h') may then be estimated from equation:

$$\delta_h = a_s / \omega_i^2 \qquad (1)$$

where $\omega_i = f_i/2\pi$ is the isolation pulsation (rad/s) and a_s the corresponding spectral acceleration;

d) subsequent iterations of above substeps provide new values of efficient stiffness, isolation frequency and shear strain for each considered isolator, until a satisfactory convergence is reached.

It should be observed that above calculations are referred to a building on hard soil, but main issues are the same for any soil stiffness: in particular, the isolation frequency is not affected by the soil, as, for any soil, the global horizontal stiffness of the isolating devices proves far lower than the global soil stiffness [5]. The only effect to be taken into account is related to different free-field spectra associated to different soils: it is observed that, at frequencies below 0.6Hz, EUR spectra for soft soils are higher than those for medium or hard soil, thus inducing higher shear strain and lower isolator stiffness. This is shown in Tables 3 and 4, which resume main results of the by-hand estimation of the efficient behaviour of selected isolators on different soils.

Table 3. Actual Dynamic Behaviour of Selected Isolators on Medium/Hard Soil

Isolator Type	Efficient Shear Strain (%)	Efficient Stiffness K_h'(kN/mm)	Efficient Isolation Frequency f_i'(Hz)	New Shear Strain (%)	New Horizontal Stiffness K_h"(kN/mm)	New Isolation Frequency f_i"(Hz)	Final Shear Strain (%)
HDS.A900	46.2	3.45	0.47	~46.0	~4.1	~0.51	~46.
HDH.A800	39.4	5.40	0.59	~40.5	~5.7	~0.60	~41.

Table 4. Actual Dynamic Behaviour of Selected Isolators on Soft Soil

Isolator Type	Efficient Shear Strain (%)	Efficient Stiffness K_h'(kN/mm)	Efficient Isolation Frequency f_i'(Hz)	New Shear Strain (%)	New Horizontal Stiffness K_h"(kN/mm)	New Isolation Frequency f_i"(Hz)	Final Shear Strain (%)
HDS.A900	77.6	2.40	0.40	~77.0	~2.4	~0.40	~77.
HDH.A800	73.0	4.20	0.52	~70.0	~4.3	~0.53	~70.

3.4 Verification of the Isolating System

The isolating devices should meet the following criteria [6], [7]:

a) the differential displacement between top and bottom of isolators, due to seismic load, should not exceed 3 T_e;
b) the distance between the vertical projection of the global centre of gravity and the isolator centre of stiffness should be less than $0.05D_{max}$, D_{max} being the maximum horizontal dimension (in this case $0.05D_{max} \cong 3.85$ m);
c) no tension load is allowed on any isolator for any load combination due to deadweight, earthquake or accidental load (verification against the uplift);
d) the overall mass associated to considered modes in the spectral analysis for horizontal excitation should not be less than 90% of the total building mass.

The above criteria are all fulfilled in the considered application, as:

a) from the calculated maximum displacements, we may observe that even in the case of soft compound isolators on soft soil, the maximum shear strain is below 100% (displacements less than T_e);
b) the eccentricity associated to the assumed isolator layout is about 1.46 m < 3.85 m (from ANSYS model);
c) a simplified approach may be used in this case for the uplift verification, showing that the eccentricity of the resultant earthquake load in the worst case (for an upward directed vertical component of seismic excitation) is well inside the basemat ellipsis of inertia; in the most pessimistic case (for a soft soil):

$e_x = M_y / N = 238690/56028 \cong 3.346$ m < 1/6 $L_{x\,min} \cong 12.83$ m

$e_y = M_x / N = 71334/56028 \cong 1.273$ m < 1/6 $L_{y\,min} \cong 6.17$ m,

where e_x (e_y) are the eccentricities along X (Y), M_x (M_y) the rocking moments around X (Y), N the minimum vertical downward load on foundations, $L_{x\,min}$ = 77 m, the minimum basemat length along X, and $L_{y\,min}$ = 37 m, the minimum basemat length along Y;
d) the overall mass associated to the significant modes retained for the seismic analysis proves very close to 100% of the total building mass on isolators.

3.5 Seismic Isolation Main Effects

Table 5 resumes main issues of the ADS building modal analysis in the case of non-isolated foundations and for both considered types of isolation (HDS or HDH isolators on hard soil). Lines 1 and 2 of table give frequency and mass participation of horizontal vessel modes (very close to the expected target value of 4 Hz to which the vessel beam model was adjusted): it should be pointed out that vessel frequencies are far from those associated to global building modes for any type of foundations, but for foundations on medium soil. In this case, a significant dynamic coupling between vessel and connected reactor building is to be expected: this is confirmed by the increase in the effective mass (about 13000 t) participating to the first vessel mode along X (at 3.89 Hz), with respect to the vessel mass (2700 t).

Results also show that the first global modes for non-isolated foundations are mainly rocking modes, whereas in the case of seismic isolation they are associated to horizontal pure translation movements (see Figures 25 and 26); the torsion mode is only significant in the case of basemat on isolators (in this case, the torsion movement is essentially associated to the global mode along Y, due to the higher eccentricity along X, see § 3.4). The maximum horizontal displacements evaluated at the foundation level were about 157 mm for HDS isolators and 105 mm for HDH isolators (in the case of classical foundations, corresponding maximum displacements were about 30 mm).

The major effect of isolating devices on the building seismic response is the drastic reduction of floor accelerations.

Table 5. Frequency (Hz) and Participating Mass(t) of Main Vibration Modes

Dominant Direction	Soil-Structure Interaction						Seismic Isolators			
	Hard Soil		Medium Soil		Soft Soil		HDS		HDH	
	Freq.	P. M.	Freq.	P. M.	Freq.	P. M.	Freq.	P. M.	Freq.	P. M.
Vessel XX	3.94	2567	3.89	13031	4.07	2485	4.01	0.05	4.01	0.4
Vessel YY	3.95	2843	4.01	2345	4.11	2900	4.00	0.05	4.00	0.4
Global YY	6.92	61302	3.56	65617	1.26	67952	.277	79293	.460	79490
Global XX	8.52	66286	4.79	65094	1.63	79581	.282	104911	.468	104897
Torsion	10.80	4193	6.59	170	2.31	28	.296	25927	.492	25726
Vertical	16.77	39998	7.94	102868	2.64	103457	16.29	57644	16.29	57624

This effect is shown by Figures 27 thru 32, which give the floor acceleration response spectra calculated at the elevation of the main vessel support structure in the considered cases (non-isolated or isolated foundations, taking into account both selected isolators) for seismic horizontal excitations. Figures show that, in the case of basemat on seismic isolators, the spectral horizontal accelerations are drastically reduced (as expected due the low frequencies observed for main building modes) with respect to corresponding accelerations evaluated in the case of a non-isolated building. The comparison is performed for foundations on hard soil, but a similar effect could be observed for any soil: it may be observed that for medium/hard soils the most efficient isolation is obtained with HDS isolators.

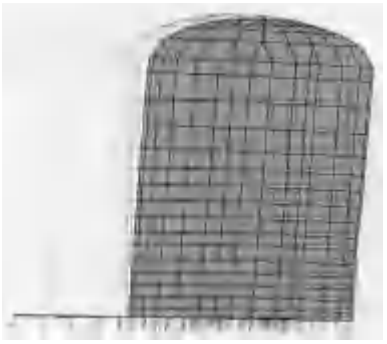

Figure 25 –YY Main Mode without Isolation (6.92 Hz)

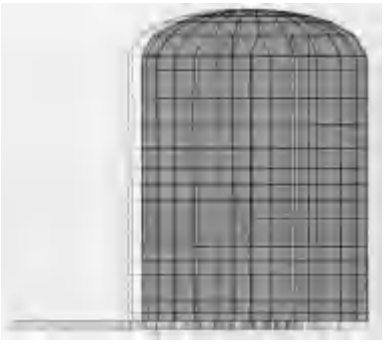

Figure 26 –YY Main Mode with Isolation (0.46 Hz)

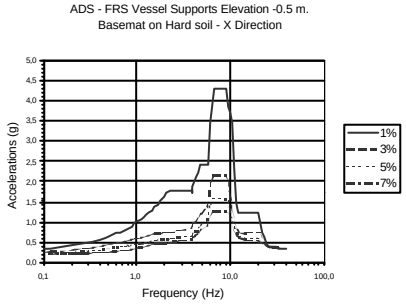

Figure 27 – XX FRS without Isolation

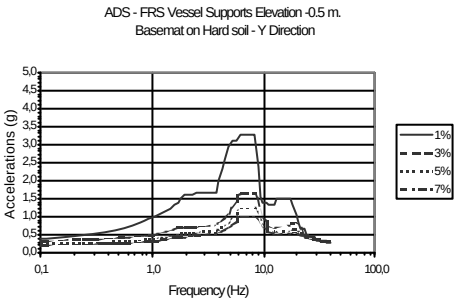

Figure 28 – YY FRS without Isolation

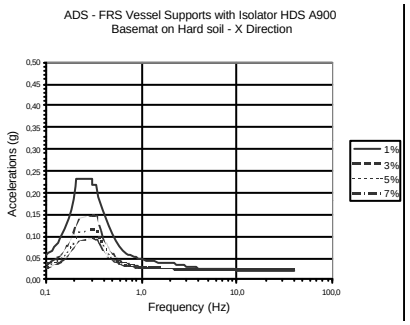

Figure 29 – XX FRS with HDS.A900

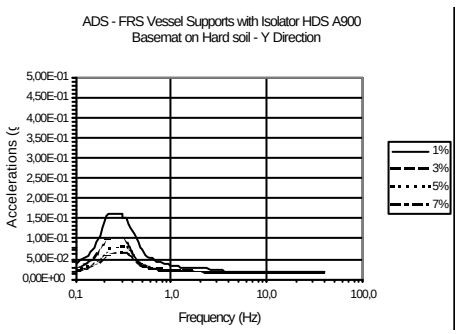

Figure 30 – YY FRS with HDS.A900

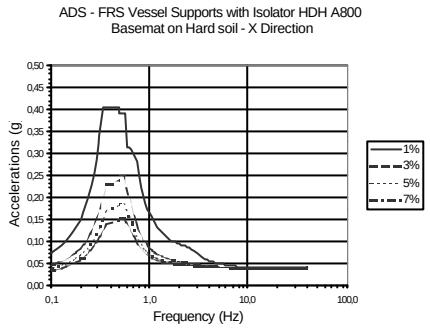

Figure 31 – XX FRS with HDH.A800

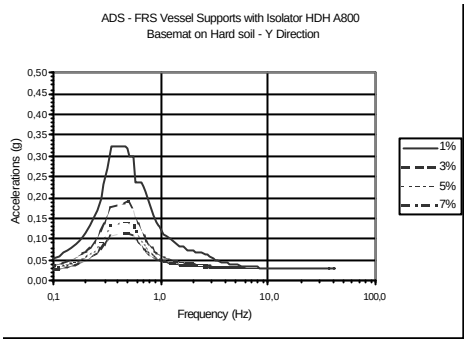

Figure 32 – YY FRS with HDH.A800

4. SUMMARY AND CONCLUSION

The present investigation on the ADS NI building response under earthquake load has confirmed that the use of aseismic isolating devices moves global horizontal modes into the low frequency range, thus drastically reducing soil/structure interaction effects under a typical free-field seismic excitation, in particular, as far as accelerations at building floors are concerned.

The higher horizontal displacements induced on the building as a rigid body motion are not likely to create any significant problems at existing connections in a proper design.

Existing criteria for the global verification of the isolation system are also fulfilled.

As a concluding remark, an isolated nuclear island appears as the most adequate choice whenever the main component design is governed by the seism-induced loads.

5. ACRONYMS

ADS	Accelerator Driven System	NI	Nuclear Island
EUR	European Utility Requirements	SRSS	Square Root of the Sum of the Squares
FRS	Floor Response Spectra	SSE	Safe Shutdown Earthquake
HDRB	High Damping Rubber Bearing	SSI	Soil Structure Interaction
HDS (HDH)	Soft (Hard) Compound HDRB	ZPA	Zero Period Acceleration

6. ACKNOWLEDGEMENTS

Ph. D. Marco Battaini of ALGA Technical Department, Milano, for the useful information and photographs provided about the HDRB Isolator and its applications.

7. REFERENCES

1. Marioni, A., *Jornadas Portuguesas de Engenharia de Estruturas*
Lisboa, LNEC, November 25 to 28, 1998
2. *Catalogue High Damping Rubber Bearing*
Algasism HDRB – 20123 Milano, I.
3. *ANSYS – Engineering Analysis System – Revision 5.2*
Swanson Analysis System Inc. August 31, 1995
4. ASCE 4-86 ASCE Standard September 1986
Seismic Analysis of Safety Related Nuclear Structures and Commentary on Standard for Seismic Analysis of Safety Related Nuclear Structures
5. ANSALDO Document ADS 2 TCLX 0202 Rev.0
Calculation Report – NI Buildings – Seismic and Static Analysis
6. *Linea guida per progettazione, esecuzione e collaudo di strutture isolate dal sisma*
Ingegneria Sismica, Anno XIV, N. 1, Gennaio-aprile 1997
Pubblicazione autorizzata dal Consiglio Superiore dei LL.PP.
7. *Extension of the Available Design Guidelines for Seismically Isolated Nuclear Power Plants to 3-D Systems Developed in the Russian Federation and Rolling Ball-Dissipative Layer System Final Report July 1998*
Contract B7-6340/95/001169/MAR/C2 between the European Atomic Energy Community and ENEA.

Design Method of Vertical Component Isolation System

Seiji Kitamura[1] and Masaki Morishita[1]

1)Japan Nuclear Cycle Development Institute, Japan

ABSTRACT

A structural concept of a vertical component isolation system for fast reactors, assuming a building adopting a horizontal base isolation system, has been studied. In this concept, a reactor vessel and major primary components are suspended from a large common deck supported by isolation devices consisting of large coned disk springs. A determination method of optimal vertical isolation characteristics, case studies of vertical isolation device and plant layout are shown in this paper.

1. INTRODUCTION

Although the horizontal component of an earthquake ground motion is sufficiently reduced by base isolation with laminated rubber bearings, the vertical component is transmitted directly. If three-dimensional isolation were achieved by adding a vertical isolation system, it would substantially enhance plant economy and safety. In order to realize a three-dimensional isolation system, two types of systems can be considered. One is a three-dimensional base isolation system, and the other is a combination of base horizontal isolation and component vertical isolation. By emphasizing the following tow points, the authors chose the latter system. The first point is that excessive rocking response doses not take place in native in the latter system, because the offset between the center of gravity and the isolation support position of the support structure can be made small. The second point is that vibration characteristics of each isolation system become simple by separating the isolation direction. The authors proposed a structural concept called "common deck isolation system", in which a reactor vessel and major primary components are suspended from a large slab structure (common deck) [1]. This common deck is supported by a couple of vertical isolation devices. The followings are considered as functional requirements for the device. The heavy weight of the installation structure should be supported, and simultaneously, a longer vertical period should be attained. It has high rigidity for degrees of freedom except for vertical direction. Assumed failure modes are not catastrophic. A coned disk spring with metallic material was chosen as vertical isolation device as it satisfies these requirements. Disk springs can be stacked in various configurations. They are adjustable to the specified load and/or deflection.

To show the feasibility of the concept of the common deck isolation system, a determination method of optimum isolation characteristics (isolation frequency and damping), case studies of the isolation device and plant layout are presented in this paper.

2. OPTIMAL VERTICAL ISOLATION CHARACTERISTICS

2.1 Method

In the vertical isolation system, it is most important to satisfy simultaneously, the reduction in the response acceleration by lengthening the period of the dynamic response of the system and the control of the response displacement. Generally, the response acceleration decreases as the isolation frequency is lowered, while the relative displacement increases. Then, a series of parametric survey by following procedures was made to identify an appropriate range of isolation frequency and damping value necessary

for vertical isolation. The procedure takes three steps (see Fig.1).

1) Input earthquake motion

Since effective isolation characteristics would be obtained for various seismic waves, three kinds of observed waves and three kinds of artificial seismic waves were chosen. The response spectra of each seismic wave with 5% damping are shown in Fig. 1.

2) Vertical response of base isolated reactor building

A series of vertical response analyses for a typical base isolated reactor building was carried out, and the acceleration response time histories at the vertical isolation device level were obtained. Soil conditions are considered ranging from a soft rock site with shear wave velocity (Vs) of 700m/sec to a hard rock site with Vs=2000m/sec.

3) Response analysis of vertical isolation system

Using a single degree of freedom model, a series of earthquake response analyses of vertical isolation system is carried out; and the maximum response acceleration and relative displacement were calculated. The natural frequency of the components supported by the deck is assumed to be 10Hz. As the measures representing the response of the component, the maximum value of acceleration response spectrum with 1% damping in the range of 5Hz to 12Hz was obtained.

2.2 Analysis

As analytical models for the vertical isolation system, a linear and a nonlinear model were used.

At first, a series of analyses using the linear model was carried out in order to identify appropriate ranges of isolation frequency and damping value necessary for vertical isolation. The ranges of isolation frequency 0.8Hz to 2.5Hz and damping ratio 2% to 60% were examined.

Next, in order to materialize the design of the coned disk spring, a series of analyses using the nonlinear model was carried out. In the analyses, an isolation system was assumed with the combination between coned disk springs and lead dampers. The restoring force characteristics of the coned disk spring were assumed to be elastic, and that of the lead damper were assumed to be elastic-perfectly-plastic (see Fig. 2). The isolation frequency, determined by the rigidity of the linear spring, was examined in the range of 0.5Hz to 5Hz. As for characteristics of the damper, both the rigidity ratio (the ratio of the rigidity of the damping element to that of the coned disk spring) and the yield ratio (the ratio of the yield load of damping element to the support weight) were given. The ranges of rigidity ratio and yield ratio examined are 1 to 20 and 0.01 to 0.2, respectively.

To identify appropriate vertical isolation characteristics, followings were used: maximum relative displacement of 50mm, normalized acceleration of 0.75, normalized response spectrum between 5Hz to 12Hz of 0.33. Here, the upper limit of relative displacement was set based on the idea that relative displacement of the piping connected the isolation system with non-isolation system in the earthquake would be allowed to the degree equal to thermal expansion. Therefore, the input seismic wave for the analyses adjusted the input level so that the maximum velocity may become an equal value.

2.3 Optimal vertical isolation characteristics

The results of the analyses using the linear model are shown in Table 1. It was found that the appropriate isolation frequency to satisfy all the criteria ranges 0.8Hz to 1.2Hz, as far as the seismic inputs used in this study were concerned. The minimum necessary damping are 15% for 0.8Hz, are 30% for 1.2Hz.

As an example of the result of the nonlinear response analyses, the following are shown: relative

displacement, normalized acceleration, normalized response spectrum for isolation frequency. It respectively shows the case in which the rigidity ratio is made to be constant, and the case in which the yield ratio is made to be constant, Fig. 3 and Fig. 4. When the isolation frequency increases, the normalized acceleration is increased, and the relative displacement is decreased. As the rigidity ratio increases, the normalized acceleration and the relative displacement decrease, and the response spectrum increases for the contrariety. It is proven that the yield ratio shows the tendency equal to the rigidity ratio.

The result of examining the appropriate region is described. To satisfy three conditions for all the seismic inputs used in this study was only the case in which they were 0.8Hz and 1.0Hz at the isolation frequency. The range of the yield ratio and the rigidity ratio is shown in Table 2. As this result, it was proven that appropriate isolation characteristics were obtained by combining the coned disk spring with isolation frequency of 0.8Hz to 1.0Hz with the hysteretic type damper with rigidity ratio of 5 to 6 and yield ratio of 0.06 to 0.07.

3. DESIGN EXAMPLE OF ISOLATON DEVICE AND PLANT LAYOUT

3.1 Isolation device

In order to examine whether the vertical isolation element with optimum isolation characteristics can apply to fast reactor plants, a design of the isolation element was attempted under following conditions: isolation frequency of 1.0Hz, displacement amplitude of 100mm, supported structure weight of 10,000ton. By the following procedures, the isolation element was designed. 1) Ordinary high tensile spring steels such as JIS SUP10 and SUP13 can be used for the coned disk. 2) Outside diameter and thickness of the coned disk are selected considering today's manufacturing performance and future feasibility from the viewpoint of machining and heat treatment. 3) Referring to a Japanese Industrial Standard (JIS) [2], the other geometries, such as inside diameter and dish free height, is determined. 4) Considering spring rate, which obtained the target frequency, and the effective deflection, number of disk springs in series is determined. 5) Considering the total length of a stack, number of disk springs in parallel is determined. 6) The following items are calculated and compared to the permissible value based on the JIS: design stress, fatigue life, relaxation of the coned disk.

An example of the structure of the isolation device is shown in Fig. 5. In this case, the outside diameter of coned disk is 1,000mm, and the thickness is 27mm. One isolation device is constituted, stacking 5 disk springs in parallel and 14 sets in series. The unloaded height of a stack becomes about 2,200mm. Support load per one unit is 260ton, and 37 units will be placed to support the common deck.

3.2 Plant layout

An example of plant layout employing the isolation device for a first reactor plant is shown in Fig. 6 and Fig. 7. Isolation devices were mainly placed in the peripheral of the reactor vessel and in the peripheral part of the common deck. While the space for construction and maintenance was considered, the details of a weight balance, etc. is not considered. There is much room for examination of optimum configuration. Likewise, a farther examination should be done on damping devices placed in the figure in the circumference of the common deck. It was confirmed, however, that the required damping would be obtained by using about 13 lead dampers for 50tonf in the design calculation.

4. CONCLUSION

The earthquake response analyses for the common deck isolation system were performed using a single degree of freedom model, and isolation frequency and damping to obtain the optimum vertical

isolation characteristics were examined. It was shown that effective isolation characteristics were obtained by using the coned disk spring of isolation frequency of 0.8 to 1.0Hz and the damping device with over 20% damping. The isolation device was designed, and in addition, a plant layout employing the isolation device for a first reactor plant was examined. As the result of the study, an outlook for the technical feasibility on the proposed vertical isolation system using the common deck was obtained.

The materialization of isolation device and damping device will be attempted, and the optimization of the plant layout will be examined.

References

1. Morishita M., "A conceptual study on vertical seismic isolation for fast reactor components", Proceedings of SMiRT-13, KH09 (1995)
2. JIS B2706, "Coned disk spring", (in Japanese), 1995

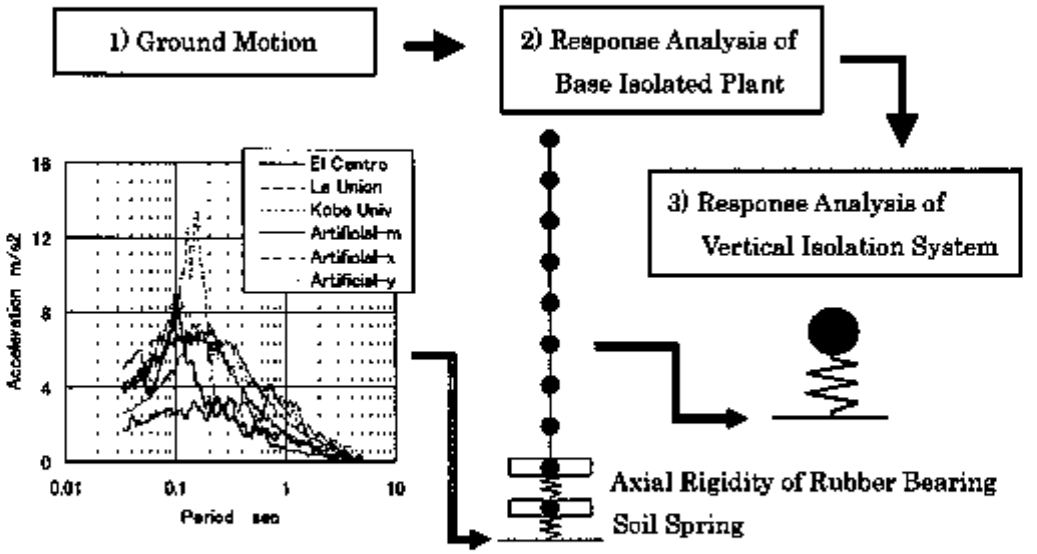

Fig. 1 Survey for optimal isolation characteristics

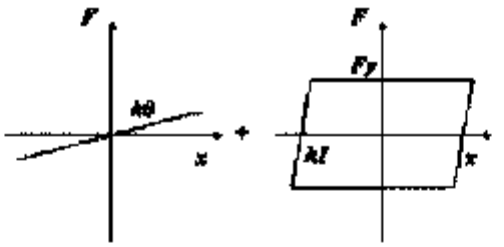

Coned disk spring
rigidity : $k0$

Damping device
rigidity : $k1$
yield force : Fy

- rigidity ratio : $k1/k0$
- yield ratio : Fy/W

W : static weight

Fig. 2 Nonlinear restoring force characteristics model

Table 1 Appropriate isolation characteristics (linear model)

Frequency	Damping ratio %					
Hz	10	15	20	30	40	60
0.8				○	○	○
1.0			○	○	○	○
1.2		○	○	○	○	○
1.5						
2.0						

50mm > Relative displacement

0.75 > Normarized accelelation

0.33 > Normarized respnse spectrum

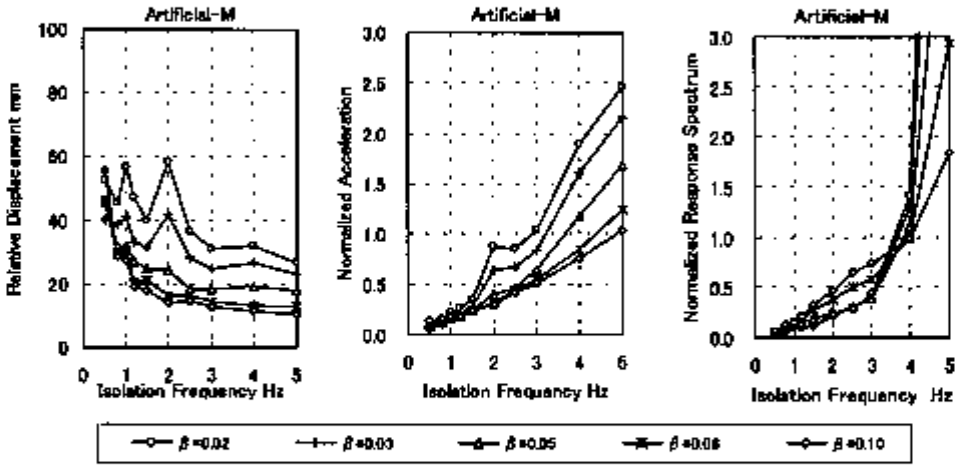

Fig. 3 Results of nonlinear analysis • =5

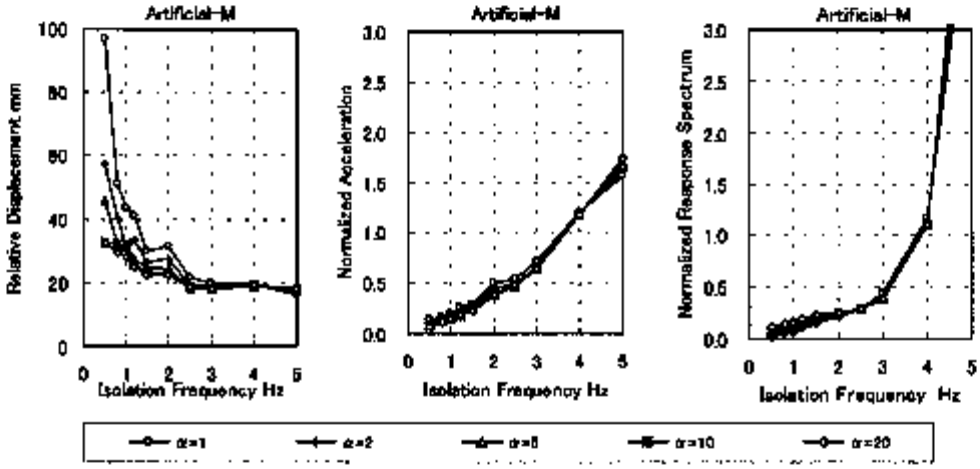

Fig. 4 Results of nonlinear analysis • =0.05

Table 2 Appropriate isolation characteristics (Nonlinear model)

Rigidity Ratio	Isolation Frequency = 0.8Hz							Isolation Frequency = 1.0Hz						
	Yield Ratio β							Yield Ratio β						
α	0.04	0.05	0.06	0.07	0.08	0.09	0.10	0.04	0.05	0.06	0.07	0.08	0.09	0.10
3										○				
4					○	○	○			○				
5			○	○	○				○	○	○	○	○	
6			○	○	○	○			○	○	○			
8		○	○	○	○	○	○		○	○				
10		○	○	○	○				○	○				
15		○	○					○	○					

50mm > Relative displacement

0.75 > Normarized accelelation

0.33 > Normarized response spectrum

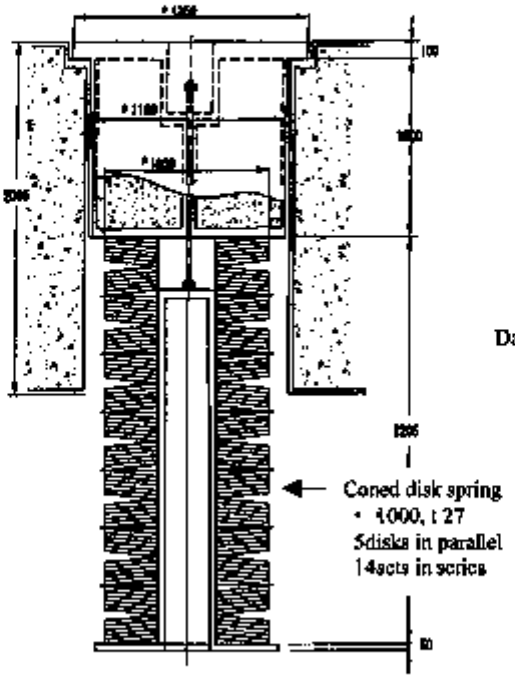

Fig. 5 Design example of vertical isolation device

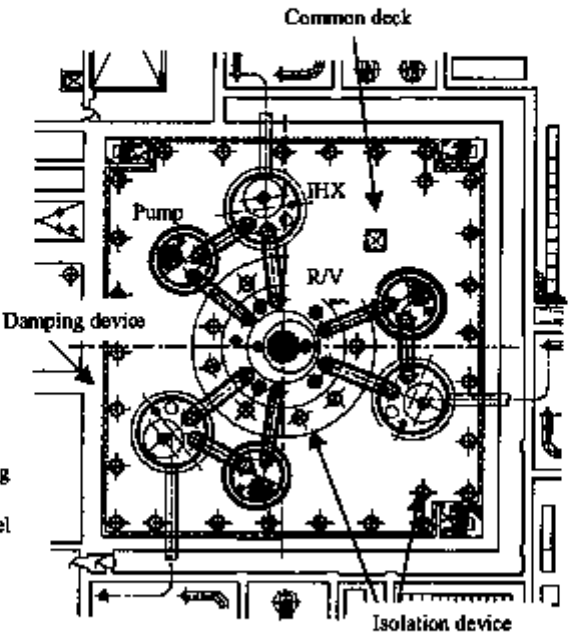

Fig. 6 Examination case of plant layout (plan)

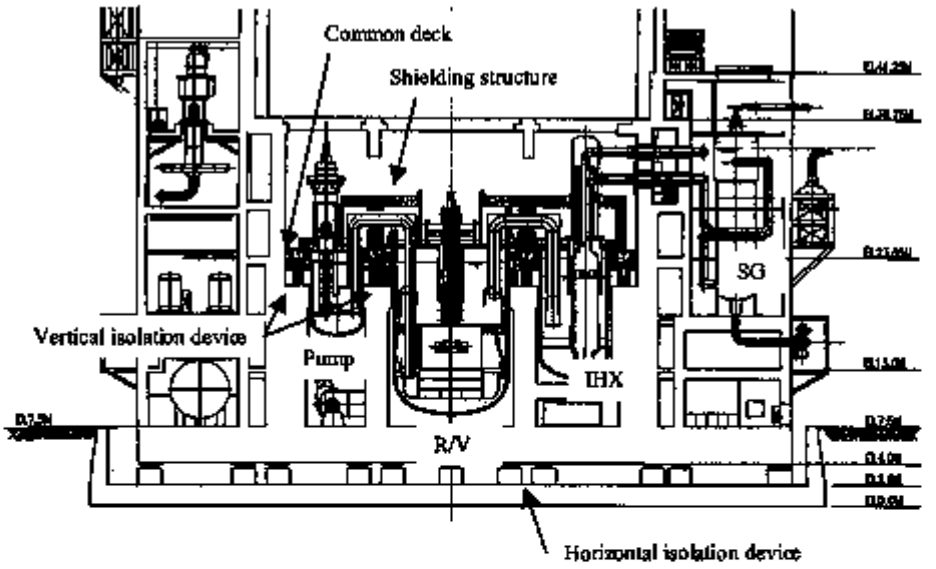

Fig. 7 Examination case of plant layout (elevation)

Aseismic Design of Structure-Equipment Systems Using Variable Frequency Pendulum Isolator

Sinha Ravi[1)] and Murnal Pranesh[1)]

1) Department of Civil Engineering, Indian Institute of Technology Bombay , Powai, Mumbai – 400 076, India

ABSTRACT

Several sliding isolation systems such as friction pendulum system (FPS) have emerged as very useful vibration control systems incorporating isolation, energy dissipation and restoring mechanism in one unit. However, these systems often have practical limitations and are not very effective when the input excitation level is significantly different from the designed level. To overcome these limitations while preserving the advantages, a new system called the variable frequency pendulum isolator (VFPI) has been developed by the authors. The natural period of VFPI varies with horizontal sliding displacement leading to a more robust isolation system. In this paper, it has been shown that isolating a structure using VFPI is very effective for vibration control of structure-equipment and other similar primary-secondary systems. An example five-storey shear structure with equipment mounted at its top has been analysed to demonstrate the effectiveness of VFPI. It is found that VFPI provides better performance compared to other friction isolation systems, and excellent response reduction is observed for a wide range of equipment properties.

INTRODUCTION

Use of base isolation systems has emerged as a very effective technique for aseismic design of structures. In base isolation technique, a flexible layer (or isolator) is placed between the structure and its foundation such that relative deformations are permitted at this level. Since the isolator is flexible, the time period of motion of the isolator is relatively long compared to that of the structure and the isolator time period governs the fundamental period of isolated structure. For properly designed isolation systems, the isolator time period is much longer than those containing significant ground motion energy. As a result, use of isolator shifts the fundamental period of the structure away from predominant periods of ground excitation thereby decreasing the energy introduced into the structure. Extensive review of base isolation systems and its applicability is available in literature [1, 2].

Isolation systems that use a sliding layer incorporate isolation and energy dissipation in one unit since energy is dissipated through friction during sliding. Such systems are very effective in controlling the vibrations of structures due to earthquake and their behaviour is relatively independent of frequency and amplitude of ground motion [3]. However friction systems that use a horizontal sliding surface (Pure-Friction System) typically experience large sliding and residual displacements that are difficult to incorporate in structural design. A modified isolation system called the friction-pendulum system (FPS) has been extensively used in which the sliding and re-centring mechanisms are integrated in one unit and the sliding surface takes a concave spherical shape [4]. The FPS isolators have many advantages over pure friction system; however, severe practical difficulties of aseimsic design using FPS isolator due to its fixed time-period have also been observed [5].

The authors have recently developed a new isolator called the Variable Frequency Pendulum Isolator (VFPI), in which a progressive period lengthening takes place with increase in sliding displacement, and which also has a restoring force softening mechanism [6, 7]. The performance of VFPI has been found to be very good under a variety of earthquake excitations and useful for many different applications [8, 9]. In the present paper, the performance of VFPI for aseismic design of structure-equipment system has been discussed. The basic mathematical formulations of structure and equipment response have also been shown. The response of a multi-storey shear building-equipment system isolated with VFPI has been evaluated for different intensities of earthquake excitations. The results have been compared with the response obtained for fixed base structure, and structure isolated by FPS and Pure-Friction (PF) isolators. It is found that a substantial reduction in the equipment response can be achieved by isolating the structure with VFPI, when compared to other systems.

VFPI GEOMETRY

Consider a rigid block of mass m sliding on a curved surface of any geometry, $y = f(x)$ representing the sliding surface of the isolator. The origin of the surface is at the centre where the sliding displacement is zero. At any instant the restoring force is given by,

$$f_R = mg\frac{dy}{dx} \tag{1}$$

Assuming that this restoring force is provided by an equivalent spring, the spring force can be expressed as the product of spring stiffness and spring deformation. The spring stiffness in turn may be expressed as product of mass and square of isolator frequency. So,

$$f_R = m\omega_b^2(x)x \tag{2}$$

where, $\omega_b(x)$ can be called the instantaneous isolator frequency, which solely depends on geometry of the sliding surface. In case of the FPS that has spherical sliding surface, the isolator frequency is approximately a constant and the restoring force is linear. The geometry of sliding surface of Variable Frequency Pendulum Isolator is derived from the basic equation of an ellipse, with its major axis being a linear function of sliding displacement [6]. The geometry can be represented as

$$y = b\left[1 - \frac{\sqrt{d^2 + 2dx\,\mathrm{sgn}(x)}}{d + x\,\mathrm{sgn}(x)}\right] \tag{3}$$

The slope at any point on the sliding surface is given by

$$\frac{dy}{dx} = \frac{bd}{(d + x\,\mathrm{sgn}(x))^2\sqrt{d^2 + 2dx\,\mathrm{sgn}(x)}}x \tag{4}$$

Defining $r = x\ \mathrm{sgn}(x)/d$ and the initial frequency when $x = 0$ as $\omega_I^2 = gb/d^2$, the instantaneous frequency can be expressed as

$$\omega_b^2(x) = \frac{\omega_I^2}{(1+r)^2\sqrt{1+2r}} \tag{5}$$

In the above equations, parameters b and d completely define the isolator properties. The ratio b/d^2 decides the initial frequency of the isolator and the value of d decides the rate of variation of the isolator frequency. Accordingly the factor $1/d$ is termed as Frequency Variation Factor (FVF). The rate of variation of isolator frequency with sliding displacement is directly proportional to FVF.

The VFPI has two distinguishing characteristics that makes it more effective than the other friction type isolators: (1) The isolator frequency decreases with increase in sliding displacement so as to provide frequency separation between the structure and the excitation and (2) The isolator restoring force has softening mechanism for large sliding displacements which limits the maximum force that is transmitted to the structure during high levels of excitation thereby providing fail-safe mechanism [6, 7].

MATHEMATICAL FORMULATION

The mathematical formulation has been given below for an N-storey shear building isolated by VFPI, although the formulation can be easily extended for general 3-dimensional structures. Due to the action of frictional forces at the sliding surface, the motion consists of two phases namely, non-sliding phase and sliding phase. The equations of motion are different in the two phases and the overall behaviour consisting of a random series of sliding and non-sliding phases is highly non-linear. Depending on the phase of motion, the corresponding equations govern the response of structure and equipment.

Non-sliding Phase

In this phase the structure behaves as a conventional fixed base structure. Due to the frictional resistance there is no relative movement between the base mass and the ground. The equations of motion governing this phase are,

$$\mathbf{M}\,\ddot{\mathbf{x}} + \mathbf{C}\,\dot{\mathbf{x}} + \mathbf{K}\,\mathbf{x} = -\mathbf{M}\,\mathbf{r}\,\ddot{x}_g \tag{6}$$

and

$$\ddot{x}_b = \dot{x}_b = 0 \text{ and } x_b = \text{constant} \tag{7}$$

with

$$\left| \left\{ \sum_{i=1}^{N} m_i(\ddot{x}_i + \ddot{x}_g) + m_b \ddot{x}_g \right\} + m_t \omega_b^2 x_b \right| < m_t \mu\, g \tag{8}$$

In the above equations, **M**, **C** and **K** are the $N \times N$ mass, damping and stiffness matrices of the structure (excluding base mass), respectively, **x** is the vector of relative displacements of the structure with respect to the base mass, x_b is the sliding displacement of isolator, **r** the force influence vector, m_i is the mass of the ith floor, m_b is the base mass and m_t the total mass of the structure (Fig. 1). The coefficient of friction is given by μ and the dots indicate derivative with respect to time. The left-hand side of Eq. (8) is the absolute value of sum of the total inertia force and the restoring force at the isolator level and the right hand side is the frictional force that must be overcome for sliding motion to take place.

Sliding Phase

The structure starts sliding when the forces on the system exceed the static frictional force leading to motion of the base mass. The structure now has one additional degree-of-freedom. The equations of motion are given by,

$$\mathbf{M}\ddot{\mathbf{x}} + \mathbf{C}\dot{\mathbf{x}} + \mathbf{K}\mathbf{x} = -\mathbf{M}\mathbf{r}(\ddot{x}_b + \ddot{x}_g) \tag{9}$$

for the structure, and

$$\left[\sum_{i=1}^{N} m_i(\ddot{x}_i + \ddot{x}_b + \ddot{x}_g) \right] + m_b(\ddot{x}_b + \ddot{x}_g) + m_t \omega_b^2 x_b + m_t \mu g \,\mathrm{sgn}(\dot{x}_b) = 0 \tag{10}$$

for the base mass; where, $\mathrm{sgn}(\dot{x}_b)$ is the signum function, which assumes a value of $+1$ for positive sliding velocity and -1 for negative sliding velocity. This value is determined from the sign of the sum of total inertia force and isolator restoring force given below [5].

$$\mathrm{sgn}(\dot{x}_b) = -\frac{\left[\sum_{i=1}^{N} m_i(\ddot{x}_i + \ddot{x}_b + \ddot{x}_g) \right] + m_b(\ddot{x}_b + \ddot{x}_g) + m_t \omega_b^2 x_b}{\left| \left[\sum_{i=1}^{N} m_i(\ddot{x}_i + \ddot{x}_b + \ddot{x}_g) \right] + m_b(\ddot{x}_b + \ddot{x}_g) + m_t \omega_b^2 x_b \right|} \tag{11}$$

The value of signum function remains constant in a given sliding phase. The end of a sliding phase is governed by the condition that the sliding velocity of the base is equal to zero, i.e.,

$$\dot{x}_b = 0 \tag{12}$$

As soon as Eq. (12) is satisfied, Eq. (6) and (7) corresponding to the non-sliding phase are to be used to evaluate the response quantities and check the validity of inequality in Eq. (8). This decides whether, during the next time step, the structure continues in the sliding phase or enters a non-sliding phase.

RESPONSE OF ISOLATED STRUCTURE-EQUIPMENT SYSTEMS

Many structures support sub-structures or secondary systems and equipments whose safety and functional integrity during earthquake ground motions is essential. A low-mass secondary structure responds to the acceleration of its supporting floor similar to response of primary structure to ground excitations. The floor accelerations at the support points of the secondary system are typically narrow-banded due to filtering effect of the structure. As a result, the response characteristics of secondary systems are strongly influenced by their dynamic properties relative

to those of the primary structure, such as frequency ratio (ratio of frequency of secondary system to the fundamental frequency of the primary system), mass ratio (ratio of mass of the secondary system to the mass of the primary system) and damping in the secondary system [10]. The secondary systems exhibit highly amplified responses when the frequency ratio is nearly equal to unity. Isolating the primary system changes the dominant frequency of excitation at the base of the secondary system as well as reduces excitation amplitude.

In the present investigations the response of a light equipment mounted on top of an example shear structure has been considered. The structure consists of a five-storey shear building (excluding base degree of freedom), 5m square in plan (Fig. 1). The storey stiffness has been taken as 112600 kN/m, and the floor mass has been chosen such that the fundamental frequency of the fixed-base structure is close to the predominant frequency of El Centro ground motion (approximately 2.0 Hz). The different storeys, including the base mass, have equal mass of 60080 kg. The investigations are carried out for El Centro ground motions with two different scaling or intensity factors: (1) intensity factor of 1.0, i.e. original recorded ground motion, and (2) intensity factor of 2.0, i.e. accelerations intensified by a factor of 2 to represent very high intensity earthquake. The natural frequencies and effective modal mass of the fixed base structure and the structure isolated by VFPI are shown in Table 1. It should, however, be kept in mind that frequencies of a structure isolated by VFPI change continuously with isolator displacement. The frequencies shown in the Table 1 indicate an upper bound on the frequencies that is obtained when the isolator displacement is zero. A light equipment, that has a mass of 1% of the total mass of the structure (including the base mass), is placed on the top storey. The equipment has been modelled by a mass with linear spring and a damper attached to the top floor of the structure. The structural and equipment damping are both assumed to be equal to 5% of critical damping to eliminate the influence of non-classical damping from this evaluation. The parameters of VFPI are chosen as $b = 0.01$ m, $d = 0.10$ m and FVF of 10 per m so that it has initial time period of 2.0 sec and the frequency reduces very sharply with sliding displacement. The coefficient of friction has been taken as 0.02. The secondary system has a mass of 1% of the total mass of the structure (including the base mass) and is attached to the top storey.

Table 1. Modal properties of fixed base and isolated structure without equipment

Mode Number	Isolator	1	2	3	4	5
Fixed-base – Frequency (Hz)	-	1.96	5.72	9.02	11.59	13.22
Effective Modal Mass (%)	-	87.95	8.72	2.42	0.75	0.16
Isolated – Frequency (Hz)	0.49	3.64	6.92	9.76	11.93	13.31
Effective Modal Mass (%)	99.93	0.07	0.00	0.00	0.00	0.00

Table 2. Peak acceleration (g) of equipment with frequency tuned to the natural frequencies of the isolated structure

Equipment frequency (Hz)	3.73	7.14	10.00	12.50
Structure Isolated by FPS	0.635	0.510	0.368	0.306
Structure Isolated by VFPI	0.440	0.353	0.328	0.262

Time-History Response

The response of structure-equipment system has been obtained by solving Eq. (6) or Eq. (9) depending on the phase of motion. The equipment frequency is chosen as 3.85 Hz since it corresponds to tuning with the second natural frequency of the isolated structure (first frequency is the isolator frequency) and represents the most severe case of tuning. The typical time-history plot of absolute acceleration and displacement of the equipment relative to the floor are given in Fig. 2(a) and (b). It can be observed from the time-history responses that there is considerable reduction in the peak response of the equipment in comparison with both the equipment on fixed-base structure and structure isolated by FPS. It is to be noted that at around $t = 5.5$ s, the response of equipment on structure isolated by PF system is greater than that on a structure isolated by VFPI and FPS isolators. This is possibly due to the stick-slip motions in PF system inducing high frequency response in the structure, which in turn affects the response of equipment. Such motions are minimised in case of VFPI and FPS isolators. However, as expected, the peak equipment response is largest in case of structure isolated by FPS.

The typical time-history for recoverable energy of equipment (kinetic energy + strain energy) [5] is shown in Fig. 2(c). This result gives additional information, which cannot be obtained from the response time-history. From this plot it is observed that the maximum recoverable energy in equipment is considerably reduced when structure isolated by VFPI in comparison to that isolated by FPS. However, as expected, it is higher than that of a PF system. As the absolute kinetic energy has been considered, the effect of rigid body movements is implicitly included, which is manifested through the various peaks in the energy time-history for FPS isolated structure. These peaks are also drastically reduced in case of VFPI and PF systems indicating more stable response of the equipment.

Floor Response Spectra of Equipment

The maximum response of single-degree-of-freedom equipment can be conveniently studied in terms of its floor response spectra. The floor response spectra enable one to evaluate the effectiveness of various isolation systems for secondary systems with different properties.

The displacement and acceleration floor response spectra have been shown in Fig. 3. The effects of structure-equipment interaction, including the effect of equipment on structure, are fully considered in the analysis. The displacement spectra are normalised with respect to the peak displacement of equipment mounted on fixed-base structure (equal to 0.28 m). In case of a fixed-base structure the equipment acceleration response is maximum when the equipment frequency tunes with fundamental frequency of the structure (approximately 1.85 Hz). However for base-isolated structures, the first natural frequency is the isolator frequency, which is much lower than that of both the fixed-base structure and the equipment. So, the possibility of equipment frequency tuning with the isolator frequency is very unlikely and has not been included. The equipment response shows a peak when the equipment frequency is close to the second frequency of the isolated structure. This can be clearly observed from the acceleration spectra (Fig. 3(b)) wherein the peak in FPS occurs at 3.85 Hz, which is close to the second isolated frequency (see Table 1). It is to be noted that the amplification of response due to tuning is almost non-existent in case of VFPI. This is due to variation in frequency of VFPI with sliding displacement, which constantly changes fundamental frequency of the isolated structure. It is further observed that response of equipment mounted on structure with VFPI performs better for the entire range of equipment frequencies. The VFPI is effective even for flexible equipment whereas a conventional FPS shows higher response.

The maximum equipment acceleration when its natural frequency is tuned to the natural frequencies of the isolated structure is shown in Table 2. It has been found that for all frequencies of equipment, the use of VFPI for isolating the structure is more effective in reducing the response than the use of FPS. This is due to the almost constant fundamental period of structure isolated by FPS wherein the structure behaves like a narrow banded filter. On the other hand the fundamental period of a structure isolated by VFPI continuously changes with sliding displacement, making it behave as a wide band filter and providing better vibration control.

The floor-response spectra of recoverable energy for medium and high intensity excitations are shown in Fig. 4. For both excitations there is a substantial reduction in the peak equipment response for VFPI-isolated structure than that for FPS-isolated structure. It is interesting to note that the recoverable energy in equipment on FPS-isolated structure increases with intensity of excitation, whereas the energy in equipment on VFPI-isolated structure and PF isolated structure is relatively independent of intensity. It is also seen that the variation in equipment response with its frequency is very small when the structure is isolated using VFPI. This shows that the performance of secondary system or equipment is relatively independent of the frequency content and amplitude of excitation when structure is isolated by VFPI. The use of VFPI for structure isolation therefore also acts as a very effective device for passive vibration control of secondary systems.

CONCLUSIONS

The mathematical formulation for response of structures isolated using the Variable Frequency Pendulum Isolator (VFPI) has been presented in this paper. The VFPI provides the ability to vary isolation time period with sliding displacement thereby eliminating the possibility of tuning between the structure and isolator or between the isolator and ground motions. The response of equipment mounted on structures isolated using VFPI and other isolators have been evaluated to evaluate the effectiveness of VFPI. Based on this investigation following conclusions can be drawn:

1. The VFPI is a robust isolation device and is very effective in controlling the response of equipment placed on VFPI isolated structure compared to the same equipment placed on structure isolated by other friction isolators.
2. The VFPI is effective in vibration control of equipment with wide range of modal properties.
3. The behaviour of structure-equipment system isolated by VFPI is relatively independent of the frequency content and amplitude of excitation.

REFERENCES

1. Buckle, I. G. and Mayes, R. L., "Seismic isolation: history, application and performance - a world view," *Earthquake Spectra*, EERI, Vol. 6, 1990, pp. 161-201.
2. Naeim, F. and Kelly, J. M., *Design of Seismic Isolated Structures: From Theory to Practice*, John Wiley and Sons, New York, NY, 1999.
3. Mostaghel N. and Tanbakuchi, J., "Response of sliding structures to earthquake support motion," *Journal of Earthquake Engineering and Structural Dynamics*, Vol. 11, 1983, pp. 729-748.
4. Zayas, V. A., Low, S. S. and Mahin, S. A. A simple pendulum technique for achieving seismic isolation, *Earthquake Spectra*, EERI, Vol. 6, 1990, pp. 317-333.
5. Pranesh, M., *VFPI: An Innovative Device for Aseismic Design*, Ph.D. Thesis, Indian Institute of Technology, Bombay, 2000.
6. Pranesh, M., and Sinha, R, "VFPI: an isolation device for aseismic design," *Journal of Earthquake Engineering and Structural Dynamics*, Vol. 29, 2000, pp. 603-627.
7. Pranesh, M. and Sinha, R., "Earthquake resistant design of structures using VFPI," *Journal of Structural Engineering*, ASCE, submitted paper, 2001.
8. Pranesh, M. and Sinha, R., "Aseismic design of tall structures using variable frequency pendulum isolator." *Proc. of 12th World Conference on Earthquake Engineering*, Auckland, New Zealand, Paper No. 284, January 2000.
9. Sinha R. and Pranesh M., "FPS isolator for structural vibration control," *Proc. of International Conference on Theoretical, Applied, Computational and Experimental Mechanics*, Kharagpur, India, December 1998.
10. Igusa, T. and Der Kiureghian, A., "Dynamic characterisation of two-degree-of-freedom equipment-structure system," *Journal of Engineering Mechanics*, ASCE, Vol. 111, 1985, pp. 1-19.

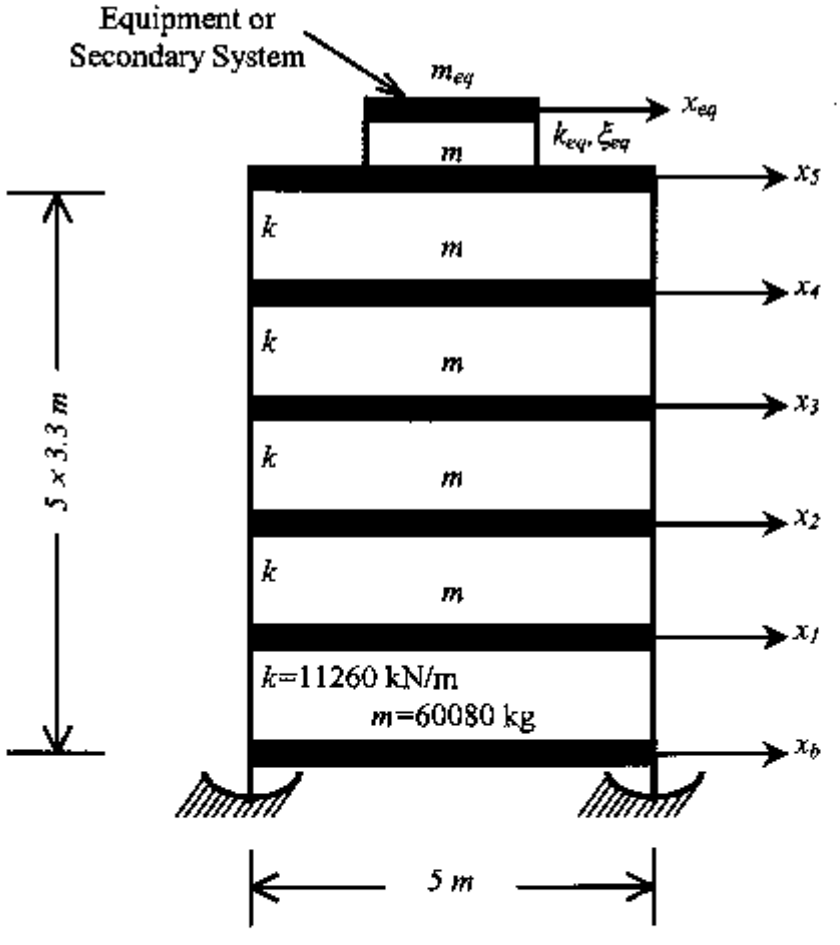

Fig. 1 Example isolated structure-equipment system

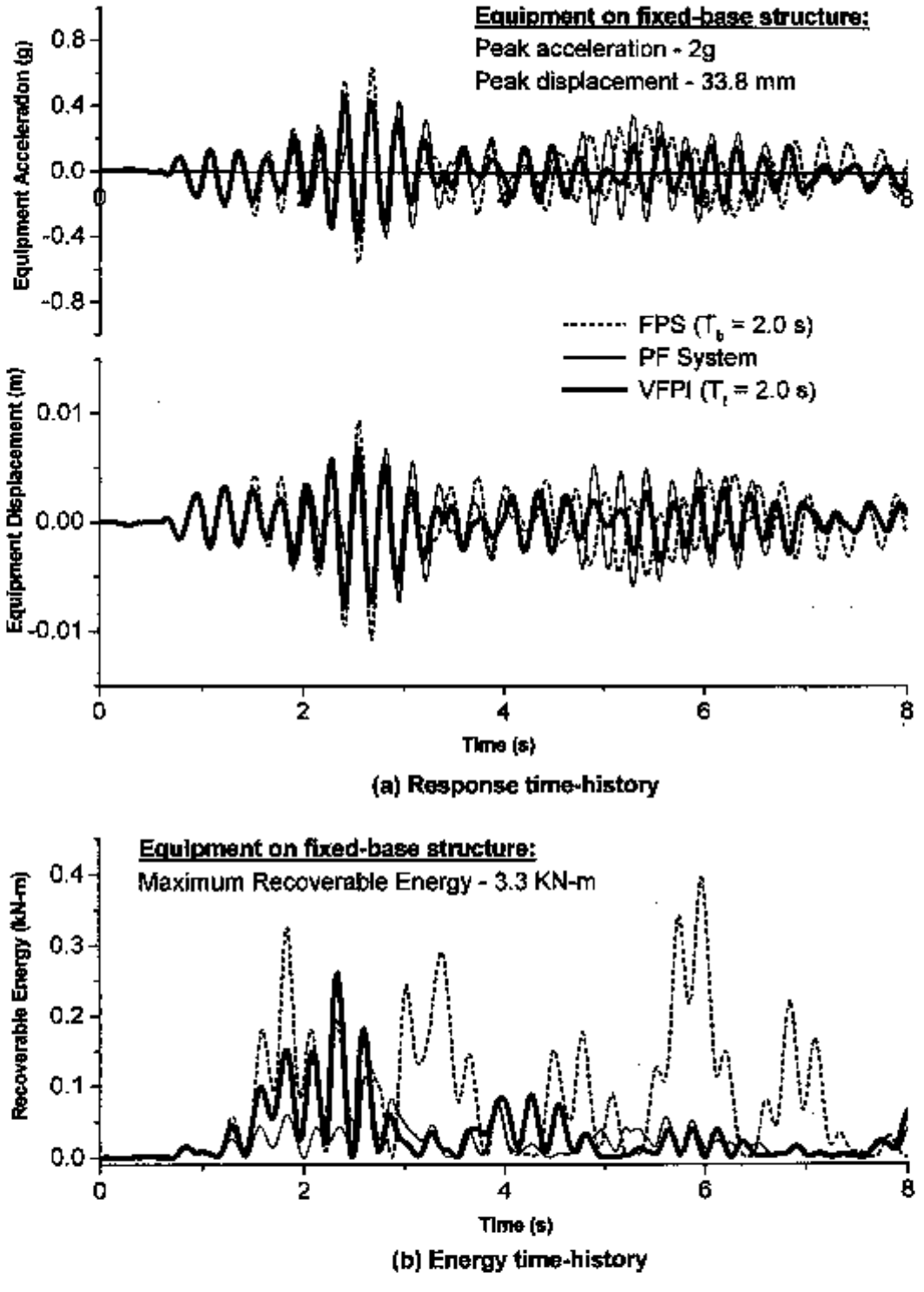

Fig. 2 Typical response and energy time-histories of light equipment mounted on example structure subjected to El Centro 1940 (NS) ground motions

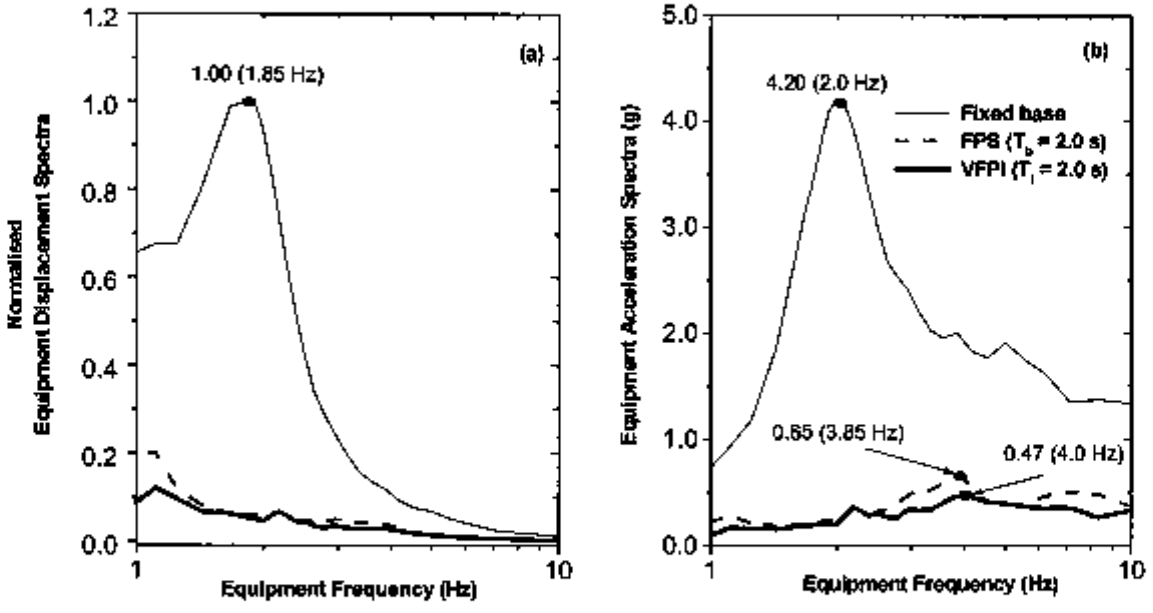

Fig. 3 Floor response spectra for light equipment on example structure subjected to El Centro 1940 (NS) ground motion (m_{eq} = 1%, ξ_{eq} = 5%, μ = 0.02, FVF = 10 per m)

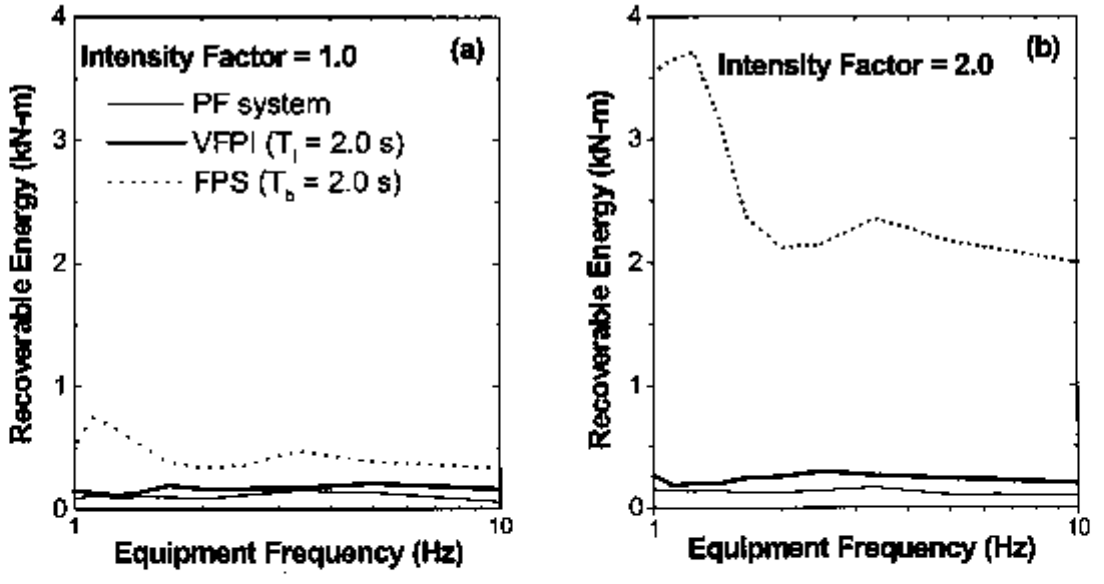

Fig. 4 Effect of earthquake intensity on response of equipment on structure isolated by sliding isolation systems (m_{eq} = 1%, ξ_{eq} = 5%, μ = 0.02, FVF = 10 per m)

Effects of Lead Plug in Lead Rubber Bearings on Seismic Responses for an Isolated Test Structure

Bong Yoo, Jae-Han Lee and Gyeong-Hoi Koo

Korea Atomic Energy Research Institute, Duckjin- Dong 150, Yusong-Ku, Daejon, Korea

ABSTRACT

The effects of lead rubber bearings are investigated by shaking table tests and seismic response analyses for 1/8-scale isolated test structure. A simple analysis model representing the actual dynamic behaviors of the test structure is developed, and the seismic analyses of the simple model are performed for lead rubber bearings with three different diameters of lead plug. The diameter of the lead plug had to be enlarged to increase isolator damping more than 24 % and this causes the isolator stiffness to increase, which results in amplifying the acceleration response of the isolated test structure in the higher frequency ranges with the monotonic reduction of isolator shear displacement.

INTRODUCTION

Much research has been carried out on seismic base isolation to verify the usefulness and to improve the earthquake resistance functions to prevent devastating damages experienced in the last decades. To reduce the seismic responses of both accelerations and relative displacements, the isolation frequency of the structure, which is determined by the stiffness of isolators, should be far away from the dominant frequency range of the earthquake ground accelerations. In parallel, the damping of the isolators implemented by either natural rubber bearings with separate dampers, high damping rubber bearings, or lead plug rubber bearings, should be decided such that it play an important role not to imperil the secondary structures attached to the primary structure of which fundamental frequencies correspond to the dominant frequencies of input motions but to reduce the accelerations and the relative displacements in the whole superstructures. The arguments of damping effects of isolation devices still continued. However there has not been much research that used shaking table tests to evaluate the damping effects of isolation devices in a seismically isolated structure to reduce seismic responses.

This paper reports on the results of shaking table tests performed to verify the damping effects on seismic responses of an isolated test structure with lead laminated rubber bearings (LLRB). The test results are presented to determine the effects on the structure responses according to the size of the lead plug diameter. A simple lumped-mass model is developed based on the modal analysis results from the detail structure model. Time history analyses to simulate test results are performed for the simple model using equivalent viscous damping obtained from the shear and compression tests of the lead rubber bearings. The comparisons between shaking table tests and analyses for the isolated structure are given for an artificial time history excitation in horizontal Y-direction.

The effects of damping and stiffness of the LLRB on the seismic responses of the isolated structure are also discussed with the analysis results.

SHAKING TABLE TEST RESULTS ON LLRBS

The input excitation motions used were Artificial Time Histories(ATH) simulating the acceleration spectrum of US NRC Regulatory Guide 1.60. For the shaking table tests, the artificial time history input motions were reconstructed through the band limited filtering of original data from 0.07Hz to 25Hz. With consideration of the similarity of the 1/8 scaled down system, the time interval of input motions is re-scaled from 0.02 second to 7.07 ms. The isolated test structure is shown in Fig. 1, which is designed to represent the dynamic characteristics of the Korea Advanced Liquid Metal Reactor (KALIMER) building. This model is composed of the rectangular basemat (lower slab,15.5 tons, 4.3m x 4.3m x 0.3m) and four columns (0.5 ton each) supporting the upper slab (5.67 tons). To increase the horizontal stiffness and provide the safety feature to the column structure, X- type crossbars were attached to the columns. The seismic isolators with the diameter of 120mm are 1/8-scaled LRB shown in Fig. 2, and four isolators are installed under the four corners of the basemat. The design isolation frequency is 1.41 Hz at 100% shear strain. The size of the 6 degrees of freedom shaking table used in the test is 4m x 4m, and the shaking capacity is 30 tons [1,2].

Fig. 1 Isolated Test Structure

Fig. 2 Scaled Laminated Rubber Bearings

Characteristic Test Results of LLRB

The hysteretic curves up to 100% shear strain for the LRBs (the natural rubber bearing(NRB) and the LLRB with three different diameters of lead plug) are represented in Fig. 3. The equivalent stiffness and damping for the several strain points are represented in Fig.4.

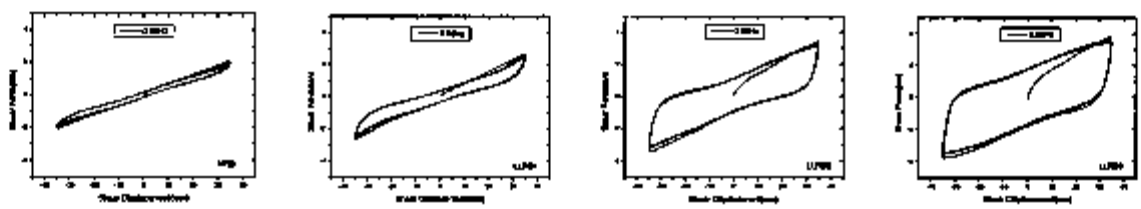

Fig. 3 Shear Strain Hysteresis of 100% Shear Strain for NRB and LLRB (0.05Hz)

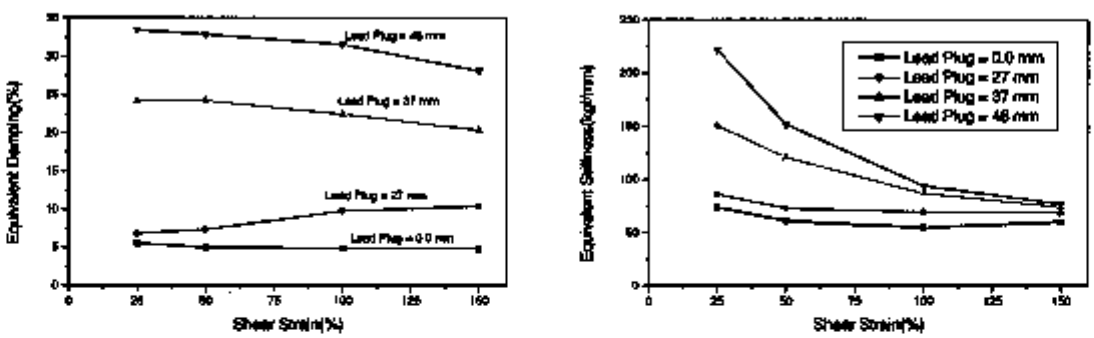

Fig. 4 Equivalent Shear Stiffness and Equivalent Damping of NRB and LLRB (0.05Hz)

Shaking Table Test Results

One of the input excitation motions is shown in Fig. 5. For the excitation levels of 0.372g to 0.439g, the shear

displacement time histories normalized with a 0.412g are represented in Fig. 6. The maximum shear displacement is reduced to 10.4mm from 27mm as the lead plug diameter increase from 0.0 to 48mm. The accelerations on the structure and the shear displacements of lead rubber bearings for the input excitation are affected by the stiffness and damping depending on lead plug diameter of LLRB.

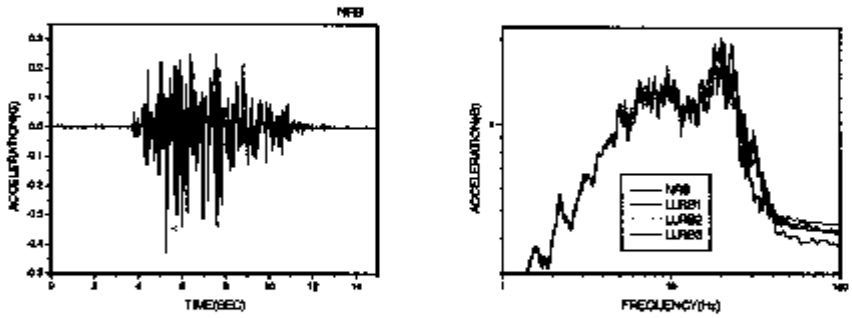

Fig. 5 Acceleration Time History and Response Spectra at Excitation Bed (2% damping)

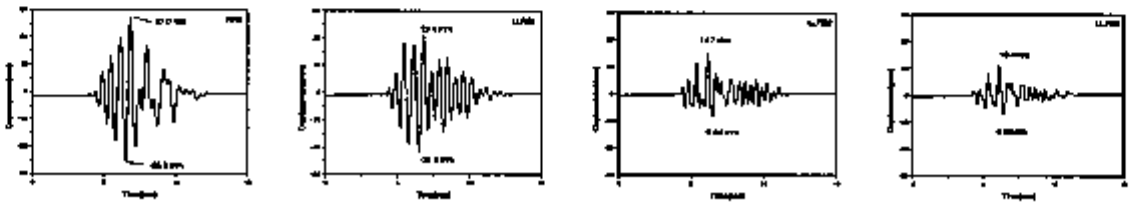

Fig. 6 Time Histories of Isolator Deformation for Input Excitations (ATH, Y-dir, 0.412g)

The equivalent stiffness and damping at the maximum shear displacements obtained from the test are given in Table 1[3]. The reduction in shear displacements for the LLRB is caused by the increases in the stiffness and damping values as the diameter of lead plug increases.

Table 1. Equivalent Damping and Stiffness for LRB Types according to Seismic Excitation

LRB Type	Excitation Input (g)	Diameter of Lead Plug(mm)	Shear Displ. (mm)	Equivalent Damping (%)	Equivalent Stiffness(Kgf/cm)
NRB	0.412	No Lead	27.0 (27.0)*	4.5	600
LLRB1	0.372	27	19.4 (21.5)*	8.0	750
LLRB2	0.439	37	15.7 (14.7)*	24.0	1250
LLRB3	0.426	48	10.8 (10.4)*	33.0	2000

()* : Scaled Values with Input Level of 0.412g

The zero period accelerations(ZPA) on the upper and lower slabs of the isolated test structure for the acceleration level from 0.367g to 0.439g are given in Table 2. The test acceleration response spectra at the upper and lower slabs normalized with 0.412g are represented in Fig. 7. In the test results, the isolation frequency is increased as the lead plug diameter increases; the accelerations in the high frequency content are amplified; and the ZPAs are also increased; but the shear displacement of LRB is greatly decreased from 27.0mm to 10.8mm.

Table 2. Test Response ZPA at Lower and Upper Slab for Input Excitations

LRB Type	Excitation Input (g)	ZPA at Lower Slab (g)	ZPA at Upper Slab (g)
NRB	0.412	0.236 (0.236)*	0.259 (0.259)*
LLRB1	0.372	0.232 (0.257)*	0.256 (0.284)*
LLRB2	0.439	0.280 (0.263)*	0.317 (0.297)*
LLRB3	0.426	0.237 (0.233)*	0.373 (0.361)*

0* : Scaled Values with the Input Level of 0.412g

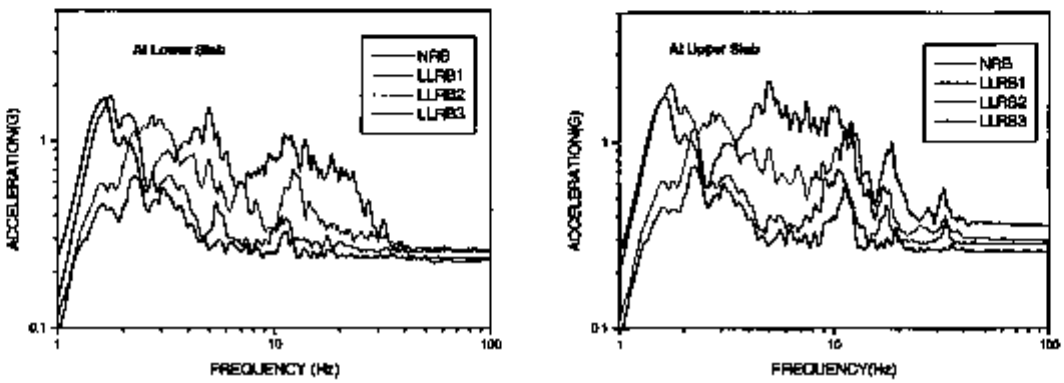

Fig. 7 Test Acceleration Response Spectra(2% Damping) of Isolated Structure (ATH, Y-dir, 0.412g)

SIMPLE ANALYSIS MODEL

To evaluate the influence of isolator damping on the structure responses, a simple analysis model (Fig.8) is developed based on the modal analysis results from the detail analysis model (Fig.9). The detail model accurately represents the dynamic characteristics of the isolated test structure with low viscous damping of about 2%, which is equivalent to no lead plug in LRB. The sample model has 16 nodes and 14 elements for reducing the computation time.

The isolators are modeled by linear spring and dashpot elements. The values for horizontal stiffness and damping are obtained from the shear and compression test results of 495.6Kg/cm and 2% viscous damping at 100% shear strain.

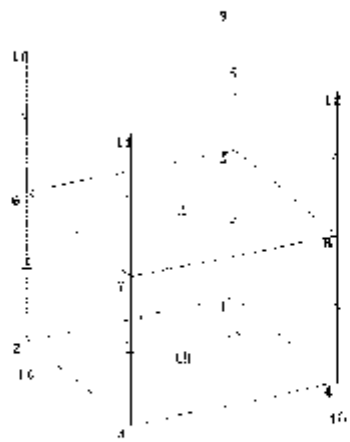

Fig. 8 Simple Analysis Model of Isolated Structure

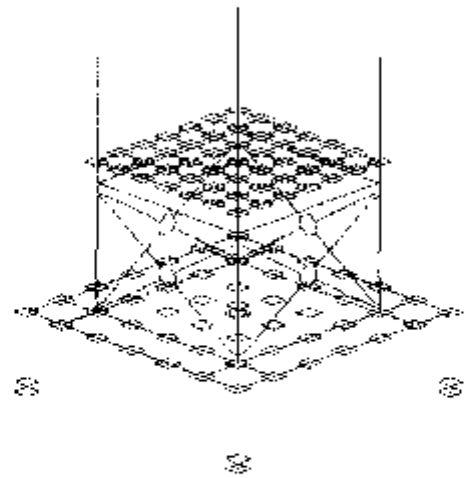

Fig. 9 Detail Analysis Model of Isolated Structure

The freqoencies of the isolated test structure were calculated by the ABAQUS program and are represented in Table 3. The almost effective mass is concentrated at the isolation frequency, but the effective mass of each structural mode is very small. The simple analysis model is compatible with the detail one. The first frequency of the simple model in Y-direction is 11.5Hz is very close to 11.3 Hz of the detail model.

Table 3. Frequency Analysis Results of Isolated Structure Models

	Detail Analysis Model			Simple Analysis Model		
Mode	Frequency (Hz)	Effective Mass (kg)	Participation Factor	Frequency (Hz)	Effective Mass (kg)	Participation Factor
Isolation (X,Y)	1.51	21,613	1.05	1.49	22,317	1.018
Isolation (Z-Rot)	3.20			7.47		
1st (X1)	10.9	2.98	0.058	10.9	2.70	0.0227
2nd (Y1)	11.3	2.69	0.044	11.5	2.26	0.0186
5-th(X2)	25.0	0.008	0.0067	28.8	0.12	0.0006
Cross-bar	9.85	0.028	0.028			

SEISMIC RESPONSE ANALYSES USING SIMPLE ANALYSIS MODEL

Time history analyses were performed using the simple analysis model subjected to the artificial time history earthquake with a time interval of 0.007sec and 15second duration. The structural damping in analysis was assumed to be 2%. Fig.10 and Table 4 show the results of the floor response spectra at the slabs. The analyses results agree well with the test results both spectrum contents and peak accelerations. The calculated ZPA of 0.197g, 0.235g and 0.233g at lower slab with LLRBs are compatible with test results of 0.232, 0.280g and 0.237g. The calculated maximum shear deflections of the LLRBs were in the range of 5.04mm to 27.2mm, which are lower than those of test results for large lead plugs.

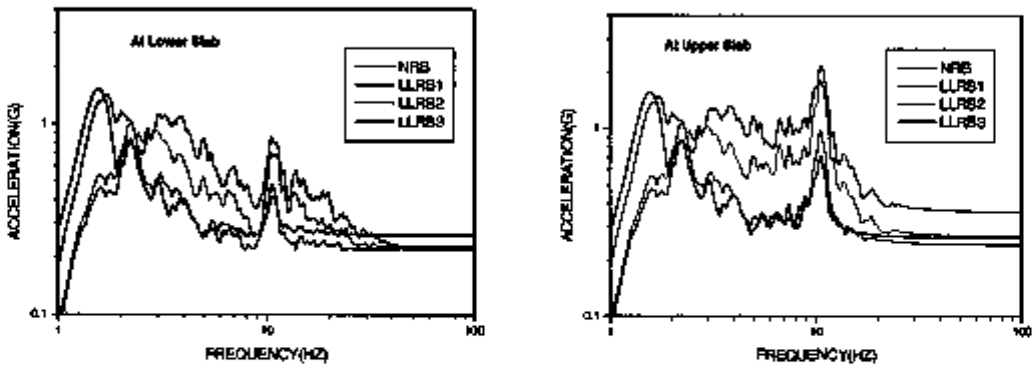

Fig. 10 Analysis Acceleration Response Spectra(2%) of Isolated Structure (ATH, Y-dir, 0.412g)

Table 4. ABAQUS Analysis Response ZPA at Lower and Upper Slabs for Input Excitations

LRB Type	Excitation Input ZPA (g)	Shear Displacement (mm)	ZPA at Lower Slab (g)	ZPA at Upper Slab (g)
NRB	0.412	27.2 (27.2)*	0.259 (0.259)*	0.260 (0.260)*
LLRB1	0.372	15.7 (17.4)*	0.197 (0.218)*	0.216 (0.238)*
LLRB2	0.439	6.84 (6.42)*	0.235 (0.220)*	0.281 (0.264)*
LLRB3	0.426	5.04 (4.96)*	0.233 (0.226)*	0.367 (0.355)*

0* : Scaled Values with the Input Level of 0.412g

The contributions to the acceleration response from the damping and the stiffness of lead plugs are not distinguished. Two parametric studies were performed: one to study the effects of damping and the other to study effects of stiffness of the LRB. The analysis results are represented in Fig. 11.

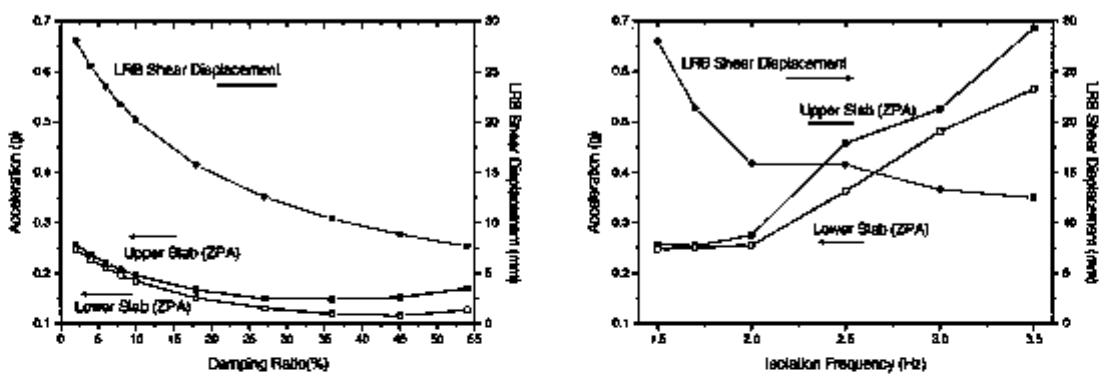

Fig. 11 Accelerations & LRB Deformations According to Damping and Isolation Frequency Variations

When the viscous damping is increased while the stiffness of the LRB is fixed, the ZPA of structure and the shear

deformation of the LRB monotonically decrease until to the damping level of about 35 %. However the ZPA of upper structure increases as increasing the damping more than 35% for upper slab of test structure. When the stiffness is increased while the damping of the LRB is fixed at 2% viscous damping, the response acceleration is increased rapidly, but the shear deformation of LRB is decreased for both cases. When the LLRB are used to reduce the seismic acceleration responses of structures, the diameter of lead plug is a key parameter because it simultaneously impacts on the structural accelerations through two points. One is the acceleration amplification of increased isolation frequency by the increase of stiffness, and the other is the acceleration reduction by the increased damping up to about 35%.

CONCLUSIONS

Test results show that increasing the lead plug diameter results in (1) amplifying the acceleration responses of the isolated test structure in the higher frequency ranges, and (2) rapidly reducing the shear displacement in the isolators.

When LLRBs are adopted to reduce the seismic acceleration response of structure, the diameter of the lead plug simultaneously affects the structural acceleration through two points, one is the acceleration amplification of increased isolation frequency by the increase of stiffness, and the other is the ZPA reduction by the increased damping up to about 35%.

Based upon tests and analyses of the isolated structures, the increased diameter of lead plug above 37mm in the isolator could give an adversary effects on the secondary systems and components attached to the primary structure because the acceleration amplification in high frequency content of the primary structure is notified.

Acknowledgement

This work was performed under the Long-term Nuclear R&D Program sponsored by the Ministry of Science and Technology.

REFERENCES

1. Yoo, B., Lee, J.-H., Koo, G.-H., "A Study of Reduced-Scale Model Tests Results of High Damping and Lead Laminated Rubber Bearings for Liquid Metal Reactor," KAERI/TR-809/97, 1997.
2. Yoo, B., Lee, J.-H., Koo, G.-H., Lee, H.-Y., Kim, J.-B.,(2000), "Seismic Base Isolation Technologies for Korea Advanced Liquid Metal Reactor," Nuclear Engineering Design 199, pp. 125-142.
3. Lee, J.-H., Koo, G.-H., Yoo, B., "A Modeling Study of Dynamic Characteristic Analysis of Isolated Structure for Seismic Exciting Tests," KAERI/TR-1038/98, 1998.

DEVELOPMENT OF 3-DIMENSIONAL BASE ISOLATION SYSTEM FOR NUCLEAR POWER PLANTS

Takahiro Somaki[1)], Testundo Nakatogawa[1)], Akinori Miyamoto[2)], Koichi Sugiyama[2)],
Yoshihisa Oyobe[3)] and Kaoru Tamachi[3)]

1) Nuclear Facilities Division, Obayashi Corporation, Japan
2) Technical Research Institute, Obayashi Corporation, Japan
3) Daido Precision Industry, Japan

ABSTRACT

This paper describes the vertical isolation system for nuclear power plants, of which 3-dimensional base isolation system is composed, assuming that some horizontal base isolation system as laminated rubber bearings.

A horizontal base isolation system brings the drastic reduction effect on equipment/piping responses in the horizontal direction. However, vertical responses of equipment/piping tend to be greater than non-isolated building.

We developed the 3-dimensional isolation system for whole building, composed of laminated rubber bearings for the horizontal directions and coned disk springs for the vertical direction.

Considering the characteristics of vertical isolation devices by elemental tests in actual size, the precise seismic response analyses show that the drastic reduction of responses can be achieved.

INTRODUCTION

In Japan, some studies on application of 2-dimensional base isolation system to FBR or PWR plants have been continued for about 15 years. So the guideline for the design of base isolated nuclear power plants will be published soon. The aims of base isolation studies are the site-free design standardization of nuclear power plants.

The horizontal isolation system brings the drastic reduction effect on equipment/piping responses in the horizontal direction. However, in the horizontal isolated building the thickness of members/walls excepting for neutron shielding walls will be designed thinner for achieving construction cost reduction, the vertical equipment/piping responses tend to be greater due to amplification in the isolation layer and in the building structure.

The development of 3-dimensional isolation system is required from a viewpoint of further construction cost reduction of nuclear power plants.

OUTLINE OF 3-DIMENSIONAL BASE ISOLATION SYSTEM

Condition for development

On the occasion of developing the 3-dimensional base isolation system, it is a basic principle to add a vertical isolation system to the 2-dimensional horizontal isolation system.

For the high seismicity area, the isolation device was developed to satisfy with the following items.

1) Developing 3-dimensional isolation for whole building, with separating the devices in horizontal and vertical directions respectively to elongate the vertical eigenperiod and to be installed in the same layer space of horizontal isolation devices
2) Installing the prevention devices for the rocking behavior occurred by the horizontal motion
3) Reducing floor response spectra in the range of less than 0.4 sec, where there is the vertical 1st eigenvalue of major equipment/piping
4) Causing no uplift force for vertical and horizontal devices

Outline of proposal 3-dimensional isolation device

The proposed 3-dimensional isolation system is composed of a couple of Devices A and B as a unit, shown in Fig. 1. As for the role of each device during earthquake, the horizontal seismic force is mainly applied to the laminated rubber bearing of Device A, and the vertical seismic force is mainly applied to the vertical isolation of Device B.

Device A is that laminated rubber bearing and coned disk springs are arranged in series. The coned disk springs on the rubber bearing are set in order to isolate from the vertical force. The horizontal shear force (Maximum: 2MN)

derived from the superstructure during earthquake is lead to the rubber bearing through the vertical sliding center guide of coned disk springs. By using the characteristics of coned disk spring as shown in attached graph of Fig. 1, the slightly fluctuating axial force is applied to the rubber bearing.

Device B is that coned disk springs and roller bearing are arranged in series. The roller bearing is connected to the superstructure by the vertical sliding center guide of coned disk springs. However the shear force applied to Device B during earthquake is negligible, as the friction coefficient of the roller bearing is only 0.005.

The total vertical design load in the couple of Devices A and B is 9.8MN. A ratio of the design vertical loads in the Devices A and B is determined based on the fluctuating vertical load during earthquake. Device B is able to cover the fluctuating vertical loads.

Design specification for actual nuclear power plants

Based on the conditions for development, the results by a preliminary analysis for S2 earthquake, the specification of the vertical isolation is determined to be 1.8Hz for the spring rate, 10% for damping factor and -60mm to +60mm for the stroke.

As shown in Fig. 2, the dimensions of the coned disk springs are 500mm in outer diameter, 230mm in inner diameter, 14.7mm in thickness (t), 26.6mm in overall height and 11.9mm in dish height (h0). The size is determined due to the manufacture and good dealing at maintenance. The material used for coned disk springs is SUP10 in Japanese Industrial Standard, which is the same one as SAE 6150 in USA.

As the result of the trial design for the vertical isolation, the combinations of single coned disk stacking are the following.

Device A : 6 assemblies with 2 disks in parallel and 15 in series.

Device B : 6 assemblies with 11 disks in parallel and 12 in series.

The share ratio of vertical load (9.8MN/pair unit) in the Devices A and B is 17%(1.7MN) to 83%(8.1MN). In this connection the fluctuating vertical load is 72% of total load.

Herein, as for the friction coefficient, which accounts for edge and inter-surface friction, since these values are different from the coating specification, they should be investigated by test. And furthermore, though the disks with h0/t=0.8 are used, it is necessary to verify the characteristics by test whether full height of h0 is available as the effective stroke or not.

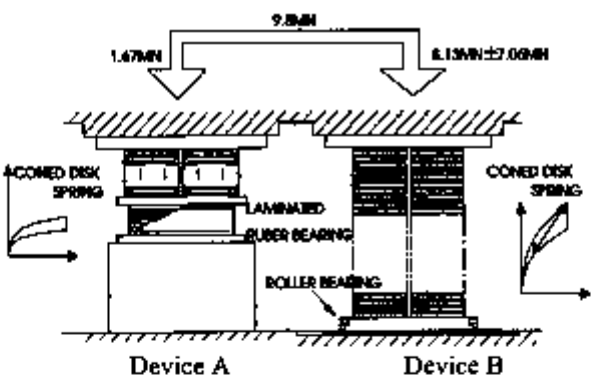

Fig.1 Illustration of 3-dimensional base isolation device

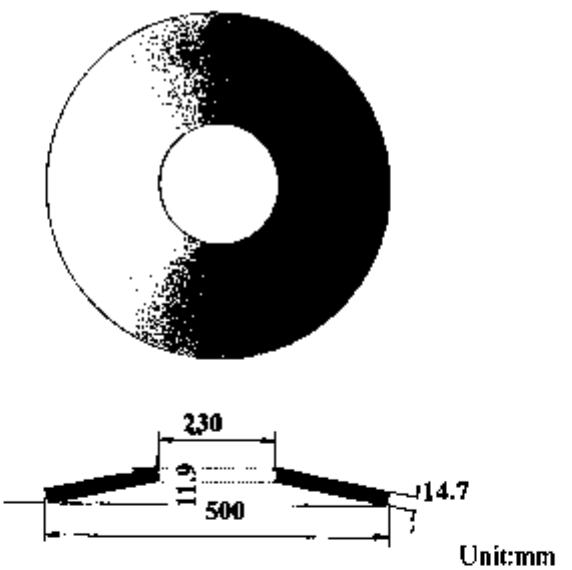

Fig.2 Details of coned disk spring

TEST AND SIMULATION ANALYSES

Objective & Specimens

Static tests, which are elemental but in actual size, are conducted to investigate the characteristics of vertical isolation device such as the load-displacement relationship. The friction coefficient for damping will be estimated by simulation analyses for test results using an approximate equation.

The actual sizes of specimen are shown in Fig. 2. After presetting, the special coating (Molybdenum Disulfide) of disks is used for rust prevention, corrosion prevention and anti-wear out, which is the glaze coating with the lubricant solid-film.

Procedure

Fig. 3 shows the loading schedule. The number of loading cycles is 16 in total with considering small amplitude for small and semi-great earthquakes and large amplitude for great (ultimate) earthquake like S2 earthquake in Japan. The first cycle for setting (bottom-out) is to investigate the full stroke.

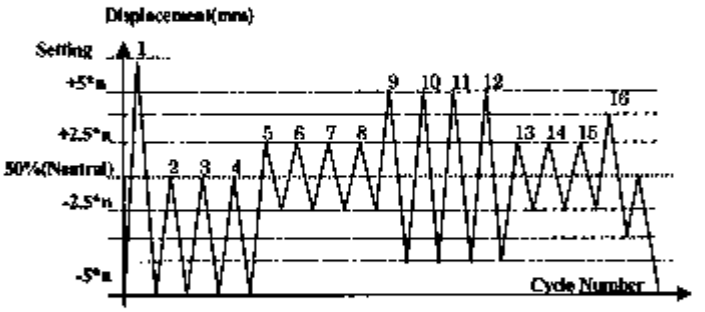

Fig. 3 Loading Schedule(n : number of disks in series)

Test cases

Table 1 shows the test cases. The case of Case 11 is the basic element model of the trial design result. At first, from Case 1 a friction coefficient Wr of edge friction is possible to be evaluated by the approximate equation. From the friction coefficient Wr and other cases, a friction coefficient Wm of inter-surface friction is possible to be evaluated in the same way.

Examples of test specimens are shown in Photograph 1.

Table 1 Test cases

Number of disks in series	Number of disks in parallel			
	1	3	6	11
1	Case 1	Case 3.1	Case 6.1	Case 11
2	-	-	Case 6.2	-
3	-	Case 3.3	-	-

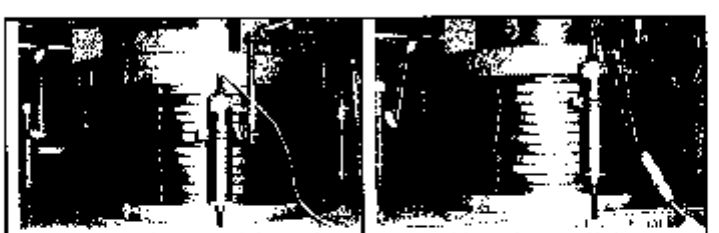

(a) 6 in parallel and 2 in series (b) 11 in parallel

Photograph 1 Examples of test specimens

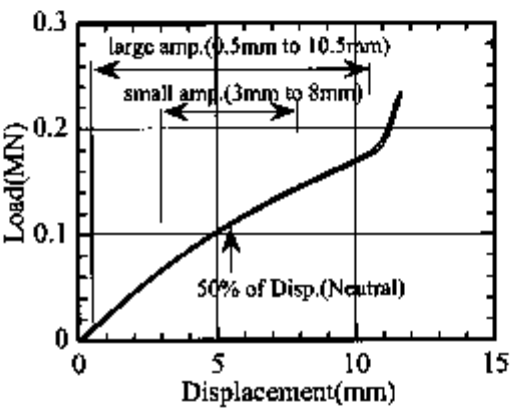

(a) Single Disk (Case 1)

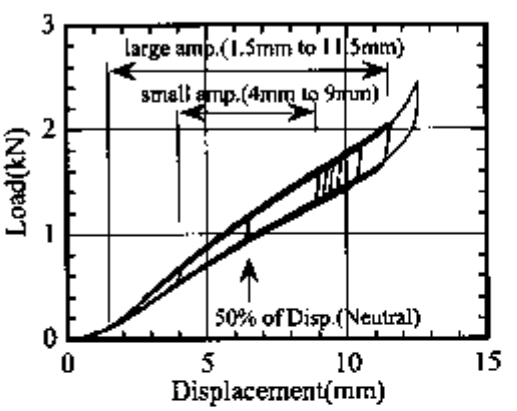

(b) 11 Disks Stacked in parallel (Case 11)

Fig. 4 Typical Load-Displacement Curves

Test results

Typical load-displacement curves are shown Fig. 4. Since the stroke of disks measured to be about 11mm, it is considered that the height of almost h0 is available as the effective stroke.

So the design stroke (-60mm to +60mm) in the case of 12 disks stacked in series is satisfied enough.

As for the surface of coating in the case of Case11, it was observed that the coat was slightly wounded only at inside bearing flats after test.

However, the hysteresis behavior is considered to be very stable even if the coating was wounded.

As for disks stacked in series, Fig. 5 shows the comparison of hysteresis loops between Case3.1 and 3.3 and between Case6.1 and 6.2, respectively.

In the case of disk stacked in series, the stroke is elongated in proportion to the number in series.

By the way, the vertical sliding center guide would be inevitably arranged in the case of disk stacked in series.

Comparing between the test results of Case 3.1 and 3.2 and between Case6.1 and 6.2 respectively, the friction between the guide and disks is negligible in these tests.

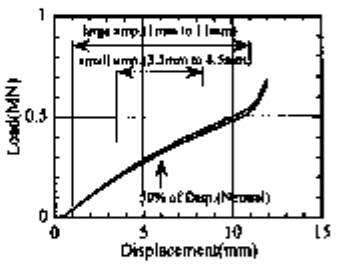

(a) Case3.1

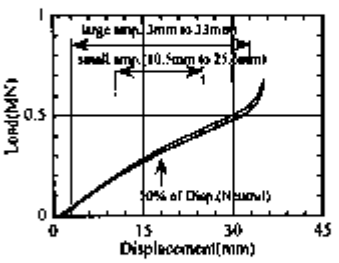

(b) Case3.3

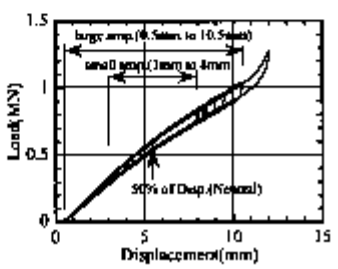

(c) Case6.1

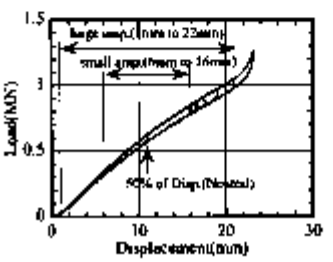

(d) Case6.2

Fig. 5 Comparison of Hysteresis Loopsbetween Disks Stacked in Series

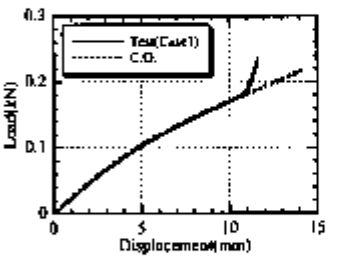

(a) Single Disk (Case 1)

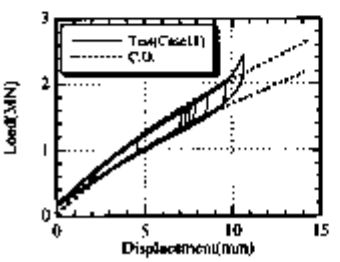

(b) 11 Disks Stacked in parallel (Case 11)

Fig. 6 Comparison between Curti-Orland and Test Results

Simulation Analyses

Fig. 6 shows the comparison between the approximate equation by Curti-Orland [1] and test results for Case1 and Case11. In the case of n disks in parallel, the load-deflection curves at loading and unloading are calculated due to the equation by Niepage [2] with the function of friction coefficients.

It is possible to simulate the test results due to the equation by Curti-Orland, as the effect of friction according with the combination of disks stacking is able to be considered in these equations.

In this connection, the friction coefficients with best simulating test results are estimated to be Wr(edge)=0.085 and Wm(inter-face)=0.035 to 0.042.

As the design formula, the proposal approximate equation by Curti-Orland could be considered to be applicable to large-sized coned disk springs.

APPLICATION TO NUCLEAR POWER PLANTS

Analytical Conditions

The soil building interaction model (shown in Fig.7) for horizontal and vertical seismic response analyses is subject to an imaginary 3-dimensional base-isolated nuclear power plant.

The dimensions of building are about 160m long and 100m width for the base-mat.

The total weight of the superstructure is 6GN.

So about 600 couples of Devices A & B are installed in the isolation layer under the superstructure.

Fig. 8 shows the response spectra (h=5%) of the design earthquake S2. The vertical spectrum is related with 2/3times of the horizontal one. The input ground motions in both directions are the artificial motions with the same random phase.

The specification of the proposal 3-dimensional isolation system is the following.

1) Horizontal directions:
Initial period T1 and isolation period T2 equal to1.0sec.and 2.0sec. respectively, and the yield strength is 0.1W. (where W is the total weight of superstructure).

2) Vertical direction:
Initial period Tv equals to 0.56sec(fv=1.8Hz). The energy dissipation for damping is considered due to the hysteresis loops.

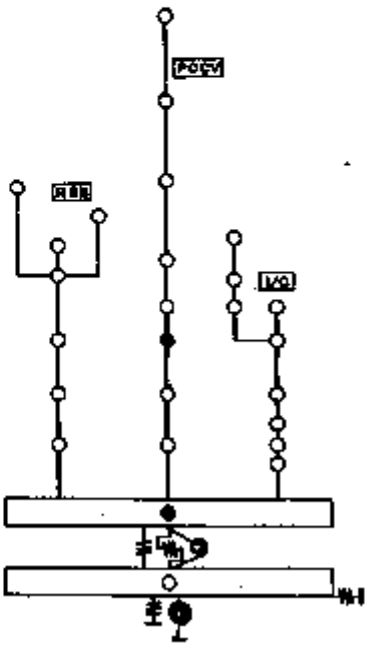

Fig. 7 Soil building interaction model

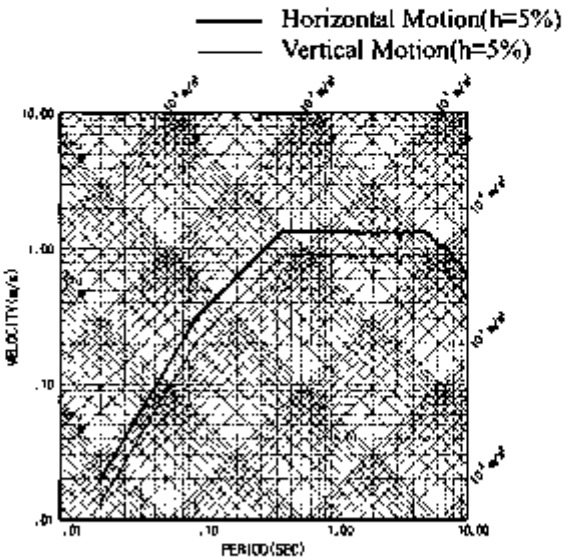

Fig. 8 Response Spectra of Input Ground Motion

Fig. 9 shows the analysis model of the vertical isolation device, comparing with the curves based on the test results. The non-linearity at loading and unloading is considered in this model, being simulated by the Ramberg-Osgood model.

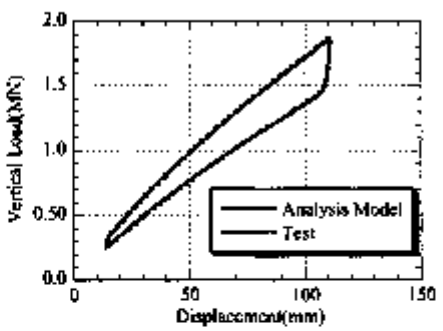

(a) Hysteresis Loop

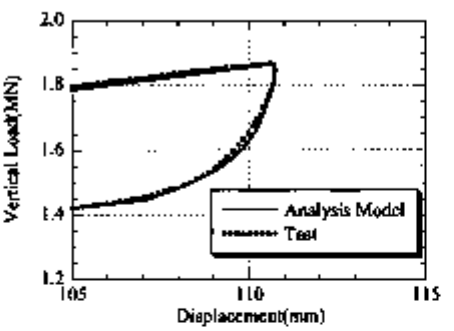

(b) Detail Curves at unloading

Fig. 9 Comparison of Hysteresis Loop between test result and analysis model

Fig. 10 shows the details and location of the proposal 3-dimensional devices. The number of coned disk springs for one couple of Devices A and B is 972.

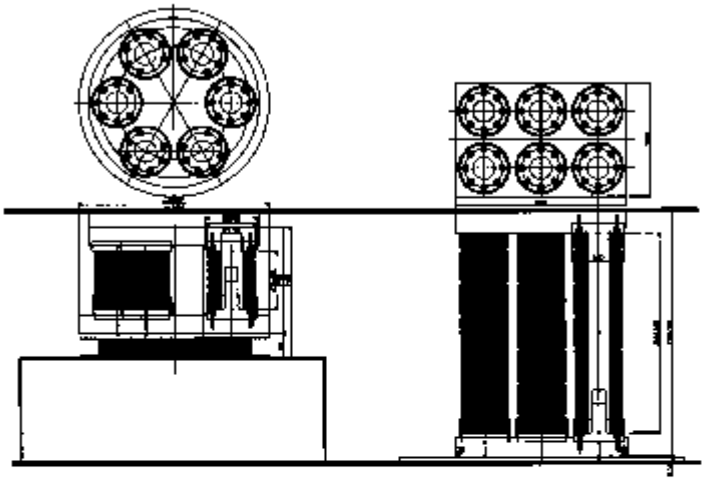

(a) Device A (b) Device B

Fig. 10 Details and Location of 3-Dimensional Devices

Evaluation for Application

Fig. 11 shows the hysteresis behavior of the vertical isolation devices. The maximum responses of displacement are 150mm in Device A and 125mm in Device B.

These responses are less than the ultimate displacement 165mm(=11 mm × 15) and 132mm(=11mm × 12) respectively.

So it is confirmed that the seismic safety margin is secured for the uplift or setting.

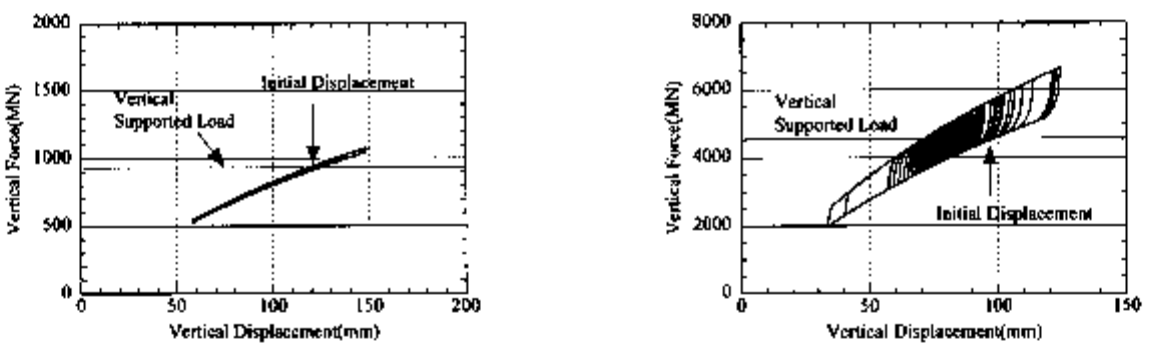

(a) Device A (b) Device B

Fig. 11 Hysteresis Behavior of Vertical Isolation Devices.

Fig. 12 shows the time history for the vertical displacement response at the isolation layer. As for the vertical displacement response due to the vertical motion, it is considered that the vibrating off the origin at the beginning of responses is due to the friction of disks stacking.

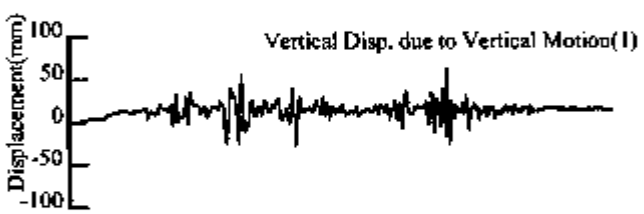

Fig. 12 Time History for Vertical Displacement Response at Isolation Layer.

Fig. 13 shows the typical vertical building acceleration responses at the operation floor(EL23.9) and at the upper base mat(EL1.7), just on the vertical isolation device, comparing with the vertical input ground motion. The vertical building acceleration responses are reduced effectively for the input ground motion.

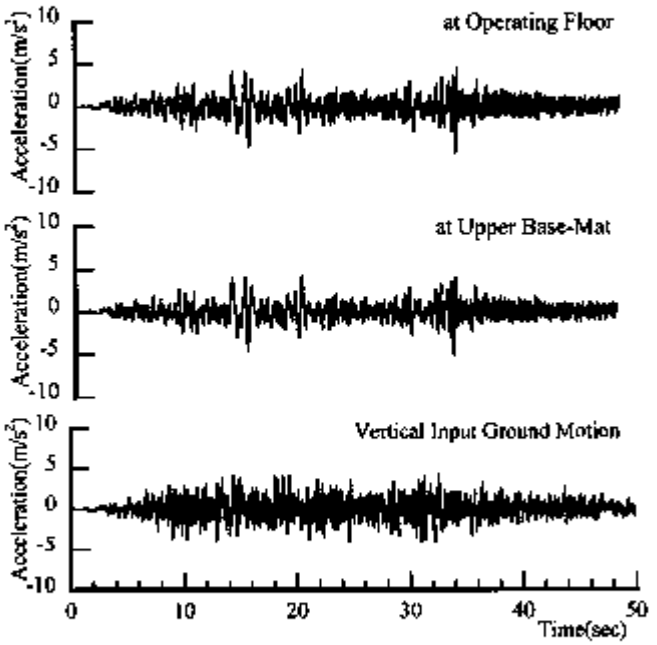

Fig. 13 Typical Time History for Vertical Acceleration Response.

Fig. 14 shows the typical vertical floor response spectra (FRS h=1%) at the operating, comparing with the case of the horizontal base isolated building without the vertical isolation.

At the beginning of development, it was worried that the friction behaviors of disks stacking would have influence on the equipment/piping response, as the friction behavior, which is the rigid non-linear characteristics, will excite the response in the short period range.

However, the response reduction effect on the design period of the equipment/piping is apparent.

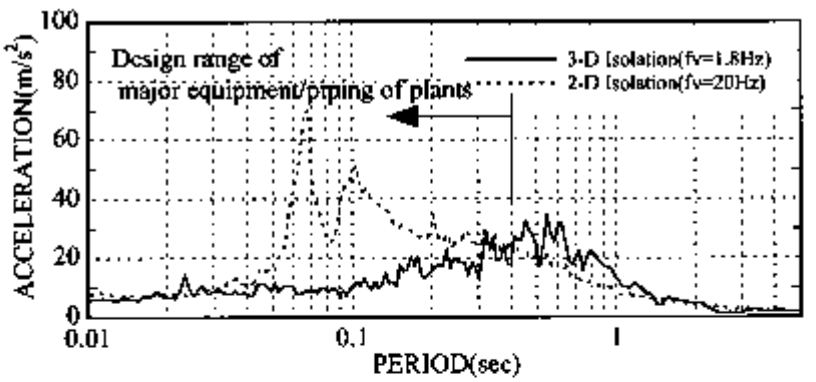

Fig. 14 Comparison of Typical Vertical FRS(h=1%) between 3-D Isolation and 2-D Isolation at Operating Floor.

It is considered that the proposal 3-dimensional isolation system could be applicable to the nuclear plants.

CONCLUSION

We developed the 3-dimensional isolation system for whole building, which is composed of the laminated rubber bearings for the horizontal direction and the coned disk springs for the vertical direction.

Considering the characteristics of vertical isolation device by the elemental tests in actual size, the precise seismic response analyses showed that the drastic reduction of equipment/piping responses could be achieved.

However it is hoped that the various verification tests for the realization would be conducted.

References

1. Curti, G. und Orland, M.: Ein neues Berechnungsverfahren fur Tellerfedern, DRAHT 30-1, pp.17-22, 1979
2. Niepage, P.: Uber den Einfluß der Reibung and kreiskegelformiger Last einleitungselement auf die Kennlinie von Einzeltellerfedrn und Tellerfederpaketen, Konstruktion, 379-384, 1984

Main Features and Conclusions of the 1999 International Post-SMiRT Conference Seminar on Seismic Isolation, Passive Energy Dissipation and Active Control of Vibrations of Structures

Alessandro Martelli [1)], Massimo Forni [2)], Hyun Min Koh [3)]

1) Chairman, Working Group on Seismic Isolation (GLIS); ENEA, Bologna, Italy
2) Technical Secretary, GLIS; ENEA, Bologna, Italy
3) Professor and Chairman, Department of Civil Engineering, Seoul National University, Korea

ABSTRACT

Summarised in this paper is the state-of-the-art on seismic protection through innovative anti-seismic techniques, namely seismic isolation (SI), passive energy dissipation (ED) and active control (AC), based on the information collected at the 6th International Post-SMiRT Conference Seminar on Seismic Isolation, Passive Energy Dissipation and Active Control of Vibrations of Structures held at Cheju (Korea) in August 1999 and even more recent information which became available to the authors. Reported is information on the most recent applications of such techniques, together with the progress of R&D activities at word-wide level, availability of design rules and the related issues and needs for further activity. With regard to the latter, somewhat more detailed information is reported for European and especially, Italian applications.

INTRODUCTION

Modern society is being more and more characterized by a strong interaction among the large systems by which it is formed: the physical, human and infra-structural systems. Seismic risk results from the interaction among seismic hazard, vulnerability of structures and social-economical effects. In the past, an earthquake mainly caused collapse of buildings and fatalities. Nowadays, a seismic event may also endanger the social-economical stability of large areas, due to the complexity of technologically advanced societies. For instance, the Great Hanshin-Awaji earthquake of 1995, which struck Kobe (where one of the most important ports of the world is located) is the first case in the history of a seismic event that occurred in a highly industrialized urban area, by producing enormous damage to the building, road and in particular, productive systems.

The earthquake which struck Izmit in Turkey on August 17, 1999, caused the fire of the biggest Turkish petrochemical plant, by leading to very difficult fuel supply and heavy pollution. A scenery similar to those mentioned above might take place in many other areas in the world, from California to Italy: in California, for instance, in case of a strong earthquake closer to San Francisco and Silicon Valley, with the respect to the 1989 Loma Prieta event; in Italy, for instance, in case of events like that which struck the now highly industrialized area around Po River in 1117, or that which destroyed South-East Sicily (where a huge number of petro-chemical plants and components is now located) in 1693.

In addition, it is worthwhile mentioning that recent earthquakes showed a fully unexpected violence, like for instance, that which struck again Turkey, with epicenter near Kaynasly (Bolu Mountains), on November 12, 1999. Since ground acceleration was much larger than the design value, this caused severe damage even to some very important modern structures, like a viaduct of the new Istanbul-Ankara freeway, being erected using the most modern anti-seismic technologies, which was extremely close to the epicenter [1]: in fact, the maximum displacement allowed by the horizontal fail-safe system (stoppers) was largely exceeded (another viaduct behaved very well, although it displaced twice the design value, but this was still allowed by the stoppers).

The aforesaid remarks demonstrate, without any doubt, the increased degree of complexity of modern society, and thus, the need for an integrated management of the territory, able to make development and safety compatible. This implies that more and more numerous shall be the structures for which design shall not be limited to prevent their collapse, but shall require the absolute integrity and full operability after the earthquake. The feature of absolute integrity is also indispensable to protect investment, taking into account that the value of contents of more and more buildings is much larger than that of the structural members, as well as to avoid spending the enormous amounts of money during both the emergency phase and reconstruction which were necessary after the recent earthquakes.

For the above-mentioned reasons, a wide extension of the use of innovative anti-seismic techniques, such as seismic isolation (SI) and passive energy dissipation (ED), which aim at ensuring the full integrity and operability of structures, is necessary for both new constructions and retrofit of existing buildings [2]. In fact, SI and ED technologies are now fully mature for such an use, as demonstrated by the results of very numerous research projects and also, by the excellent behavior of seismically isolated buildings in both the Great Hanshin-Awaji earthquake and the Northridge earthquake which struck the Los Angeles area the year before [2]. This conclusion has been confirmed in all the recent Conferences on seismic

engineering, in particular at the 6th International Post-SMiRT Conference Seminar on Seismic Isolation, Passive Energy Dissipation and Active Control of Vibrations of Structures held at Cheju, Korea in 1999 [3].

RECENT APPLICATIONS

The invited lectures and contributed papers presented at the Cheju Seminar and the extensive discussion both following their presentation and during the Closing Panel, demonstrated that not only SI, but also several ED systems are already fully mature for wide-ranging applications. They also showed that, at last, the benefits of such systems have been well understood in several countries and that they are now being more and more used. The aforesaid benefits had already been very well understood by Japanese after the 1995 Kobe earthquake and to a certain extent, by Californians after those of Loma Prieta (1989) and Northridge (1994). Even before, this had occurred in New Zealand, where there are still new applications of SI to both new and existing ancient constructions, in spite of the limited population; more recently, it also occurred in other countries, like the P.R. China, Russian Federation (especially after the Sakhalin earthquake in 1994) and Italy (after the 1997 earthquake of Umbria and Marche Regions, which severely damaged famous frescos of Cimabue and Giotto in the "San Francesco Basilica Superiore" at Assisi). It is also worthwhile citing again that, according to the information provided at the Cheju Seminar, SI and ED are now considered of great interest also for areas characterized by low or moderate seismicity [3].

Applications in Japan

In Japan the number of buildings provided with innovative anti-seismic systems is still considerably increasing, in spite of the need for still asking for a specific approval for each design including these techniques [3]. The number of licenses began to drastically increase in September 1995, some months after Kobe earthquake (60 new applications) and the annual number reached 207 in 1996, while the overall number during the 10 previous years was 79; such a dramatic increase ended in 1997, when a probably steady progress began (the new licenses were 135 in 1997 and 131 in 1998).

In this country, the use of SI was recently extended from new constructions to retrofit of existing buildings (e.g. Le Courboisier Museum at Tokyo), as well as to many new or existing bridges and viaducts (in some cases, at least in Kobe, becoming compulsory for the latter). SI is having many variations in application objects, application methods of rubber bearings and kinds of devices. The variations include SI of tall buildings of about 100 m height, SI of artificial grounds for multiple buildings, and application of non-rubber type SI devices. SI is finding new applications which include wooden houses, masterpieces in museums, automatic storage systems of warehouses, etc.: for wooden houses, non-rubber type SI systems using ball/rubber bearings or sliding bearings to support the superstructure have been developed and used; for masterpieces in museums, various types of SI have been developed and used for the containing showcases; for automatic storage systems of warehouses, a new type of SI floor has been developed and used. It is also noted that SI is beginning to be used for very important public buildings and facilities, such as, for instance, the new official residence of the Prime Minister.

Applications in the USA

In the USA (especially in California), new constructions of important isolated strategic buildings, including emergency control centers (e.g. those at San Francisco and Long Beach) are going on and retrofit of even large public buildings using SI (e.g. the San Francisco City Hall and San Bernardino Medical Center) is progressing [3]. Most applications make use of rubber bearings, namely High Damping Rubber Bearings (HDRBs) or Lead Rubber Bearings (LRBs).

However, the extent of the aforesaid progress is much less than in Japan. In fact, although the first U.S. seismically isolated building was completed in 1985, in 1999 there were in this country only 25 applications to new constructions and 22 retrofits of existing buildings: this is due to very complex and conservative regulations.

Conversely, SI is now being widely used in the USA for highway bridges, for which it is governed by a simple and not overly conservative code.

Applications in New Zealand

There were 10 isolated buildings in New Zealand in 1999 (in addition to several applications to bridges and viaducts), four of which being retrofits of ancient constructions (those of the Old Bank of New Zealand and Wellington Museums were completed in 1999) [3]. Most applications make use of LRBs, in some cases in conjunction with teflon sliders.

Applications in Other Non-European Countries

As regards other non-European countries, in the P.R. China there were already 160 buildings isolated by means of rubber bearings in 1999 [3]; the total numbers of Chinese isolated buildings and bridges & viaducts reached 230 and 20, respectively, in May 2000 [4]. In Taiwan 10 bridges had been supported by LRBs, in addition to others being erected using viscoelastic devices (VEDs) and elastic-plastic (EP) dampers [3]. It is also worthwhile noting that the number of seismically

isolated bridges using LRBs was approaching 30 in Korea in 1999, in spite of its low and moderate seismicity [3]: the main reason is that the use of SI is generally accepted in Korea as an alternative way to reduce the additional construction costs caused by the seismic design requirements recently adopted in this country.

With regard to important new applications of ED systems to bridges and viaducts, to be cited are also those to: (a) three new viaducts of the Istanbul-Ankara freeway in the Bolu Mountains in Turkey (Figure 1), two of which completed and one under construction, which have been provided with multidirectional EP devices (as previously mentioned and explained in [1], two of these viaducts behaved in an excellent way in the earthquake of November 12, 1999); (b) the Bangabundhu Bridge over the Jamuna River in Bangladesh, with hysteretic devices [5, 6]; (c) twenty six important railway viaducts in Venezuela, again with hysteretic devices [5, 6]; (d) five bridges along the North-South Route in Chile, with VEDs [5, 6].

In Chile, the new hospital of the Catholic University has been isolated with HDRBs [5, 6].

Applications in Western Europe

As regards Europe, to the knowledge of the authors, most new applications of the innovative anti-seismic techniques (in progress or under design or planned) concern Italy, where there were already over 30 applications of such techniques in 1998 [2] and such new applications take advantage of the results of important projects funded by the European Commission (EC).

In Italy to be cited are the following recent / new applications to [3, 5, 6]:

- The "San Francesco Basilica Superiore" at Assisi (Umbria Region), which had been severely damaged by 1997 earthquake: in October 1999, it was equipped with Shape Memory Alloy (SMA) devices and innovative shock transmitters (the latter developed in the EC-funded REEDS Project, in the framework of the restoration of the Basilica (see Figure 2 and [7]).
- The "San Giorgio in Trignano" Bell Tower at San Martino in Rio (Reggio Emilia, Emilia-Romagna Region), which had been severely damaged by the Reggio Emilia and Modena earthquake of 1996: in November 1999, it was also retrofitted using SMA devices, in the framework of the EC-funded ISTECH Project.
- The San Feliciano Cathedral at Foligno (Umbria), again damaged by the 1997 earthquake and retrofitted with SMA devices.
- The "La Vista" and "Domiziano Viola" schools at Potenza (Basilicata Region), which were retrofitted in 1999 using dissipative braces (see Figure 3).
- The "Gentile Fermi" school at Fabriano (Marche Region), a reinforced concrete building constructed in the years '50s, being one of the few examples of rationalist architecture in the town, which had been also heavily damaged by the 1997 earthquake: it is being retrofitted using VEDs (see Figure 4).
- An apartment building, under construction with HDRBs at Rapolla (Potenza, Basilicata Region) close to a twin conventionally founded building (see Figure 5); this application is similar to the twin isolated and non-isolated buildings already existing at Squillace (Catanzaro, Calabria Region) [2].
- The "Rione Traiano" Civic Center at Soccavo (Naples, Campania Region), a very large construction erected with conventional foundations before the 1980 Campano-Lucano (Irpinia) earthquake, when the area was not considered as seismic: this is being retrofitted using approximately 500 HDRBs.
- A new hospital at Frosinone (Lazio Region), which has been designed using HDRBs.
- Several buildings of the new Emergency Management Center for Central Italy at Foligno (Perugia, Umbria Region), being designed using various innovative anti-seismic systems (see Figure 6).
- The new hospital at Perugia and an apartment building at Città di Castello (Umbria Region), to be isolated with HDRBs.

Figure 1a. Viaduct N. 1 of the Istanbul-Ankara freeway provided with EP devices.

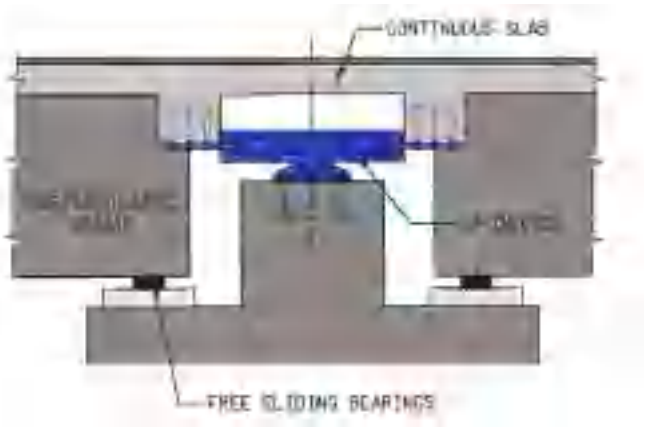

Figure 1b. Detail of the pier top of the Viaduct of Figure 1a.

Figure 2 a. SMA devices installed on the "San Francesco Basilica Superiore" at Assisi (PG).

Figure 2 b. Shock transmitters installed between nave and transept of the "Basilica Superiore".

- Two new buildings at the Navy Base of Augusta (Siracusa, Sicilian Region), to be probably isolated using HDRBs, similar to those already existing at such a Base [2].
- An electric substation at Laino (Calabria Region), to be isolated by the Italian Electricity Board (ENEL) with wire ropes, based on the results of an extensive numerical and experimental study (this will be the first electric equipment in Italy to be provided with a SI system).
- Several viaducts of the Salerno-Reggio Calabria freeway (Campania, Basilicata and Calabria Regions), for which retrofits using ED systems are being designed.
- A bronze statue of Germanicus Emperor, located in a museum at Perugia (Umbria Region), which was provided with a multistage SI system using HDRBs (this will be the second Italian application of SI of this kind, following that to the famous Bronzes of Riace at the Reggio Calabria Museum [2]).

In addition, SI might be adopted in Italy for other buildings or structures; in particular, based on the already promising results of an ongoing study funded by the National Group for the Defense from Chemical, Industrial and Ecological Risks of the National Research Council (CNR), it may be adopted for Liquefied Natural Gas (LNG) tanks, such as an existing spherical butane storage tank located in a highly seismic site, as a possible pilot application in Italy for chemical plants [8].

Finally, the possibility of reconstructing ancient villages in Marche and Umbria Regions using the original masonry materials and to make it feasible, SI is being considered in Italy: to this aim, under consideration are the village of Mevale di Visso in Marche Region (which was almost fully destroyed by the Marche and Umbria earthquakes of 1997-98, after being severely damaged by previous earthquakes) and villages around Nocera Umbra in Umbria Region (which were also severely damaged by the 1997-98 earthquakes).

Data concerning the Italian applications are available on Internet at the GLIS address: http://192.107.65.2/glis. It is noted that some applications, in particular those of the new Emergency Management Center at Foligno and (if confirmed)

Figure 3. Dissipative braces installed on the "La Vista" and "Domiziano" schools (Potenza).

Figure 4. Gentile Fermi school (Fabriano). Cut of the wall for the introduction of the braces supporting the VED.

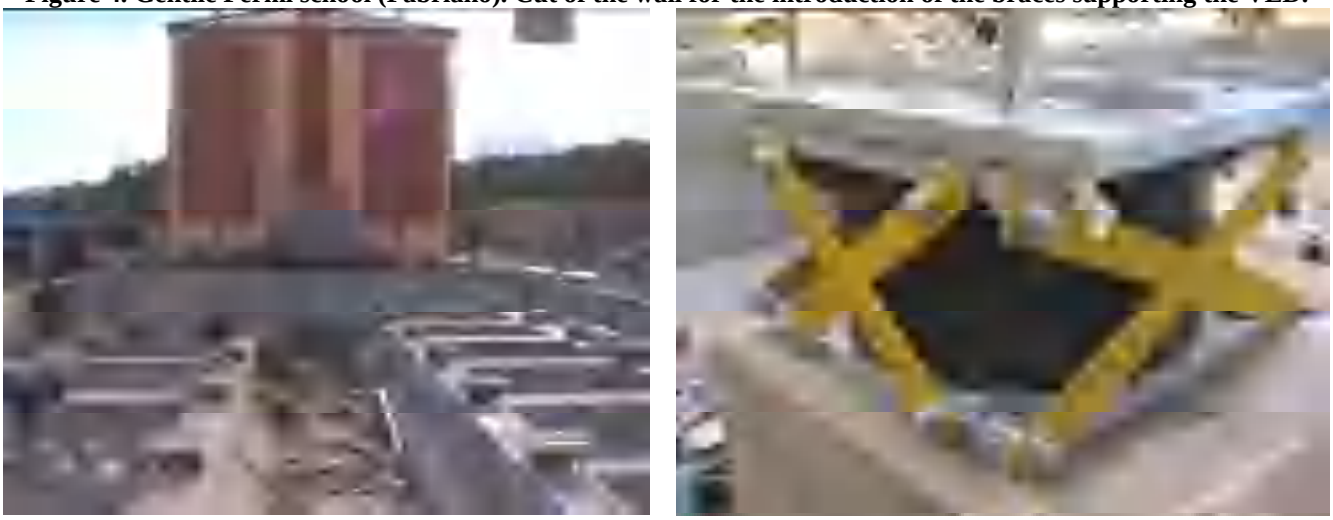

Figure 5. Isolated under construction and already erected conventional buildings at Rapolla (PZ).

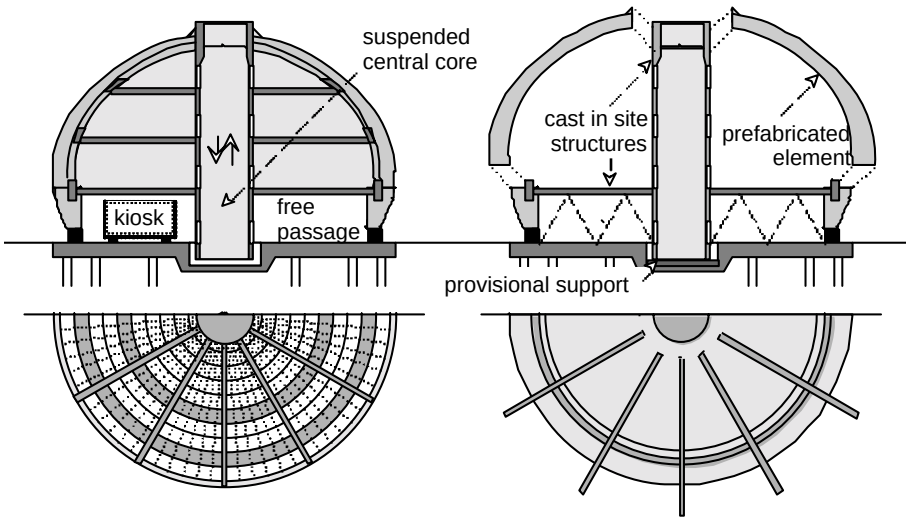

Figure 6. Sketch of one of the buildings of the Center of the new Emergency Management Center of Central Italy, Foligno, Umbria, which will be seismically isolated using HDRBs.

that to the reconstruction of Mevale di Visso, will take advantage of collaborations recently established (or being established) between ENEA and Italian Regions for carrying out pilot applications on buildings, by joining the use of innovative anti-seismic systems with the energetic-environmental quality [5, 6].

With regard to other Western European countries, new / recent important applications known to the authors are to [3]: (a) two storage tanks of Lonza Company for hazardous chemical materials, which were retrofitted at Visp (Switzerland) using HDRBs; (b) bridges in France, including a "TGV" fast train bridge at Marseille, which were provided with VEDs; (c) a French building at La Martinica to be provided with VEDs in conjunction with cables; (d) the 4 km long Santarem cable-stayed bridge over Tagus river, isolated using HDRBs (Portugal); (e) the "21th April" suspension bridge over the Tagus river (Portugal), which was upgraded using viscous dampers (VDs); (f) the new "Vasco de Gama" Tagus crossing (Portugal), which was provided with shock transmitters, VDs and elastic-plastic (EP) devices; (g) some small bridges in Greece, provided with HDRBs.

Applications in the Former USSR Countries

Some new building applications of SI were also carried out in the former USSR countries (where the total number reached 306 in 1999 [3]: these were performed in Russia, Armenia and Uzbekistan and made use of HDRBs (the previous applications mostly made use of so-called "low cost isolators"). To be cited among the aforesaid recent applications of HDRBs is the retrofit of the bank of Irkutsk-City (Russia), where isolators manufactured in the P.R. China were installed.

STATE-OF-THE-ART ON R&D

The papers presented at the Cheju Seminar also showed that most necessary R&D activity has already been completed, not only for SI, but also for most types of ED systems (further work remaining necessary for very new devices such as electromagnetic dissipators [3]). With regard to studies performed in the European Union on SI and ED systems, those previously mentioned, concerning the REEDS and ISTECH Projects for the optimization of hysteretic, viscous and viscoelastic dampers and shock transmitters, as well as the development of innovative rolling SI systems and SMA devices, had been just completed at the time of the Seminar and confirmed the excellent behavior of such devices [3].

To be cited is also the present availability, of test equipment - not only in Japan, but also in the USA (for instance, that of Caltrans at San Diego) - capable of qualifying full or at least, large scale devices, as necessary to correctly estimating safety margins: in fact, such tests, if performed on small scale devices, may be not very satisfactory even for rubber bearings (for instance because bonding conditions could be different from those of the real scale device) and are certainly not adequate for VDs, because they cannot correctly describe fluid heating conditions [3].

Regarding future studies and application of SI and ED systems, issues which were stressed were the importance of: (a) extending retrofit using the innovative anti-seismic techniques; (b) improving studies concerning innovative systems applicable to cultural heritage; (c) improving knowledge and develop systems for vertical isolation; (d) promoting more

applications to hospitals and chemical plants and components; (e) widely extending application from strategic to apartment buildings; (f) performing adequate monitoring; (g) improving knowledge on seismic input, in particular for near-field earthquakes (how correct is this point was confirmed later by the aforesaid earthquakes in Turkey); (h) improving studies concerning some reliability and uncertainty issues which have not been yet fully analyzed (including scale effects for qualification tests of SI and ED devices, the behavior of such devices at earthquake levels exceeding the design value, and failure modes, at extremely violent beyond design earthquakes, of structures provided with the anti-seismic systems); (i) considering other sources of vibrations which may damage or weaken structures (for instance, traffic).

Finally, with regard to non-passive control systems (active, semi-active and hybrid systems), the papers presented by the experts at this topic stressed that also their development is further progressing well. Thus, it was decided that the attention devoted at Cheju to this topic has to be kept also at the next Seminar, to be held at Assisi (Italy) on October 2-5, 2001.

DESIGN GUIDELINES DEVELOPMENT

The only still remaining problems for a wide-ranging application of SI and ED systems that were stressed at the Cheju Seminar concern the design rules for structures provided with such systems [3]. In general, the situation did not improve much with respect to the previous 5th Seminar held at Taormina (Italy) in 1997 [9], especially because such rules are still different in the different countries, frequently still penalize the use of SI with respect to the conventional design and their application still requires heavy approval processes. The only important improvement is that there are now, at least, design guidelines available in most countries (in Italy they were published by the Ministry of Construction at the end of 1998).

An interesting recommendation made in the Closing Panel of the Cheju Seminar was to try to find the way to develop international design guidelines for structures provided with the innovative anti-seismic systems. Among others, these international guidelines should explain such systems correctly and leave official codes out of consideration. They would not have any legal value, but may be useful, because they would be based on knowledge and experience of real experts. This guidelines' development might be part of the activities of the International Earthquake Research Center that had been proposed at the main SMiRT Conference, held at Seoul (Korea) the week before that of Cheju Seminar. The problem to allow for these activities is to find the necessary funding. In the aforesaid Closing Panel, it was also proposed the guidelines of all countries represented in the Seminar to be translated in English and published in an appropriate volume at the next venue of Assisi, and that, at such a venue, there shall be papers on applications, each containing sufficiently detailed reference to the codes used in the related country. With regard to non-passive control systems, it was stressed at Cheju that the development of these techniques suffers from the fact that they are not considered at all by design rules [3].

CONCLUSIONS

Based on information collected at the 6th International Post-SMiRT Conference Seminar on Seismic Isolation, Passive Energy Dissipation and Active Control of Vibrations of Structures, held at Cheju (Korea) in 1999 and more recent information that became available later to the authors, the state-of-the-art on the applications of SI and ED systems has been shortly reported and some remarks on the progress of R&D activities at word-wide level and design guidelines development have been made. It has been stressed that SI and ED technologies, which aim at ensuring the full integrity and operability of structures, are fully mature, as demonstrated by both the results of very numerous research projects and the excellent behavior of seismically isolated buildings and viaducts in violent earthquakes. It has been shown that, consequently, a wide extension of the use of these techniques is in progress, for both new constructions and retrofit of existing buildings.

The state-of-the art on the development and application of the innovative anti-seismic techniques will be updated at the 7th International Seminar to be held at Assisi, Italy, on October 2-5, 2001.

REFERENCES

1. Marioni, A., "The Effects of Recent Earthquakes on the Base Isolated Bridges of the Istanbul Ankara Motorway near Bolu", *Proc.Of IASS Symposium on Bridging Large Spans – From Antiquity to Present*, pp. 261-270, Istanbul, Turkey, 2000.
2. Martelli, A., and Forni, M., "Seismic Isolation of Civil Buildings in Europe", *Progress in Structural Engineering and Materials*, Construction Research Communications Ltd., London, Vol. 1 (3), 1998, pp. 286-294.
3. Koh, H.M., and Martelli, A., Preface – "Overview and Summary of the International Post-SMiRT Conference Seminar on Seismic Isolation, Passive Energy Dissipation and Active Control of Vibrations of Structures", *Seismic Isolation, Passive Energy Dissipation and Active Control of Vibrations of Structures - Proceedings of the Post-SMiRT Conference Seminar, Cheju, Korea, August 23-25, 1999*, Vol. 1, Seoul, Korea, August 2000.
4. Zhou, F.L., Recent Development on Isolation and Energy Dissipation Used in New Seismic Design or Retrofit for

Structures in China. *Proc. Of the IASS Symposium on Bridging Large Spans – From Antiquity to Present*, pp. 230-240, Istanbul, Turkey, May-June 2000.
5. Martelli, A., and Forni, M., State-of-the-Art on Seismic Protection through Innovative Techniques. *Proc. Of the IASS Symposium on Bridging Large Spans – From Antiquity to Present*, pp. 251-260, Istanbul, Turkey, May-June 2000.
6. Martelli, A., and Forni, M., State-of-the-Art on Recent Applications and Research Needs, Session on Base Isolation System. *Proc. Of the Final Workshop on "Protezione Sismica dell'Edilizia Esistente e di Nuova Edificazione attraverso Sistemi Innovativi*; Programma MURST PRIN 97, Naples, Italy, June 2000.
7. Castellano M.G., and Martelli, A., The Influence of Shape Memory Alloy Ties on the Seismic Behaviour of Historical Masonry Buildings. *Proc. IASS Symp. on Bridging Large Spans – From Antiquity to Present*, pp. 271-280, Istanbul, 2000.
8. Martelli, A., Forni, M., Poggianti, A., and Spadoni, B., R&D in Progress at ENEA, with Particular Attention to the Industrial Plants. *Proc. Of the 16th SMiRT International Conference*, Washington, DC, USA, August 2001.
9. GLIS, *Seismic Isolation, Passive Energy Dissipation and Active Control of Seismic Vibrations of Structures - Proceedings of the International Post-SMiRT Conference Seminar, Taormina, Italy, August 25 to 27, 1997*, A. Martelli and M. Forni eds., Bologna, Italy, 1998.

Product Specification and Mechanical Properties of Chinese Rubber Bearings

Wenguang Liu[1)], Fulin Zhou[1)], Feng Sun[1)], Da Huo[2)], Weiming Yan[2)]

1) Guangzhou University, 510405,Guangzhou, P R China
2) Beijing Polytechnic University, 100022, Beijing, P R China

ABSTRACT

Firstly, the basic mechanical properties of rubber bearings are provided in the paper, such as the vertical stiffness, and horizontal stiffness of the rubber bearings with diameter from 400mm to 1000mm. Then the duration properties of acceleration aging, creep test are considered followed by the product specification. The dependence properties, vertical compressive stress 5MPa to 25MPa, frequency 0.001Hz to 0.5Hz, temperature -25ºC to 40ºC, are also introduced in the paper. According to the product specification, rubber bearings should have enough fireproof capability under the action of natural fire lasting one hour, the fireproof properties of rubber bearings and lead rubber bearings was tested. The mechanical properties of rubber bearings with rotation are also provided in the paper, they show that Chinese rubber bearings have stable properties not only can be used in base isolation system but also in column top isolation system. At the end of the paper, the main features of product specification of laminated rubber bearings are introduced.

INTRODUCTION

Base isolation system shows an effective avenue to aseismic design, there are nearly 250 isolated buildings in China since the first one was built in 1994. The isolated buildings are distributed widely according to the statistics provided by Chinese Committee of Seismic Control for Structures (CSACE), especially in Xinjian, Shanxi and Yunnan province. The usage of base isolation system has been extended from special purposes such as computer centers or hospital to normal residential buildings, and the structural types include reinforcement concrete and masonry. In the mean time, rubber bearings have been used in railway and highway bridge to decrease the response under the action of earthquake. Being an important part of the structure, the properties of rubber bearings are the key factors to support the vertical load and provide enough displacement, or provide enough damping for lead rubber bearings.

In 1997, China began to compile product specification of laminated rubber bearings in order to promote the development of isolated building, and the specification is published in October of 2000. In this paper, the properties of rubber bearings and test results that we completed in China and Japan are summarized and compared, and then the product specification are introduced in the end of the paper.

MECHANICAL PROPERTIES OF RUBBER BEARINGS

Vertical Stiffness and Yield Stiffness

The vertical stiffness and yield stiffness of specimens with diameter from 400mm to 1000mm are tested, the properties of natural rubber used in the specimens are as follows: Gr=0.55MPa; Eb=2kN/mm^2; κ=0.77; IRHD (hardness)=48. The comparison between design value and test value of vertical stiffness are provided in figure 1, which includes 10-ϕ400 to 10-ϕ1000 specimens. The equations of vertical stiffness and yield stiffness are:

$$K_v = \alpha \frac{E_{cb} G_r}{A} \tag{1}$$

$$K_d = \frac{K_{eq}\delta - Q_d}{\delta} \tag{2}$$

Extreme Properties

The monotonic shear failure tests with vertical compressive stress 10MPa were performed using 4 different diameter LRB specimens and 2 different diameter RB specimens. The hysteresis loops of LRB specimens are shown in

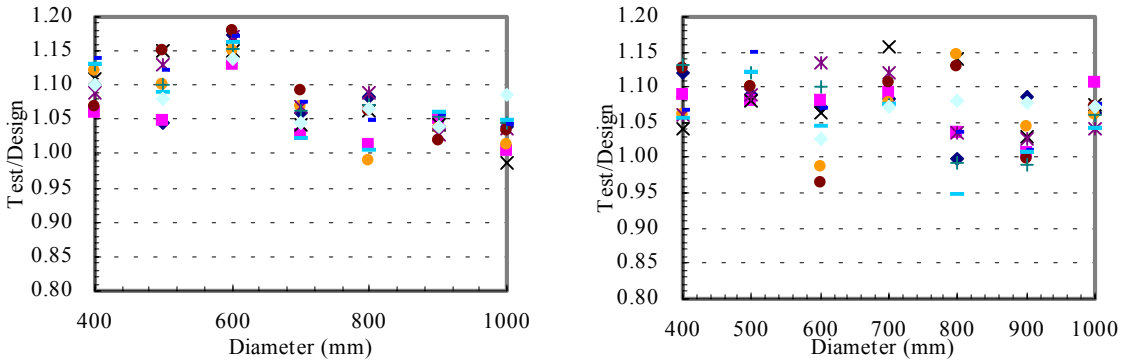

Fig. 1 Vertical stiffness and yield stiffness (test value/design value, design compressive stress 10MPa)

figure 2. The extreme shear strain of all specimens are more than 350% which is the minimum extreme strain published by the product standard, and the largest shear strain is 478%.

Creep and Aging Test

The tests were planned based on the Arrhenius's Theory. From the results of the raw rubber material test, it was found that the condition 100°C × 168 hours corresponded the condition 20°C×60 years for rubber bearings. All durability tests followed this condition. A RB-ϕ300 and LRB-ϕ300 specimen was used to perform creep test to keep vertical load small enough. The result is shown in figure 3. The vertical displacement does not include elastic deformation of the specimen. The creep is small as much as 1.38 mm and 0.91 mm or 2.38% and 1.58% by strain respectively.

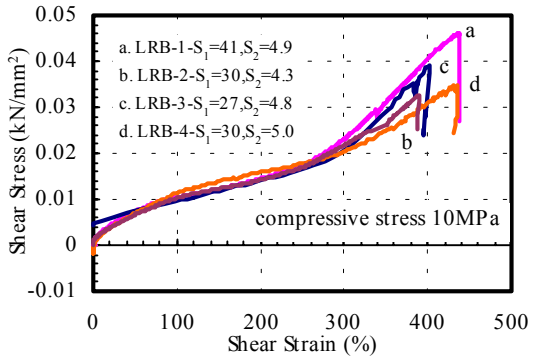

Fig. 2 Extreme shear strain

Four specimens, RB-ϕ300, RB-ϕ400, LRB-ϕ300 and LRB-ϕ200 are used for the acceleration aging test in the terms of corresponded condition 20°C×60 years respectively. The horizontal and vertical stiffness of both RB and LRB specimens increase nearly 10% when specimens cooled more than 24 hours after the aging test. The extreme shear strain of aging specimens are tested to compare with the original specimens under the same test condition, and the LRB-ϕ300 specimen are not failure when the shear strain is more than 360% for the reason to protect the test facilities, see in figure 4.

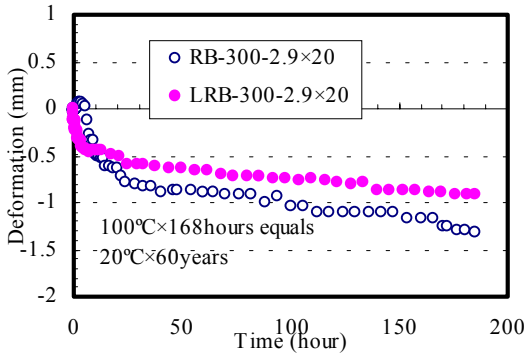

Fig. 3 Creep of RB-300 and LRB-300 with constant compressive stress 10Mpa

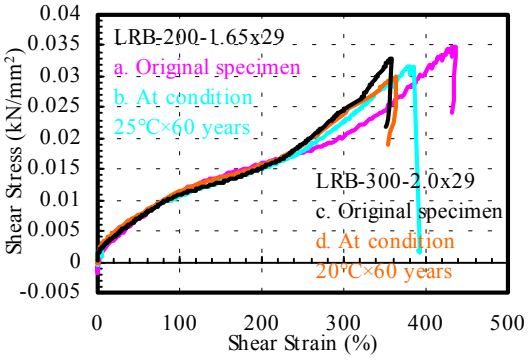

Fig. 4 Extreme shear strain of aging test

Fireproof Test

2 specimens are used for the fireproof test according to the demand of specification. The test is to imitate the engineering condition of rubber bearings, adding stable vertical load to design value and using wood with a little patrolling around the specimen, keeping the fire lasting for one hour. There are 2 temperature transducers to collect the variation of inner and outer temperature of the specimens, see in figure 5. The outer average temperature of the specimen is 350°C, the temperature of the inner specimen increases about 15% in the first 20 minutes, and then the temperature of the inner increases apparently. The vertical stiffness decrease nearly 7% and the horizontal stiffness decrease nearly 8% compared to the original specimen. The extreme compressive property has no apparent difference for both 2 types specimen when the stress is no more than 70Mpa, the extreme compressive stress is more than 90MPa determined by the specification from the figure 6. The inner rubber is nature rubber and the outer is neoprene rubber, it is observed that nearly 3mm thick carbonization is formed on protection rubber surface after the fireproof test.

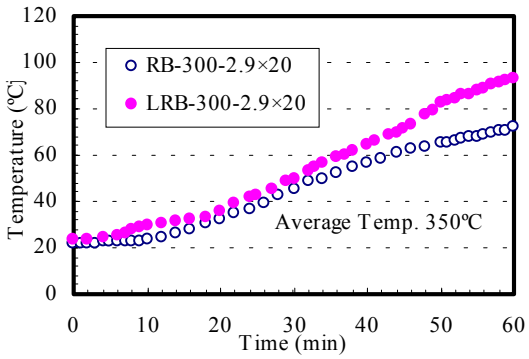

Fig. 5 Temperature of inner rubber

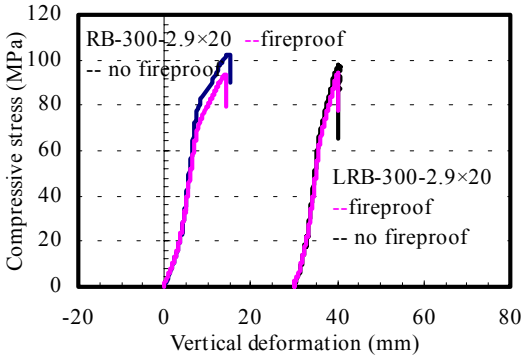

Fig. 6 Extreme compressive stress after fireproof test

Dependence

Dependence properties, such as compressive stress, shear strain, frequency, fatigue and temperature dependence, are also tested to grasp the characteristics of rubber bearings. The mechanical properties of stiffness and damping of rubber bearings should have little decline or increase. The environment temperature of rubber bearings varies according the climate. The vertical load to the rubber bearing changes greatly under a moderate to large earthquake. It is important that the building has enough safety under all these handicaps. The compressive stress from 5Mpa to 25MPa, temperature –25to 40ºC and load frequency 0.001Hz to 0.5Hz dependence of LRB-ϕ300 are shown in one figure with different horizontal axis, and another axis is a relative ratio normalized with the stiffness of 100% shear strain, see in figure 7.

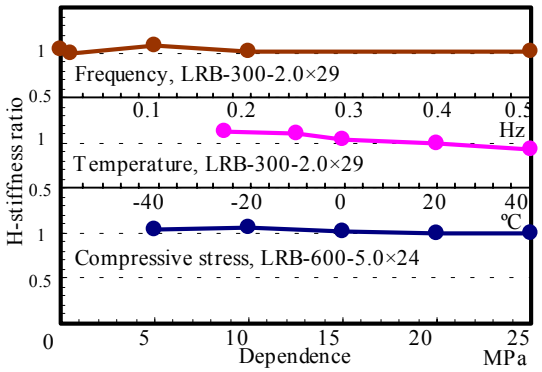

Fig 7. Dependence Properties (Compressive stress 5-25MPa, Temperature -25-40ºC, Frequency 0.001-0.5Hz)

Rotation

The mechanical characteristics take vertical stiffness, horizontal stiffness and yield stiffness for example, will vary when the test specimens create shear strain with fixed or unfixed rotation. 5 cases with different compressive stress, rotation and shear strain are considered to compare with a traditional test without rotation, the test contents are shown in table 1. The specimens used in the test are RB-ϕ300 and LRB-ϕ300.

The test results of both RB and LRB specimens are close in case 1,2 and 3, which have fixed rotation according to the shear strain-horizontal stiffness relationship shown in Figure 8. On the other hand, the load-displacement curve turns low when rotation of specimens vary in the test process in case 4 and 5.

Table 1. Test Contents with Rotation

Case	Compressive stress (MPa)	Rotation (rad.)	Shear strain (%)
1	10	0.0	10%~300%
2	5~15	0.0	10%~300%
3	10	+0.01	10%~300%
4	10	-0.01~+0.01	10%~300%
5	5~15	-0.01~+0.01	10%~300%

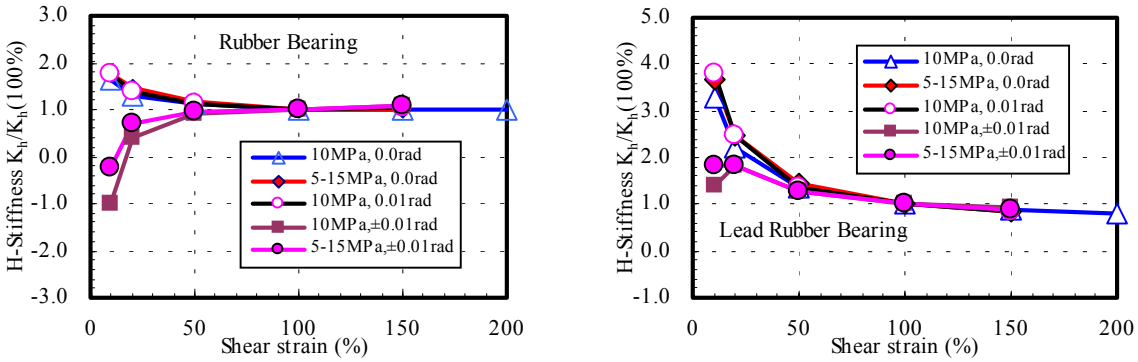

Fig. 8 Comparison of horizontal stiffness (Left: RB, Right: LRB)

The stiffness of RB turns stable with the increase of shear strain indicated in Figure 8, which is normalized with the value at shear deformation γ=100% in 5 cases. The test results of LRB are shown in Figure 8 too, it shows that mechanical characteristics are not stable in small shear deformation, however, the curve turns more stable when shear strain is more than 50%. The horizontal stiffness of RB specimen and yield stiffness of LRB specimen at shear strain γ=100% are shown in Table 2, which are normalized with the values tested in case 1.

Table 2. Horizontal stiffness and yield stiffness (Normalized with the value tested in case 1)

Specimen	Case 1	Case 2	Case 3	Case 4	Case 5	Case 1/numerical value
RB	1	0.913	0.903	0.699	0.728	0.985
LRB	1	1.001	0.904	0.746	0.811	0.982

PRODUCT SPECIFICATION

Properties of Rubber Bearings

Vertical and horizontal mechanical properties are shown in table 3.

Table 3. Vertical and horizontal mechanical properties

Item		Properties
Vertical properties	Stiffness	±20% of design value, ±10% of average value
	Deformation	$\left\|\frac{K_v(1,2,4,5)-K_v(3)}{K_v(3)}\right\| \le 10\%$ K_v(i): stiffness of i cycle
	Extreme compressive stress	≥90Mpa
	Elastic compressive stress	≥70Mpa
	Extreme compressive stress with horizontal displacement 0.55 rubber diameter	≥30Mpa
	Extreme tensile stress	≥1.5Mpa
	Elastic tensile stress	≥1.0Mpa

Horizontal properties	Stiffness	±20% of design, ±10% of average value (For inspection, shear strain 50,100,250% should be tested)
	Yield stiffness	
	Effective damping ratio	
	Extreme strain	≥350%

Durability properties, such as aging, creep, fatigue properties are shown in table 4.

Table 4. Durability properties

Item		Properties
Aging	Vertical stiffness	Varying percentage less than 20%
	Horizontal stiffness	
	Horizontal extreme strain	
	Effective damping ratio	
Creep	Deformation of rubber	Less than 5% of total thickness of rubber
Fatigue	Vertical stiffness	Varying percentage less than 20%
	Horizontal stiffness	
	Effective damping ratio	

Varying percentage of vertical stiffness, horizontal stiffness and effective damping ratio is less than 30% after the fireproof test. Dependence of rubber isolator should consider the vertical compressive stress, large shear strain, loading frequency and temperature.

Horizontal Conversion Intensity

A new concept, horizontal conversion intensity, is provided for analyzing the structural earthquake response instead of protected intensity used in calculating the earthquake response in China aseismic design code for traditional building. The horizontal conversion intensity is defined as follows:

(1) The intensity value is determined through the comparison of layer shear force between isolated building and non-isolated building. The horizontal conversion intensity equals to the protected intensity which is lowed, when isolated structure layer shear force less than 80% layer shear force of non-isolated structure with protected intensity lowed.

(2) For masonry structure and structures with basic period no more than site characteristic period, horizontal conversion intensity can be derived as follows:

The basic period of isolated structure is no less than the first critic period and the ratio to site period is no less than the minimum ratio that is shown in table 3, the horizontal conversion intensity is 1 degree lower than the protected intensity of site.

The basic period of isolated structure is no less than the second critic period and the ratio to site period is no less than the maximum ratio that is shown in table 5, the horizontal conversion intensity is 2 degree lower than the protected intensity of site.

(3) Horizontal conversion intensity should not be 2 degree lower than the protected intensity, and it should not be lower than 6 degree.

Table 5. Critic period and ratio of site characteristic period

Effective damping ratio	First critic period	Minimum ratio	Second critic period	Maximum ratio
0.05	1.1s	2.8	2.4s	6.0
0.10	0.85s	2.1	1.9s	4.8
0.15	0.72s	1.8	1.6s	4.1

Computation of Earthquake Response

The methods to calculate the earthquake response of isolated structure have effective lateral method and time-history method of earthquake response analysis.

The earthquake affective coefficient α_{max} with the damping ratio 0.05 can be adopted by protected intensity, site type and free vibration period of structure, which is shown in figure 1. Shape coefficient of the curve is constituted as follows:

(1) Linear ascending part, the period is less than 0.5s.
(2) Level part, 0.1s to characteristic period T_g.
(3) Descent part, T_g to 5 T_g, and the attenuation coefficient are 0.9.
(4) Slant part, 5 T_g to 6s, descent slope is 0.02.
(5) Characteristic period T_g, determined by the site and earthquake environment: 1st distinct shown in table 6, 2nd distinct $T_{g2} = \frac{7}{6} T_g$, 3rd distinct $T_{g3} = \frac{4}{3} T_g$.

Table 6. Characteristic period T_g of 1st distinct

Site	I	II	III	IV
T_g (s)	0.20	0.30	0.40	0.65

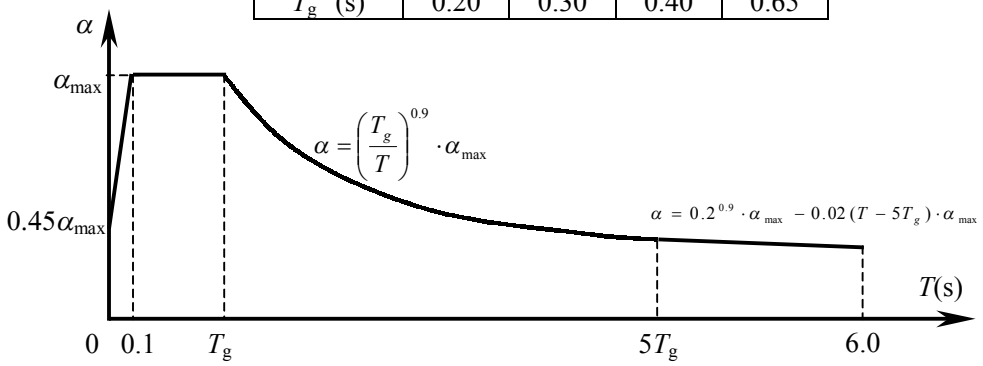

Fig. 9 Earthquake affective coefficient curve

When damping ratio of structure is not 0.05, the lateral earthquake affective coefficient curve is same as figure 1, but the shape coefficient should be corrected as follows:

(1) The attenuation coefficient γ of descent part is:

$$\gamma = 0.9 + \frac{0.05 - \zeta}{0.5 + 4\zeta} \tag{3}$$

(2) Slope η_2 of slant part is:

$$\eta_2 = 0.02 + \frac{0.05 - \zeta}{8} \tag{4}$$

The maximum affecting coefficient of lateral earthquake α_{max} should be adopted as follows:

(1) When structural damping is 0.05, α_{max} is shown in table 7.

Table 7. The maximum affecting coefficient of lateral earthquake α_{max}

Intensity	6	7	8	9
Little Earthquake	0.04	0.08	0.16	0.32
Middle Earthquake	0.113	0.23	0.45	0.90
Large Earthquake	0.25	0.50	0.90	1.40

(2) When structural damping ratio is not 0.05, α_{max} should consider of the correction coefficient η_1:

$$\eta_1 = 1 + \frac{0.05 - \zeta}{0.06 + 1.4\zeta} \tag{5}$$

The standard value and distribution of earthquake action should be considered as follows:

(1) The equations of standard value of total lateral earthquake action are:

$$F_{ek} = \alpha_1 G \tag{6}$$

$$\zeta = \frac{\sum K_i \zeta_i}{\sum K_i} \tag{7}$$

(2) For masonry structure and structures with height-width ratio less than 2, the lateral earthquake action of mass point is:

$$F_i = \frac{G_i}{\sum G_i} F_{ek} \tag{8}$$

(3) For other structures, the lateral earthquake action of mass point is:

$$F_i = \frac{G_i H_i}{\sum G_i H_i} F_{ek} \tag{9}$$

The equation to calculate the lateral displacement of isolation layer with effective lateral method is:

$$U_h = k \frac{F_{ek}}{\sum K_i} \tag{10}$$

The lateral displacement of isolator or damper should corrected with displacement coefficient η_t when torsion is considered, and η_t is:

$$\eta_t = 1+12\ e\ r\ /\ (b^2+l^2) \tag{11}$$

The choice of earthquake input wave, computation model and torsion action of 2-direction lateral earthquake action should be considered with time history method of earthquake response analysis to calculate structural response for isolated building.

CONCLUSION

The basic mechanical properties of Chinese rubber bearings are stable according to the statistics provided in the paper, the duration properties of acceleration aging, creep test show that Chinese rubber bearings have enough safety after 60 years followed by the product specification. The further, the dependence properties, such as different compressive stress, frequency, shear strain, temperature dependence, testify that all specimens have stable properties even if work in different conditions. The vertical stiffness and horizontal stiffness tested after the fireproof test decrease no more than 8% and the extreme compressive stresses are still more than 90MPa. The mechanical properties of rubber bearings with rotation are also provided in the paper, they show that Chinese rubber bearings have stable properties not only can be used in base isolation system but also in column top isolation system. A new concept, lateral conversion intensity is provided for design and analyzing the isolated structure in specification. Structural elements above isolation layer can be designed with lateral conversion intensity that is lower than protected intensity, reducing the cost of isolated building while structural safety is ensured.

NOMENCLATURE

K_v = vertical stiffness
α = coefficient
G_r = shear modulus
A = area of section
K_d = yield stiffness
K_{eq} = equivalent stiffness
δ = shear deformation
Q_d = yield load
ζ = damping ratio
F_{ek} = standard value of total lateral earthquake action of structure
α_1 = affecting coefficient of lateral earthquake action corresponded to free vibration period of isolated structure

G = total gravity value of structural elements above isolation layer
ζ = effective damping ratio of isolation layer
K_i = effective stiffness of single isolator
ζ_i = effective damping ratio of single isolator
U_h = displacement of isolation layer.
k = near site coefficient, the distance to causative fault d≤5km, k=1.5; 5km<d≤10km, k=1.25; d>10km, k=1.0.
r = distance between isolator and rigidity center of isolation layer
b, l = short, long side of structural plane.
e = eccentricity between mass center of structure and rigidity center of isolation layer, which include actual eccentricity and occasional eccentricity (0.05b)

REFERENCES

1. Chinese Committee of Seismic Control for Structures, "Product standard of rubber isolator for building ", 2000, pp. 1-10.
2. Japan Society of Seismic Isolation, "An Introduction to Seismic Isolation", Ohmsha, 1995, pp. 73-80.
3. Zhou, F.L., , "Seismic Reduction and Control of Structures", Seismological Press, 1997, pp. 102-104.
4. "Eurocode 8-Design provision for earthquake resistance of structures-Part2: Bridge", European Prestandard ENV 1998.
5. Skinner, R.I., W.H. Robinson and G.H. McVerry, "An Introduction to Seismic Isolation", John Wiley & Sons Ltd, England, 1993.
6. Architectural Institute of Japan, "Recommendation for the Design of Base Isolated Buildings", Architectural Institute of Japan, 1993.
7. Feng, D.M., Liu, W.G. and Zhou, F.L., "Characteristics of Large Size Rubber Isolator with Lead-Damper", Theories and Applications of Structural Engineering, Yunnan Science & Technology Press, 1998, pp. 254-260.
8. Yang, Q.R., Liu, W.G. and Zhuang, X.Z., "Entire stiffness, Rotational Stiffness and Properties of High Compressive Stress of Rubber Bearings", Earthquake Engineering and Engineering Vibration, Vol. 20, No.4, Dec., 2000, pp. 118-125.
9. Liu, W.G., Zhuang, X.Z. and Zhou, F.L., "Duration and Fireproof Properties Research on Rubber Bearings", Journal of South China Construction University (West Campus), Vol. 8, No.3, Sept., 2000, pp. 1-10.

R&D in Progress at ENEA on the Innovative Anti-Seismic Techniques, with Particular Attention to the Industrial Plants

Alessandro Martelli [1)], Massimo Forni [1)], Alessandro Poggianti [1)], Bruno Spadoni [1)]

1) ENEA & GLIS, Bologna, Italy

ABSTRACT

Reported in this paper are some features of R&D recently performed and in progress at the Italian Agency for New Technology, Energy and the Environment (ENEA) on seismic protection of structures, in particular industrial plants, through innovative anti-seismic (IAS) techniques, namely seismic isolation, passive energy dissipation and semi-active control. This work is being performed in the framework of both new projects funded by the European Commission and a national project funded by the National Research Council. The first (SPACE and SPIDER) aim at the development of floor isolation systems, semi-active systems and systems formed by energy dissipation devices and cables. The second (ISI), to which this paper mainly refers, aims at the development of suitable IAS systems for the protection of high risk components in highly seismic areas and already provided very important results, in particular for tanks containing hazardous materials: in fact, ISI makes reference to a real component, located in a highly seismic Italian site, which will be possibly retrofitted using IAS techniques.

INTRODUCTION

Large R&D efforts are going on in Italy, in particular at the Italian Agency for New Technology, Energy and the Environment (ENEA), on seismic protection of structures, in particular industrial plants, through innovative anti-seismic (IAS) techniques, namely seismic isolation (SI), passive energy dissipation (ED) and active (AC) semi-active control (SAC). This work is being performed in the framework of both new projects (SPACE and SPIDER) funded by the European Commission (EC) and a national project (ISI) funded by the National Research Council (CNR).

ISI, to which this paper mainly refers, aims at the development of suitable SI systems for the protection of high risk plants and components in highly seismic areas. While the EC-funded projects began in March-April 2000, the CNR-funded project began in 1998. It already provided very important results, in particular for tanks containing hazardous materials: for these, the study is being based on a real chemical component, located at a highly seismic Italian site, which will be possibly retrofitted using IAS techniques at the end of the study. Should this pilot application be carried out, it will be the first in Italy to a high risk component and may lead to an extensive use of SI in industrial plants.

The SPACE Project ("Semi-active and PAssive Control of the dynamic behavior of structures subjected to Earthquakes, wind and vibrations") aims at developing new devices for the AC and SAC of the earthquake effects on civil buildings, industrial plants and bridges. This project also includes the development of innovative devices for SI of single floors or parts of buildings containing cultural heritage objects (museums), costly tools (computers) or critical components from a safety point of view (control rooms, surgeries and other hospital facilities). SPACE is coordinated by Maurer-Söhne (Germany); the partnership includes, in addition to ENEA, the German Billfinger+Berger, the Italian ENEL.HYDRO, ENEL.HYDRO-ISMES and "Roma Tre" University, the Swedish Stockholm University, the French Thomson-Marconi and the British TARRC Center.

The most important and innovative aspect of the SPACE Project is the development of semi-active magneto-rheological devices. These devices permit the variation of stiffness and energy dissipation of the SI system using a small quantity of power (only a few Watts). Furthermore, this system provides a basic "passive" behavior that gives the structure a good level of protection also in case of failure of the control system. In particular, these devices make use of fluids with mechanical characteristics dependent on the magnetic field in which they are immerged. During an earthquake the magnetic field can be easily changed using a low current flux controlled by a computer. The computer elaborates data coming from the sensors and intervenes to modify the characteristics of the system to obtain a sort of "intelligent control".

The SPIDER Project ("Strands Prestressing for Internal Damping of Earthquake Response") aims at developing an IAS system based on the use of dampers connected in series with pretensioned cables (Damper Cable System, DCS), which act on the whole structure by reducing the seismic effects on its various floors. This system acts by transferring the whole interstorey drifts of all floors (or sets of them), by means of a special steel cables, to dampers installed at the building base (or only on some selected floors): in this way, dampers are able to dissipate a large seismic energy, since they are subjected to large differential displacements. The cables are pretensioned to keep positive the tension stresses during the earthquake and to provide a re-centering force at the end of the seismic event. DCS is particularly beneficial for retrofit of existing structures, for instance for civil buildings, due to its low cost and easy application.

SPIDER is coordinated by Bouygues (France); the partnership includes, in addition to ENEA, the Italian ENEL.HYDRO-ISMES and Udine University, the French Jarret e VSL and the Portuguese A2P Consult Ltd.

MAIN FEATURES OF THE ISI PROJECT

The ISI Project is devoted to the seismic protection of high risk industrial plants, in particular chemical plant components. While in several countries there are already numerous applications of SI systems to civil buildings (more than one thousand) and to bridges and viaducts, the number of those to industrial plants and components is still rather limited. In particular, very few (none in Italy) are still the chemical plants or components making use of such systems, in spite of their demonstrated large benefits to improve safety without complicating plant layout.

These are the reasons why, in 1998, the Italian Agency for the Environment (ANPA), ENEA and the University of Roma "La Sapienza" jointly undertook a study, funded by CNR, to evaluate the benefits of applying SI to the protection of industrial (in particular, chemical) plants and components. This study includes the following activities:

1. Identification of a reference typical component. The aim is also to make a real SI application possible, at the conclusion of the study. Thus, an existing component had been selected.
2. Analysis of the selected component with regard to both chemical and structural / mechanical engineering aspects, with the evaluation of seismic risk and consequences of possible accidents due to seismic events.
3. Definition of structural and functional requirements of the SI system.
4. Definition of the design vibratory motion for the site where the reference component is installed.
5. Choice of the most adequate SI system for the selected component and its detailed design.
6. Analysis of the isolated component, with evaluation of SI effects on seismic resistance, functionality, layout and costs.
7. Collection of data for general application of results to other components.

The first results of the ISI Project where jointly presented by the partner at the 2nd European Conference on Structural Control [1] and at the 2000 ASME-PVP Conference [2]. The most important are reported below.

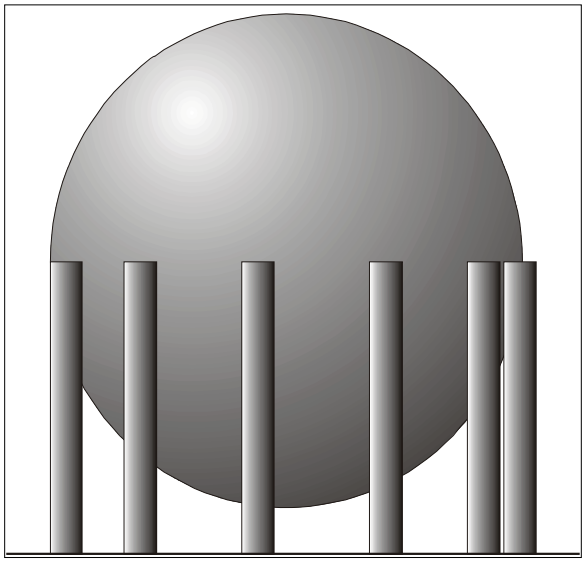

Figure 1: Sketch of the tank selected

SELECTED STRUCTURE

A tank has been selected for the study. More precisely, it is an existing spherical storage tank for liquids, located in the South of Italy. The tank has a diameter equal to 21 m (Volume 5000 m^3) and is supported by eleven 12.5 m high columns, with a diameter of 1 m (Figure 1). The tank walls are 22 mm thick and the total height of the structure is 23.5 m. The mass of the structure depends on the level of liquid in the tank: it ranges from about 310 tons (empty tank) and about 3,300 tons (full tank). Thus, the vertical load acting on the each column varies from about 280 kN to about 3,000 kN. This makes it necessary that great care is devoted to the design of the SI system, as stressed in the following sections.

PROPOSED SEISMIC ISOLATION SYSTEM

In general, a SI system must ensure the following two functions:

1. support the dead load of the structure by avoiding rocking motions during earthquakes;
2. allow for horizontal displacement during earthquakes.

Moreover, a good SI system should also satisfy two further function:

1. provide an adequate restoring force during and at the end of the earthquakes;
2. dissipate a sufficiently large amount of energy.

Aim of function (2) is to move the natural frequency (f) of the structure in a range of the response spectrum which is characterized by a low energy content. This depends on the supported mass M, since $f=\sqrt{(K/M)}$, where K is the total stiffness of the SI system. Thus, in order to have a constant isolation frequency, a SI system with a stiffness proportional to the supported mass would be necessary. Since active control technology is not yet mature for application in the seismic field, especially to high risk plants, the only available system which is able to provide such a behavior is a passive SI system based on friction devices. In fact, the reaction force provided by such SI devices is proportional to the mass through the

friction coefficient.

The SI systems which have been analyzed in this study are formed by Sliding Devices (SDs), High Damping Rubber Bearings (HDRBs) or Elastic-Plastic Devices (EPDs). SDs consist of dimpled lubricated PTFE sheets sliding on a polished stainless steel surface, similar to those usually used for SI of bridges and viaducts. For low-speed (thermal) movements**,** the quasi-static coefficient of friction of the sliding elements has been assumed to be μ_s=0.003, while in the presence of high-speed (seismic) movements**,** the dynamic coefficient of friction to be assumed is μ_d =0.01.

In the mixed (HDRBs coupled with SDs) SI system, SDs provide reaction forces and energy dissipation related to the fluid mass contained in the tank, while HDRBs provide the needed restoring force and further energy dissipation. Thus, such an SI system ensures that the previously mentioned four functions are all satisfied.

NUMERICAL MODELS

Two finite-element models (FEMs) of the selected tank were implemented in the ABAQUS code [3]. The first is a simplified model formed by beams, springs and concentrated masses, which has been used for quick parametric analyses. The second is a detailed FEM of the whole structure consisting of over 900 nodes and 850 beam and shell elements (Figure 2), which was used for the final analyses. In both cases the fluid mass was represented by a concentrated mass rigidly connected with the tank wall. Similar model have also been developed and implemented in SAP 2000 code. A simple model with a one degree of freedom oscillator was also used .

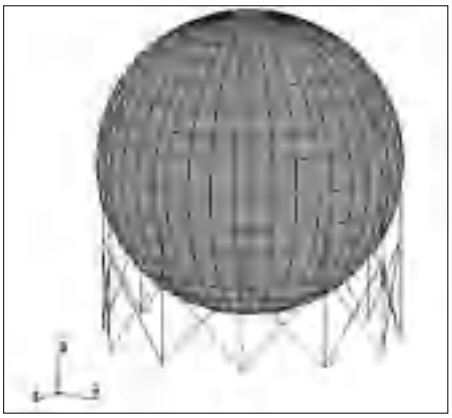

Figure 2: Detailed Finite Element Model

In the calculations, different condition corresponding to empty, full (80% of internal volume filled with liquid, in normal condition) and semi-full (50% of volume filled) has been considered. In a further step of the analysis, the effects of the liquid level and related sloshing-induced forces were also taken into account, according to Nuclear Reactors and Earthquakes standards, Sect. 6.3 (Vibrations of Liquids in Tanks).

The HDRBs (see an example in Figure 3) and the SDs devices were numerically modeled in ABAQUS code by coupling a spring and an elastic-plastic truss, which is a beam working only in the axial direction, that provides the energy dissipation (Figure 4).

Figure 3: HDRB isolation device

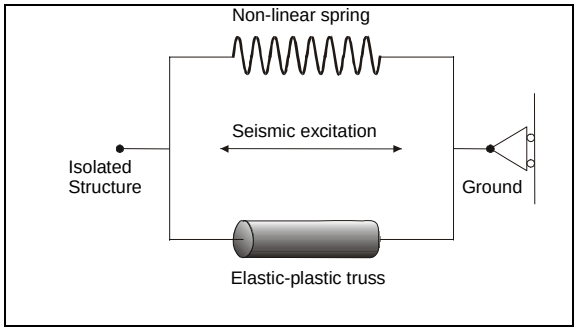

Figure 4: Simplified model of the HDRB

Thus, the hysteresis loop of the HDRB model results to be bilinear, which provides a good approximation of the real behavior. In the SD model, the stiffness of the spring is neglected and the related hysteresis loop simply has a rectangular shape. An example of an EPD is shown in Figure 5, his hysteresis loop is shown in Figure 6.

SEISMIC INPUT

Based on a design response spectrum, which satisfies the requirements of the Italian design guidelines for isolated structures [4] for the site, multiplied by an 'Importance Factor' of 1.4 to take into account the importance of the structure from the risk point of view), several acceleration time-histories were generated and used in the analyses with ABAQUS code.

Figure 5: Elastic-Plastic Device

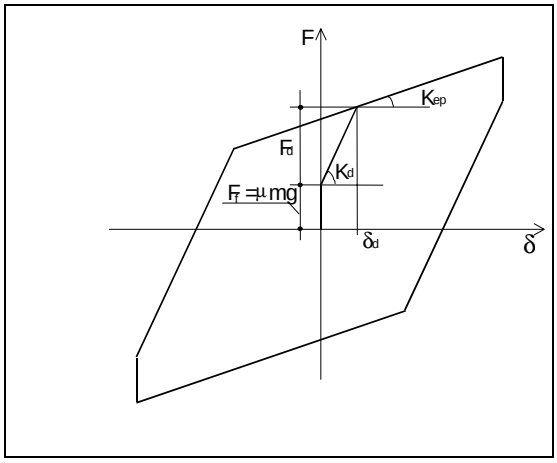

Figure 6: Hysteresis loop of the EPD

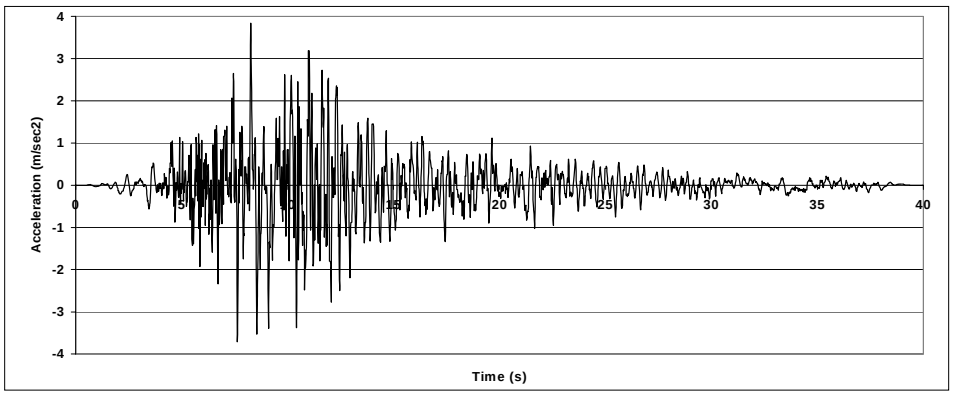

Figure 7: Ground acceleration time-history used in the dynamic analysis

Figure 7 reports, as an example, a 40 s time-history with a peak acceleration equal to approximately 0.4 g. In this way the earthquake considered has a probability of occurring once every 1000 years.

VERIFICATION CRITERIA

In this study, the first yielding of the base of the columns supporting the tank was assumed as a verification criterion of the structure in the analysis performed using the ABAQUS code. Stresses in the columns were evaluated taking into account the dead load of the structure, the maximum bending moment and the shear force calculated during the dynamic analyses.

NUMERICAL ANALYSES

Fixed base configuration.

The detailed and simple models described above were used to evaluate the values of natural frequencies and related participation factors of the tank. Table 1 reports the first 3 natural frequency values in the case of empty and full tanks, in

Table1: First natural frequencies of the tank in the fixed base configuration.

	Frequency (Hz)							
	Empty tank				**Full tank**			
Mode	ABAQUS		SAP	One DoF	ABAQUS		SAP	One DoF
n°	Simpl.	Comp.	2000	Osc.	Simpl.	Comp.	2000	Osc.
1	3.39	3.39	2.78	3.45	1.09	1.10	0.93	1.19
2	3.39	3.39	3.85		1.09	1.10	1.14	
3	4.27	4.16			4.27	4.16		

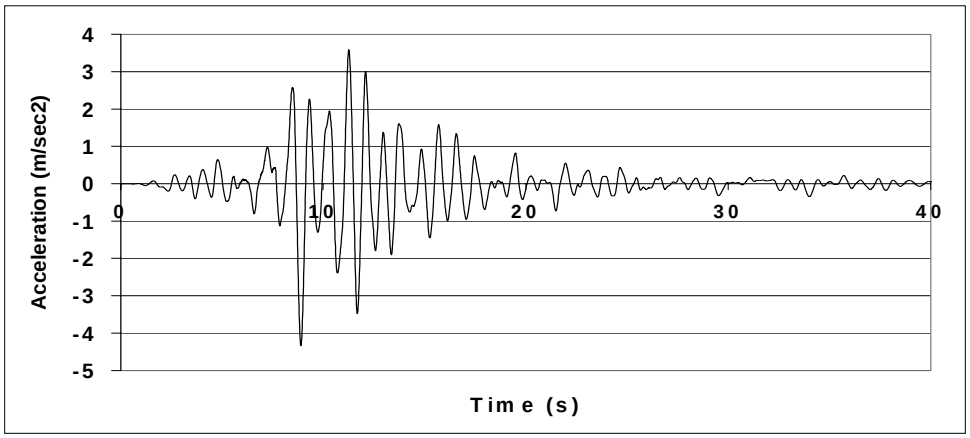

Figure 8: Full tank acceleration in fixed base condition

the fixed-base configuration, which characterizes the tank at present. It is worthwhile noting that the first two bending modes participate with over 95% of the total mass of the structure in the case of empty tank, and over 99% in case of full tank, the third mode is a torsional mode and it is not activated by the earthquake. The comparison of the results obtained by the different models demonstrates that the structure behaves like a single degree of freedom oscillator and that the simplified model can be correctly used. In spite of this simple behavior, the structure must be analyzed using a step by step procedure, due to the non-linear features of the anti-seismic devices.

After completing the modal analysis, some dynamic calculations were also performed on the tank in the fixed-base configuration. It was found that, based on the criteria discussed in the previous section and for the considered seismic input of Figure 7, the structure is positively verified in the case of empty tank. On the contrary, in the case of full tank, the deformation of the columns resulted to be too large and calculations showed that plasticization of the steel occurs.

In Figure 8 is reported the full tank acceleration during the earthquake calculated by ABAQUS with a step by step analysis

Isolated configuration.

Since in the case of empty tank the structure had been positively verified at fixed base, only the case of full tank has been considered for the analysis with SI using ABAQUS code and a step by step integration.

In this analysis the tank was conservatively considered full at 100% of the internal volume. First, a SI system formed by 11 HDRBs (with no SDs) was considered. Two different sizes of HDRBs were analyzed in order to obtain some parametric data on the dynamic response of the structure. The first HDRB (H1) was characterized by a diameter of 800 mm, a rubber height of 100 mm and a shear (G) modulus of 0.8 MPa, which lead to a stiffness of 4,000 N/mm. The second HDRB (H2) had a diameter of 700 mm a rubber height of 150 mm and the same G modulus as H1; thus, the stiffness results to be equal to 2,000 N/mm. In both cases a value of 10% was assumed for the equivalent viscous damping ratio.

The results of dynamic analyses showed a strong reduction of the acceleration of the tank with respect to the input time-history. In addition, the deformation of the devices (about 150 mm) resulted to be very close to the rubber height of the isolator (100% shear strain). However, unfortunately, the deformation of the columns resulted to be too large and the

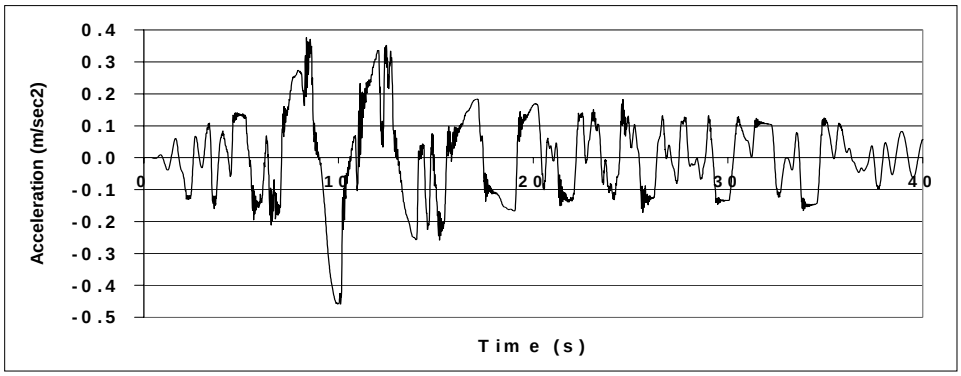

Figure 9: Full tank acceleration in the case 3 H2 and 8 Sliding Devices

verification criteria of the structure were not respected in both cases.

Thus, further analyses were performed with a modified SI system. Since the case of H2 isolators had provided the best results, a softer SI system, formed by sliding devices and HDRBs of the H2 type was considered. In this case also, two different configurations were considered, which were characterized by 5 and 3 type H2 HDRBs, respectively. In this case in order to distribute uniformly the load on the columns, they were connected one with the other by means of rigid bars positioned just above the SI system.

In both cases, the tank acceleration strongly decreased compared to the fixed base configuration, even of a factor 10, in the case with 3 HDRBs, (Figure 9). Moreover, in this case, deformation of the columns was calculated to be 11 mm; and the verification criteria were satisfied. Of course, the deformation of the devices, that is the relative displacement between the structure and the ground, increased. However this increment was not so dramatic, especially in the case with 3 HDRBs. In fact, in this case, the deformation of the HDRBs was calculated at about 190 mm, corresponding to 125% rubber shear strain, which is an admissible value according to the Italian design guidelines for seismically isolated structures [4].

In the last step of the study the effects of the liquid level and related sloshing-induced forces were taken into account. To simulate the sloshing effect, according to Nuclear Reactors and Earthquakes standards, Sect. 6.3 (Vibrations of Liquids in Tanks), a system formed by two concentrated masses substituted the mass of the fluid. One of them, rigidly connected to the tank wall, simulating the part of the fluid that acts as a solid mass and the other, connected to the tank wall by a spring, simulating the portion of the fluid oscillating inside the tank.

Comparing the stress and the deformation of the most loaded column both in fixed base and isolated condition with and without the sloshing effect, we can see that it reduces the stress and the deformation of the columns and increases the natural frequencies.

All the results are summarized in Table 2 in terms of maximum Tresca equivalent stress at the base of the most loaded column and of maximum tank displacement.

Table 2: Summary table for the ABAQUS calculations

Empty	Full 100%	Full 80%	Sloshing	Seismic Isolation	TRESCA Stress MPa	Displac. Mm	Accel. m/sec^2
X				NO	227	26	12.3
X				3 HDRB + 8SD	99	71	1.60
	X			NO	901	107	4.12
	X			11 HDRB H=100	341	187	1.57
	X			11 HDRB H=150	346	199	1.14
	X			5 HDRB +6 SD	264	232	0.68
	X			3 HDRB +8 SD	215	205	0.42
		X		NO	758	90	4.33
		X	X	NO	660	77	5.14
		X		3 HDRB +8 SD	183	187	0.46
		X	X	3 HDRB +8 SD	161	118	0.52

Different solutions were studied using different models. The SAP 2000 model was used to analyze the present situation for full, semi-full and empty tank, finding that the full tank is not able to withstand the design earthquake, and than used to study a SI system formed by 11 HDRB with 600 mm diameter and 156 mm high rubber.

Also with the SAP 2000 model the sloshing effect was analyzed, following the mentioned standards, and finding that the sloshing has a positive effect in reducing the stresses at the columns base.

Table 3: Results of SAP 2000 analysis fixed base and isolated (in brackets) tank

Tank analysis	1st Period s	2nd Period s	$\sigma_{max.}$ at the column base Mpa	σ_{min} at the column base Mpa	Max Tank Displacement cm
Full without sloshing	1.08 (3.08)	0.880 (2.5)	380 (-12)	-532 (-160)	9.7 (21.8)
Full with sloshing	4.63 (4.93)	0.86 (2.26)	278 (-58)	-425 (-115)	7.6 (16.3)
Semi-full with sloshing	5.30 (5.23)	0.59 (1.59)	194 (-36)	-295 (-76)	5.3 (12)
Empty	0.36 (1.03)	0.26 (0.8)	129 (10)	-147 (-30)	2.9 (9)

The results of the SAP 2000 analysis are summarized in Table 3, in brackets are indicated the value for the isolated tank. It is possible to see that the isolation has strongly positive effects in all the situations evaluated.

Using the simple one degree of freedom (DoF) oscillator model, several situations were studied. First of all it was used to evaluate the actual situation with the tank rigidly connected to the ground. A conventional base isolation with Rubber Bearings (RBs) was than analyzed. The RBs are schematized adding a new spring with stiffness K_d to the spring with stiffness K_s simulating the structure stiffness, (Figure 10), where C_s is the structure damping). The results are reported in Table 4 in terms of oscillation period and total shear force at the base of the columns.

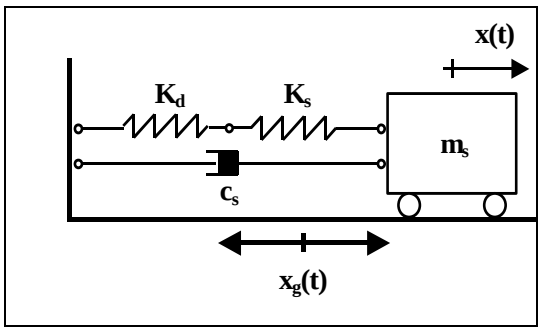

Figure 10: Simplified model for base isolation with Rubber Bearings

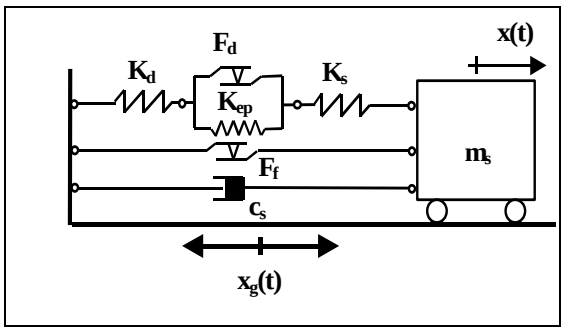

Figure11: Simplified model for base isolation with Elastic-Plastic Devices

Table 4: Results of one degree of freedom analysis for base isolation with Rubber Bearings

Load Condition	80%	50%	Empty
T (s)	3.00	2.24	1.00
F (kN)	2900	2250	1000
Displacement (m)	0.243	0.181	0.080

The second solution foreseen an increase of the dissipation of the structure by means of internal or external device (Figure 12). In this case, due to the mechanical characteristics of the structure, the reduction of the lateral load induced by the seism is not sufficient, thus this solution was considered not suitable for this type of application.

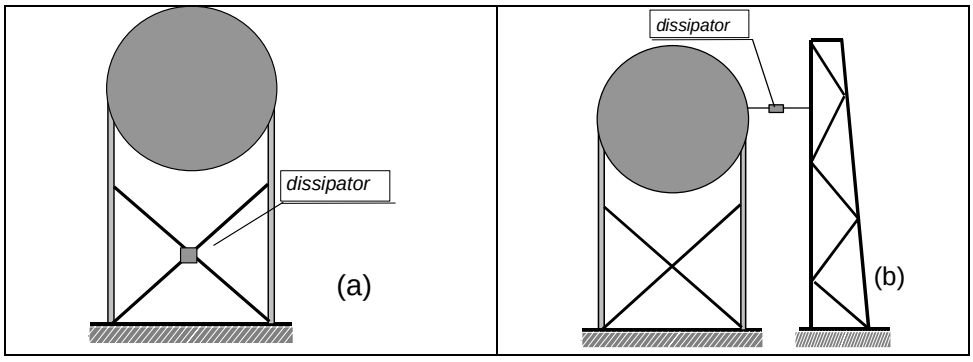

Figure 12: Internal and External Dissipative Devices

The third solution studied considered the application of elastic-plastic devices (an example is shown in Figure 5), positioned between the base of the columns and the foundation. These devices are largely used in bridges and viaducts and their aim is to change the natural frequencies of the structure but, above all, to increase the dissipation capability of the structure. Their hysteresis loop is shown in Figure 6 where K_d is the initial elastic stiffness, K_{ep} the secondary elastic-plastic stiffness, F_d the yield force, F_f the friction force, δ_d the yield displacement. These devices are introduced in the single DoF model as shown in Figure 11. Some parametric calculations were performed with different values of the elastic stiffness K_d, of the friction coefficient μ and of the plastic stiffness K_{ep}.

The best design solution to reduce the shear force and the mass displacement was the one with $K_d=0.5K_s$. In Table 5 the results obtained with $K_d = 0.5K_s$, $\mu = 0.01$ and $K_{ep} = 0$ are shown in terms of period of oscillation, total shear force at the

columns base, displacement of the tank as regards to the device and displacement of the tank.

Table 5: Results of one degree of freedom analysis for isolation with Elastic-Plastic devices

Load Condition	80%	50%	Empty
T (s)	1.45	1.09	0.50
F (kN)	1195	1080	961
Displacement (m)	0.144	0.061	0.041
Rel. Displacement (m)	0.006	0.006	0.006
Acceleration (g)	0.050	0.080	0.325

A summary of the most promising solutions proposed, in terms of total shear force at the base of the columns and tank displacement reported in Table 6.

Table 6: Comparison of the different solutions

	Total Shear Force (kN)		Displacement (mm)	
	Full	Empty	Full	Empty
Fixed Base	14400	3890	90	32
11 HDRB	2900	1000	243	80
Mixed	1260	470	187	71
11 EP	1195	961	144	41

CONCLUSIONS

The main features of ongoing EC-funded projects (SPACE and SPIDER) on the development of IAS techniques, which involve ENEA, have been shortly summarized. More details have been provided on the ISI national project; in particular, the benefits of SI of an existing spherical tank were analyzed in this study. Different SI systems were considered by ANPA, ENEA and the University of Rome "La Sapienza". The most promising solutions resulted to be a system formed by 3 HDRBs (acting as isolators, dissipators and re-centering devices) and 8 SDs (acting as isolators and energy dissipators) and a system formed by 11 EPDs. The mixed SI system provides a sufficient restoring force and an energy dissipation related to the fluid mass inside the tank, but with a displacement of about 200 mm during the earthquake. The SI system formed by 11 EPDs offers a lower displacement during the earthquake, but with a small residual displacement after the earthquake (about 40 mm). Both the systems offer a strong reduction of the forces transmitted to the structure during the earthquake. Being the benefits of the SI system confirmed, it might be used to really retrofit the considered tank.

The ISI project is fully consistent with the recommendations of the 6th International Post-SMiRT Conference Seminar on Seismic Isolation, Passive Energy Dissipation and Active Control of Vibrations of Structures held at Cheju (Korea) in 1999, [5] where the importance of application of the IAS techniques to chemical plants had been stressed.

ACKNOWLEDGMENTS

The authors warmly thank their colleagues of ANPA (Dr. T. Sanò and A. Pugliese) and University of Rome La Sapienza (Prof. V. Ciampi and Dr. D. Addessi) for having made available their results for comparison with those of ENEA.

REFERENCES

[1] Forni, M., Martelli, A., Poggianti, A., Spadoni, B., Pugliese, A., Sanò, T., Addessi, D., Ciampi, V. and Foraboschi, F. P., "Development of Innovative Anti-Seismic Passive Systems for the Protection of Industrial Structures and Components", *Proc. Of the 2nd European Conference on Structural Control*, Champ sur Marne, France, July 2000.

[2] Forni, M., Martelli, A., Poggianti, A., Spadoni, B., Pugliese, A., Sanò, T. and Foraboschi, F.P., "Studies Performed in Italy for Seismic Isolation of Chemical Plant Components", *Proc. Of the 2000 ASME-PVP Conference*, PVP-Vol. 402-1, pp. 185-192, Seattle, Washington, USA, July 2000.

[3] Hibbitt, Karlsson & Sorensen, Inc., *ABAQUS User's and Theory Manuals*, Pawtucket, RI, USA, 1998.

[4] CSLLPP, *Linee Guida per la Progettazione, Esecuzione e Collaudo di Strutture Isolate dal Sisma*, Ministero dei Lavori Pubblici, Presidenza del Consiglio Superiore dei Lavori Pubblici, Servizio Tecnico Centrale, Rome, Italy 1998.

[5] Martelli, A., Forni, M., Koh, H.M., "Main Features and Conclusions of the 1999 International Post-SMiRT Conference Seminar on Seismic Isolation, Passive Energy Dissipation and Active Control of Vibrations of Structures", *Proc. Of the 16th SMiRT International Conference*, Washington, DC, USA, 2001.

Performance Tests of Reactor Containment Structures of the HTTR

Kazuhiko IIGAKI, Nariaki SAKABA, Satoshi KAWAJI and Tatsuo IYOKU

Department of HTTR Project, Oarai Research Establishment, Japan Atomic Energy Research Institute, Oarai-machi, Higashiibaraki-gun, Ibaraki-ken, Japan

ABSTRACT

The containment structures of the high temperature engineering test reactor (HTTR) consist of a reactor containment vessel (CV), a service area (SA) and an emergency air purification system, which minimize the release of fission products from the reactor facilities in the postulated accidents. In the high temperature gas-cooled reactor, the pressure boundary of coolant in the leakage test should be closed to prevent from releasing of fission products into the CV. Thus, we propose to perform the overall leakage test of the CV keeping the pressure boundary of coolant closed and the local leakage test of the CV isolation valves. Results of performance tests of the CV, the SA and the emergency air purification system could meet the requirement for them.

INTRODUCTION

The high temperature gas-cooled reactor (HTGR) is expected to be one of alternative energy sources in the near future because it can supply high temperature heat and has high thermal efficiency. The high temperature engineering test reactor (HTTR) [1] built by Japan Atomic Energy Research Institute (JAERI) as the first HTGR in Japan, attained its first criticality on November 10 in 1998. The HTTR is a graphite-moderated and helium-gas-cooled test reactor with an outlet gas temperature of 850℃ at the rated operation and 950℃ at the high temperature test operation as well as a thermal power of 30MW. Table 1 shows the major specifications of the HTTR.

Table 1 Major specifications of the HTTR

Thermal power	30MW
Outlet coolant temperature	850/950℃
Inlet coolant temperature	395℃
Primary coolant pressure	4MPa
Fuel	Low-enriched UO_2
Fuel element type	Prismatic block
Direction of coolant flow	Downward flow
Pressure vessel	Steel
Plant lifetime	20yr

Fig.1 shows an outlined description of the containment structures of the HTTR [2]. The containment structures of the HTTR consist of the reactor containment vessel (CV), the service area (SA) and the emergency air purification system, which minimize the release of fission products from the reactor facilities in the postulated accidents.

Prior to startup core physics tests of the HTTR, the JAERI carried out performance tests of the reactor containment structures with no fuel conditions in 1996. These tests are also perfomed every year afer fuel loading.

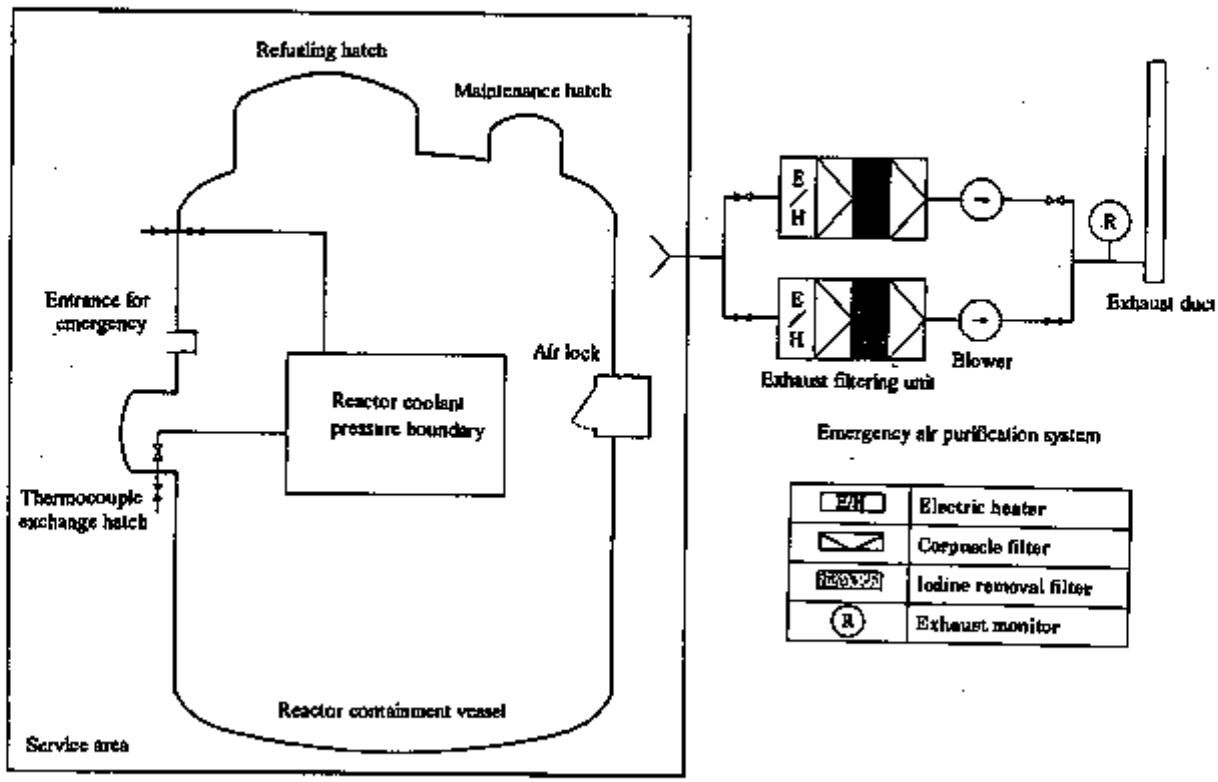

Fig.1 Outlined description of containment structures of the HTTR

In conventional light water reactors (LWRs), the leakage test of the CV is conducted keeping the pressure boundary of coolant open [3]. However, the pressure boundary of coolant in the leakage test of the HTGR should be closed to prevent from releasing of fission products into the CV. Thus, we put forward to perform the overall leakage test of the CV keeping the pressure boundary of coolant closed and the local leakage test of the CV isolation valves. The leakage rate of the CV is estimated considering results of the overall and local leakage tests.

In this paper, the conditions and the results of the performance tests of the reactor containment structures are described.

OUTLINE OF REACTOR CONTAINMENT STRUCTURES

Reactor Containment Vessel

The CV made of carbon steel is 30.3m in height, 18.5m in inner diameter, and 2800m^3 of free volume. Its configuration is shown in Fig. 1. The CV is designed to withstand the temperature and pressure transients and to be leak-tight within the specific limits in case of a rupture of primary piping; i.e. depressurization accident [4]. The size of the CV is smaller than that in the LWRs to minimize the amount of air which may react with in-core graphite components during the depressurization accident.

The CV is also designed to maintain less than 0.1%/day of air weight in the CV at room temperature and 0.9 times that maximum service pressure of 0.4MPa. Table 2 shows the major specifications of the CV.

Table 2 Major specifications of CV

Type	Cylindrical vessel
Maximum service pressure	0.4MPa
Maximum service temperature	150℃
Size	
Inner diameter	18.5m
Overall height	30.3m
Body thickness	30mm
Top head closure thickness	38mm
Free volume	2800m^3
Material	Carbon steel
Allowable limit of leakage rate	Less than 0.1%/day of air weight in CV at room temperature and 0.9 times that maximum service pressure of 0.4MPa

Service Area

The SA surrounding the CV is the space containing the fuel handling and storage systems as well as the primary helium purification system. The free volume of the SA is about 23000m^3. The air pressure inside the SA is maintained to be slightly lower than that of atmosphere by the air ventilation system in the normal operation and by the emergency air purification system in an accident.

Emergency Air Purification System

The emergency air purification system removes airborne radioactivities and maintains proper pressure in the SA during the accidents. Also, it has two lines as shown in Fig. 1. Each line is composed of an exhaust filtering unit, an exhaust blower and butterfly valves. The exhaust filtering unit discharge the purified air to atmosphere through an exhaust duct. Table 3 shows the major specifications of the emergency air purification system.

Table 3 Major specifications of emergency air purification system

Exhaust filter unit	
Type	Corpuscle and iodine removal filter
Number	2
Each volume velocity	3360m^3/h
Charcoal layer thickness	50mm
Allowable limit of removal efficiency	
Iodine	More than 95%
Corpuscle	More than 99%

PERFORMANCE

CV Leakage Test

The overall CV leakage test is based on the absolute pressure method according to the rule of the CV leakage experiment by JEAC 4203-1994 [5]. The leakage rate, obtained from the change of air weight using variations of air temperature and pressure in the CV, treats statistically. Accuracies of thermometer for air temperature and quartz manometer for air pressure are ±0.01℃ and ±0.01%, respectively.

Amount of leakage Q (%) is evaluated through the absolute air pressure and temperature in the CV, and is given by equation (1).

$$Q = \frac{G_1 - G_2}{G_1} \times 100 = \left(1 - \frac{Pm_2 T_1}{Pm_1 T_2}\right) \times 100 \quad (1)$$

Q: amount of leakage	(%)
G: air weight	(kg)
Pm: absolute air pressure in CV	(mmHg)
T: absolute air temperature in CV	(K)

Prior to the overall leakage test, it is confirmed that the CV retains the boundary under the air pressure condition of 0.44MPa. After that, the overall CV leakage test was performed keeping the air pressure of 0.36MPa and the coolant pressure of 0.05MPa. Fig. 2 shows a transient of amount of leakage in the CV between October 24 and 31 in 1996. As a result of the leakage test, the leakage rate of the CV was 0.018%/day, which was well below the allowable limit of 0.1%/day.

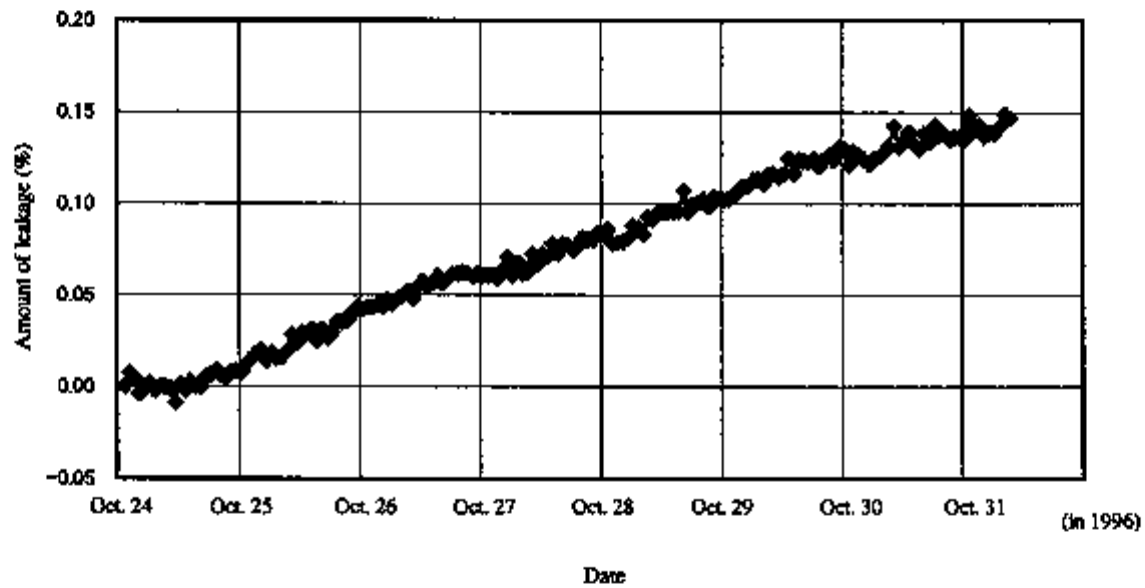

Fig.2 Transient of amount of leakage in CV

Table 4 CV leakage test results

	First test (Oct. 1996)	Second test (Sep. 1999)	Third test (Dec. 2000)
CV leakage rate	0.018%/day	0.017%/day	0.034%/day

Table 4 shows CV leakage test results at each year. It can be seen from the Table 4 that the CV leakage rate was well below the allowable limit of 0.1%/day at each year. Thus, it was confirmed that the integrity of the CV is maintained.

In order to minimize the release of fission products, the CV isolation valves are designed to be closed within 5s after sending the CV isolation signal if the depressurized accident and rupture of piping for the primary helium

purification system occur. The CV isolation valves are divided into the following three type valves.

(1) Isolation valve inside CV on piping of helium purification system

(2) Isolation valve outside CV on piping of helium purification system

(3) Isolation valve outside CV on piping of helium purification system leading to auxiliary cooling system

As shown in Table 5, the time from the startup of signal to the close of the CV isolation valves for inside and outside the CV isolation valves were 0.17s and 0.24s, respectively. The time of all the CV isolation valves was well below the allowable limit of 5s.

Table 5 Performance test result of isolation valve of CV

Isolation valve	Time from startup of signal to close of isolation valve	
	Allowable limit	Measurement value
Isolation valve inside CV on piping of helium purification system	Less than 5s	0.17s
Isolation valve outside CV on piping of helium purification system	Less than 5s	0.24s
Isolation valve outside CV on piping of helium purification system leading to auxiliary cooling system	Less than 5s	0.24s

Airtight Test Of Service Area

If the depressurized accident and rupture of the piping for the primary helium purification system happen, the SA is isolated by signals such as ' pressure difference between primary coolant and pressurized water is low'. The SA needs to maintain the air pressure of less than –59Pa after the startup of the emergency air purification system. In the airtight test of the SA, the opening of air regulation damper of the emergency air purification system changes from 20 to 55% as a parameter. Table 6 shows the relationship between the air pressure in the SA and elapsed time after the startup of the emergency air purification system at the opening of the air regulation damper of the emergency air purification system of 55%. By the opening of the air regulation damper of 55%, the air pressure of the SA was kept to be below –59Pa within 1min from the startup of the emergency air purification system.

Table 6 Relationship between air pressure in SA and elapsed time after startup of emergency air purification system at opening of air regulation damper of 55%

System	Elapsed time(min)	0	1	2	3	4	5
A	Air pressure in SA (Pa)	17	-75	-86	-82	-85	-87
B	Air pressure in SA (Pa)	18	-71	-79	-81	-81	-82

Performance Test Of Emergency Air Purification System

A performance test of the emergency air purification system confirms functions of filter for corpuscle removal and iodine removal. The allowable limits of the corpuscle removal efficiency and the iodine removal efficiency are more than 95% and more than 99%, respectively. After the smoke of dioctryl phtalate (DOP) of 0.7 μ m produces from its generator to obtain the corpuscle removal efficiency, the concentrations at upstream and downstream paths to the filter are measured. The iodine removal efficiency was evaluated by the use of adsorption efficiency of active carbon and leakage

rate of bypass filter path through freon gas (R-112). The corpuscle and iodine removal efficiencies are calculated as follows:

Corpuscle removal efficiency (%)= $\{1-(X/Y)\} \times 100$ (2)

X: DOP concentration at downstream path to filter

Y: DOP concentration at upstream path to filter

Iodine removal efficiency (%) = adsorption efficiency of active carbon×(1-R/100) (3)

$R = (B-D)/(A-C) \times 100$ (4)

R: leakage rate (%)

A : freon gas concentration at upstream path to filter

B : freon gas concentration at downstream path to filter

C : air concentration at upstream path to filter

D : air concentration at downstream path to filter

As a result of the test, the corpuscle and iodine removal efficiencies were estimated to be 99.99% and 99.59%, respectively.

In addition, the startup time of the emergency air purification system is very important to prevent the public people from suffering the excessive radiation exposure. In the safety analyses of the HTTR, the startup time of 13min was employed considering conservatively from the viewpoint of the radiation exposure. The startup time corresponds to total time from the following items (1) to (4).

(1) Time from the startup command to the startup of blowers and electric heaters of the emergency air purification system

(2) Time from the startup time of the blowers and the electric heaters to the difference between temperatures at inlet and outlet of the electric heaters of 4℃.

(3) Time from the loss of off-site electric power simulation to the restartup of the emergency air purification system by the emergency power feeders.

(4) Time from the restartup time of the blowers and the electric heaters to the difference between temperatures at inlet and outlet of the electric heaters of 4℃.

As shown in Table 7, the startup of the emergency air purification system was less than 3min, which was well below the allowable limit of 13min.

Table 7 Performance test result of emergency air purification system

Number	Items	Time		
		Regulation value	Measured value	
			System A	System B
①	Time from startup command to startup of blowers and electric heaters of emergency air purification system	—	0.09s	0.08s
②	Time from startup time of blowers and electric heaters to difference between temperatures at inlet and outlet of electric heaters of 4℃	5min	1min	1min
③	Time from loss of off-site electric power simulation to restartup of emergency air purification system by emergency power feeders	1min	49.8s	53.8s
④	Time from restartup time of blowers and electric heaters to difference between temperatures at inlet and outlet of electric heaters of 4℃	5min	1min	1min
	Total	(13min*)	3min	3min

* Total time of ②, ③ and ④ as well as safety margin of 2min

CONCLUSION

The followings are the major conclusions from the performance tests of the reactor containment structures of the HTTR

1. The leakage rate of the CV was 0.018%/day, which was well below the allowable limit of 0.1%/day in 1996 and the CV leakage rate was also well below the allowable limit of 0.1%/day in 1999 and 2000. The time of all the isolation valves was well below the allowable limit of 5s.
2. The air pressure of the SA was kept to be below –59Pa within 1min from the startup of the emergency air purification system.
3. The corpuscle and iodine removal efficiencies of the emergency air purification system were estimated to be 99.99% and 99.59%, respectively. The startup of the emergency air purification system was less than 3min, which was well below the allowable limit of 13min.

REFERENCES

1. Saito S., " Design of High Temperature Engineering Test Reactor (HTTR)," JAERI 1332, 1994
2. Sakaba N., "Performance Tests of the Reactor Containment Structures of HTTR," JAERI-Tech 98-013, 1998
3. Japan Electric Association, "Definitions Code of Reactor Coolant Pressure Boundary and Reactor Containment Vessel Boundary," JEAC 4602, 1992
4. Kunitomi K., "Thermal Transient Analyses during a Depressurization Accident in the High Temperature Engineering Test Reactor (HTTR)," JAERI-M 91-163, 1991
5. Japan Electric Association, "Primary Reactor Containment Vessel Leakage Testing," JEAC 4203, 1994

CONTAINMENT PROTECTION DURING SEVERE ACCIDENTS

Henrik Dubik[1)], Ola Jonsson[1)], Thomas Augustsson[1)], Lars Engsund[1)], Lennart Agrenius[2)], Robert Henry[3)], William Berger[3)]

1) Oskarshamn Nuclear Power Station, Oskarshamn, Sweden
2) Agrenius Engineering, Stockholm, Sweden
3) Fauske & Associates, Inc., Burr Ridge, Illinois

INTRODUCTION

It is imperative during any accident condition to minimize the release of fission products to the environment. The Containment serves as this last barrier to guard against a release. It is important then to understand how the containment will respond to an accident and to implement where possible features that will assist the structure in serving its design function as a barrier to the release of any fission products. The design of the Swedish Nuclear Facilities have adapted a number of protective measures that will assist in ensuring that the containment will serve its function. Much of the decision as to the types of systems that were to be employed was made under the Reactor Accident Mitigation Analysis research project (RAMA, 1984). The systems implemented included a large vent system with a rupture disc and two normally open isolation valves. This vent was designed to a Large LOCA event with a condensation pool bypass. Such an event would lead to containment failure and loss of piping systems penetrating the containment wall. The result would be a core melt due to lost injection sources. Following containment isolation signal and a time delay the vent system isolation valves would close. This would prevent the vent from operating late in an accident sequence, providing a direct path from containment to the environment. A second vent system was also added to address over pressure beyond the expected time of a pool bypass event. This vent, smaller in size also included a rupture disc and a parallel manual valve. The output from the vent is directed through a sparger and into a water pool where fission products are scrubbed from the gas stream. This vent is intended to preclude over pressure failure given that a core melt had occurred. The systems generated from the RAMA study included an independent spray system whose source of water is taken external to the plant and its operation is independent of plant power. As a result after manually initiating the system, spray water can be directed to containment to help control pressure and scrub fission products. Depending upon the containment design, a lower drywell flood system was implemented. The intent of this system is to ensure a deep water pool under the reactor vessel in the unlikely event the vessel fails and debris is discharged. Also included in the design were special shields for the penetrations that passed through the lower drywell floor. The implementation of these systems was as a result of rulemaking from the Swedish regulatory body (SKI). This paper will focus on the influence that the lower drywell water pool has on the accident and the contribution that the independent sprays and the filtered vent have on reducing the risk of an unfiltered release. The design and implementation of these systems varies depending upon the plant. Each unit has unique features and as a result the description used in this paper is not reflective of any one of the three units at Oskarshamn. These differences will be noted in the paper.

Accident Progression

The response of the containment during a severe accident is dependent upon the type of accident and selected plant features, which can influence the containment response. To facilitate the application of containment protective features, it is necessary to first understand the progression of a severe accident and its influence on the containment.

The decay heat generated during any reactor scram is transported to the condensation pool from the primary system through the (314) safety relief valves and from containment via the downcomers. As water is added to the reactor vessel the steaming that occurs initially continues to be transported to the pool. The condensation pool eventually begins to rise in temperature and it then becomes necessary to remove heat from the pool. The failure to provide this heat removal will eventually lead to pool saturation and a gradual rise in containment pressure. Failure to recover the pool cooling function will result in pressure values reaching the containment ultimate failure pressure. Figure 1 typifies a containment response to a lack of condensation pool cooling.

The Figure shows a gradual rise in pressure due to the steaming from the condensation pool. The rise in pressure is at a rate of about 3Pa/ sec. This sequence certainly provides adequate time to implement recovery actions and re-establish condensation pool cooling.

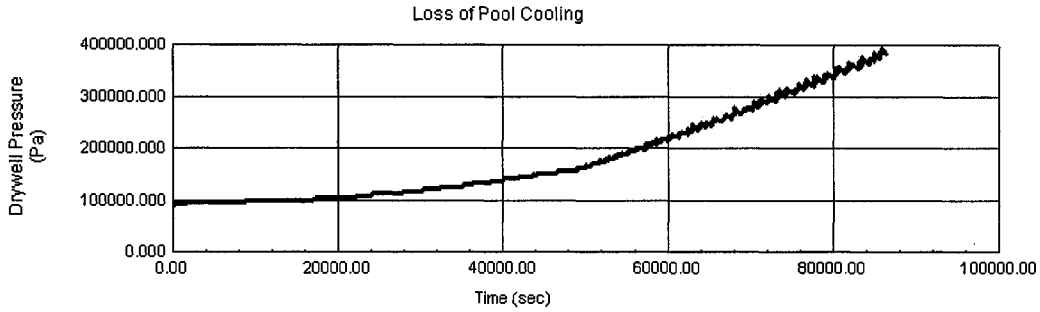

Figure 1 Containment Response No Pool Cooling

In this sequence a transient was the initiator and injection is being provided by the Auxiliary Feedwater System (327). The auxiliary feed water system uses as its suction source the condensation pool or a supply tank external to the drywell depending upon the unit design. If the pump takes suction from the condensation pool then its time of operation is limited to either NPSH limitations or high pool temperatures causing seal problems. If the water supply is an external tank then the pump is not subjected to the adverse conditions occurring as a result of the condensation pool reaching saturation conditions. The reactor core is being cooled and decay heat is transferred to the condensation pool. Without pool cooling, eventually saturation and steaming occur which is shown as the gradual growth in pressure. In this case the containment will eventually reach failure conditions and should a core melt occur with the containment already failed a direct path for release of fission products would be provided, this typically can result in large unfiltered releases.

As stated in the introduction, one measure employed in these designs is to flood the lower drywell with a deep water pool (i.e. 7 meters) to cool any debris which may be released from the failed vessel. Some stations have a lower drywell floor over the condensation pool. Thus instead of flooding, a mechanistic means is provided to allow debris to enter the condensation pool from the lower drywell floor effectively creating the same situation as flooding of the lower drywell. For designs where the debris enters directly a deep-water pool following vessel failure, the failure pressure can have an influence on the interaction of the debris with the water pool. The failure pressure will determine the velocity with which the debris enters the water pool, and the hydrodynamic forces that will act on the debris jet. The net result will be a particle size determined by these conditions. As the debris particles are quenched in the pool, they oxidize as part of this cooling process. The higher the velocity, the more break up and the higher the oxidation rates. The result is that a significant amount of non-constable gases can be formed which will create a more dynamic rise in drywell pressure. This was simulated assuming such an occurrence for a plant design where the debris enters a water pool; this is depicted in Figure 2.

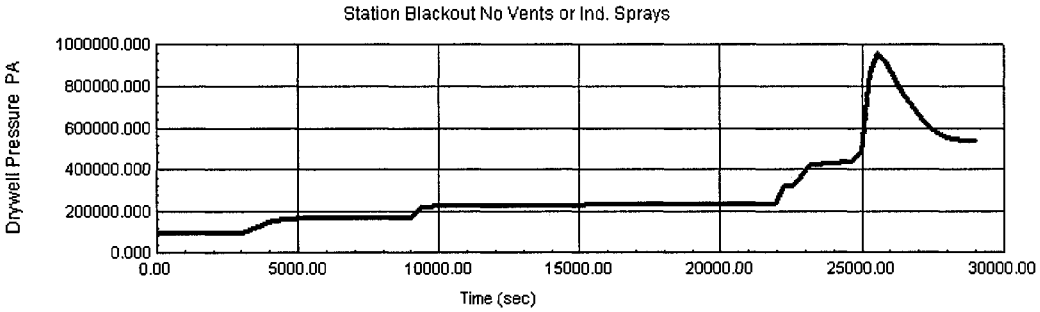

Figure 2 Drywell Pressure

In this sequence, the pressure rises in two small steps prior to 10,000 seconds. The first step occurs at the time the core uncovers and there is a release of hydrogen into the drywell gas space. The second step is the oxidation of debris particles as the debris enters the water pool in the lower vessel plenum. The drywell pressure remains at a fairly constant value until the first vessel failure at about 22,000 seconds and then the failure of the vessel lower head at about 25,000 seconds. In both of these failures, debris is entering the water pool in the lower drywell and oxidation of this debris is resulting in the production of hydrogen. The Figure shows a rapid rise in pressure reaching containment failure conditions. It is evident from these two sequences that the variability of the drywell response could have far ranging effects.

As the containment pressurizes it is expected that initially it will form many cracks and begin to leak. This leakage will allow the flow of steam and aerosols that may be present in the gas space to escape, but will not be sufficient to depressurize

the containment. As the pressure rises further cracking will occur until the point is reached where the openings created are sufficient to relieve the drywell pressure. At this point the constituents within the gas space will be swept out with the blow down. The source term implications can be far reaching when an opening to the environment is created during accidents of this magnitude. It is important to understand how the fission products behave during these events so that appropriate actions can be taken. At the onset of core damage the volatile fission products as well as the noble gases are released form the fuel assemblies. The volatile fission product vapors will condense and form aerosols. These aerosols then deposit within the primary system and later revaporize. Those that do not settle within the primary system are transported to the containment depending upon the type of accident. For transient cases where the primary system remains in tact, the aerosols are transported to the condensation pool via the safety relief valve system (314) and to a high degree of efficiency filtered out of the gas stream and remain trapped in the condensation pool. If the initiator was a LOCA then the aerosols that initially escape the primary system enter the drywell gas space where they remain airborne until they settle in containment. Once the vessel fails then the aerosols plated out in the primary system have a release path when they revaporize and they then enter the drywell. It can be seen that there numerous release scenarios that could result in volatile airborne aerosols and if containment failure occurs while these products are airborne then they have a release path to the environment. Figure 3 depict for a station blackout sequence the mass of airborne fission products in containment.

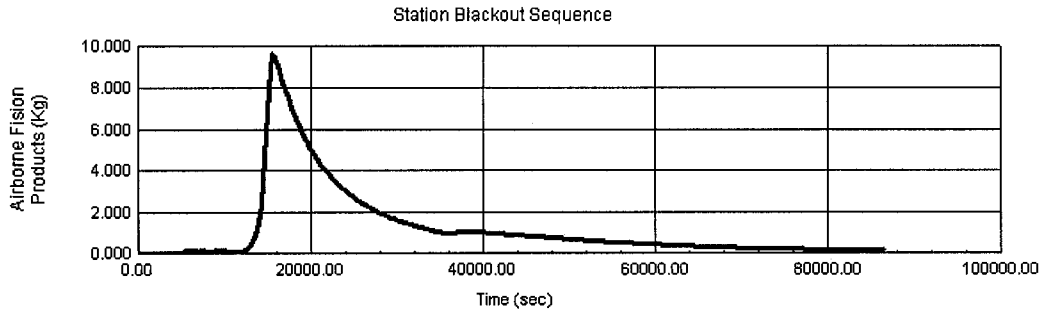

Figure 3 CsI in Containment

In this particular sequence, the vessel failed at around 12,500 seconds. The volatile aerosols became airborne within containment and then began to settle on structures and components. At anytime during their presence in the gas space should containment failure occur, these fission products would be swept out into the environment. It is important to recognize the timing of events and how they can play a role in effecting releases. If the containment failure precedes possible vessel failure as shown in Figure 1 then a direct release path is provided for the fission products depicted in Figure 3. On the other hand, if containment failure occurs within a time period close to that of vessel failure then the same effect could occur. This latter case may be the result of the sequence described by Figure 2.

Containment Protective Features

The containment protective features discussed in the introduction are depicted in Figure 4 with nominal values for their operation; the Figure reflects the Oskarshamn Unit 3 design.

If the event is a LOCA combined with a condensation pool bypass, then the 361 vent rupture disc would operate. After a time delay the vent is isolated. The 358 system would respond based on vessel level and isolation to flood the lower drywell . If this system should fail then any molten debris would attack the penetrations. The independent sprays 322 and the filtered vent would also be employed to protect from an unfiltered release.

To assess the level of protection that these systems afford a plant design, a PSA model has been developed which employs nominal probability Figures for these systems. An initiating event frequency of 1.0 has been used so that the outcome probabilities would be representative of a per unit or per cent contribution to the overall outcome and derivation of absolute Figures would not be required. The event tree and its probabilities are representative of Swedish facilities, not any one unit. The event tree and its probabilities are shown in Figure 5.

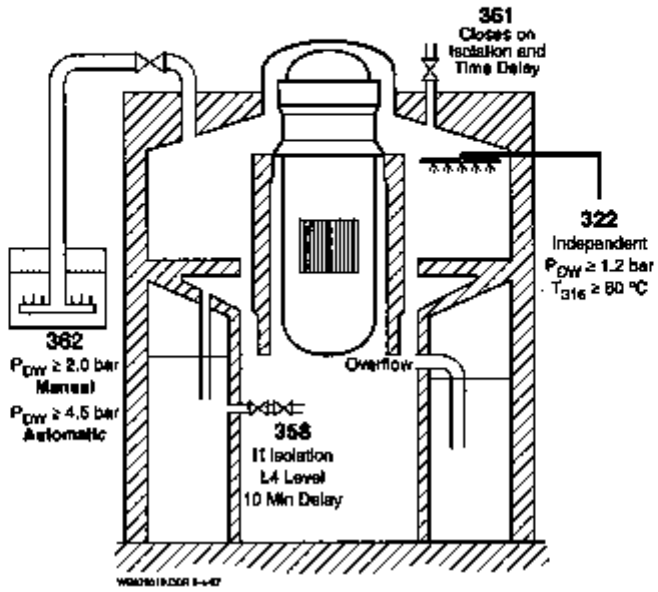

Figure 4 Containment Protective Features

358 Flood	322 Sprays	362 manual	362 rupture	End State	% Cont.
5.00E-03	1.00E-01	2.00E-01	1.00E-02		
				Scrubed	89.55%
				Filtered	7.96%
				Filtered	1.97%
				OVP	0.02%
				Pent	0.50%

Figure 5 Containment Event Tree

The initiating event to this tree would be the composite core damage frequency from the level 1 analysis. The outcomes to the event tree are revered to as end states and depict the various states where the containment may end. These end states include scrubbed, filtered, OVP and Pent. Scrubbed refers to spray operation and implies that any airborne fission products will be removed form the containment gas space. This mechanism of spraying also reduces the containment pressure. Filtered is the end state associated with the vent system operating to reduce pressure. The end state designated as OVP refers to a state of containment over pressure. Finally the end state designated as Pent represents penetration failure.

Following the initiating event, the tree first checks to see if the lower drywell flooding system worked and if it has not then as stated before a breach of containment through the penetration will occur. Failure of this node results in a Pent. end state. After success of the flooding a check is made to see if the sprays have functioned. The outcome of this action will be a scrubbed release through the leakage paths in containment. If the sprays fail then the operator acts to manually open the filtered vent and should the manual system fail the rupture disc would be the next action to reduce pressure. The sprays are employed at first to reduce pressure thus eliminating the need to vent, which would be the preferred method of pressure reduction. If a rapid pressure rise had occurred due to formation of non-condensable gases from the debris water pool

interactions then the tree would have to be revised inorder to show that the rupture disc would have been required. The rupture disc would have been the only mechanism to respond to the rapid rise in pressure.

It should be emphasized that the event tree of Figure 5 does not address the nominal containment spray system used to control pressure. It is assumed that it has failed, as the tree is entered. Should it have functioned then the release would have been limited to that of leakage paths. The key feature identified by this tree is that only a very small fraction of the sequences would result in some type of unfiltered or unscrubbed release. This is depicted clearer in Figure 6, which shows the release breakdowns.

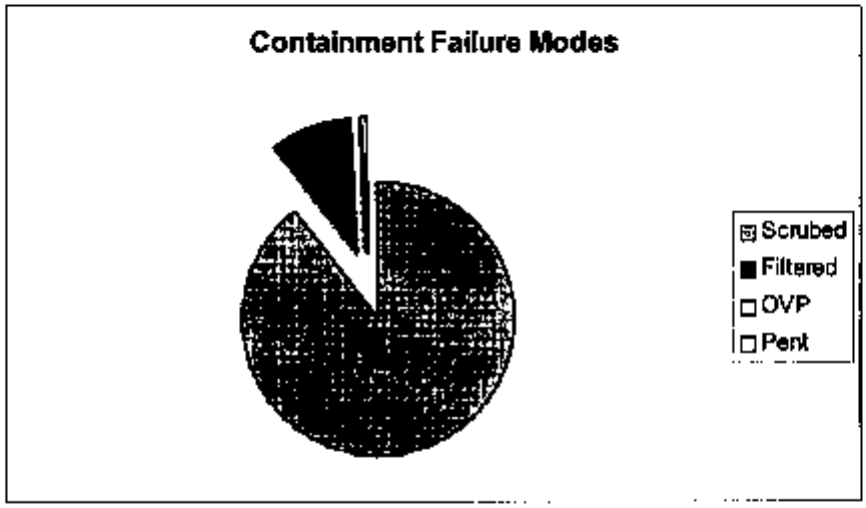

Figure 6 Consequence Break Down

Clearly the scrubbed and then the filtered release dominate the results. The scrubbed release exceeds the filtered release because procedurally it is preferred to first reduce pressure without having to create any containment openings. Less then 1% of all challenges to the containment result in a unfiltered or unscrubbed release.

Conclusions

The primary function of the containment is to serve as the final barrier to the release of fission products. The progression of an accident can result in unique challenges that may result in a breach of this final barrier. The accident can be of such a nature that the pressure rises quickly to levels challenging containment and not allowing for adequate operator intervention. Accordingly, the progression can be where the rise in pressure is at a slow rate providing time for mitigating actions. The simplified analyses outlined in this paper shows that the typical design considerations in the Swedish plant result in about 0.7% of all challenges resulting in a unfiltered or unscrubbed release. Over 99% of the challenges will be scrubbed, thus minimizing public risk. To gain a better perspective, assume a nominal core damage frequency of E-05. This would necessitate an unfiltered release frequency of about 7.0E-08. Regulatory Guide 1.174 lists as the minimum LERF for which changes in the LERF need to be assessed as 1E-05. Thus, these features offer a significant reduction in the LERF figure for the plant.